Republic of Iraq
Ministry of Higher Education
and Scientific Research

BUCKLING AND POST-BUCKLING ANALYSIS OF STIFFENED PLATES BY FINITE ELEMENT METHOD

A Thesis

Submitted to the College of Engineering
of the University of Babylon in Fulfillment of Partial
Requirements for the Degree of Master
of Science in Civil Engineering
(Structures)

By

BAHAA HUSAIN MOHAMMAD

Supervised by

PROF. DR. HUSAIN M. HUSAIN

ASST. PROF. DR. HAITHAM H. AL- DAAMI

November 2005

جمهورية العراق
وزارة التعليم العالي والبحث العلمي

تحليل الانبعاج و ما بعد الانبعاج للصفائح المُجسأة بطريقةِ العناصر المحددةِ

رسالة
مقدمة إلى كلية الهندسة في جامعـــــة بابـــــل
كجزء من متطلبات نيل درجة الماجستير
في علوم الهندسة المدنيـــــة
(إنشاءات)
من قبل

بهاء حسين محمد

إشراف

أ. د. حسين محمد حسين
أ. م. د. هيثم حسن الدعمي

تشرين الثاني 2005

[قالوا سبحانك لا علم لنا إلا ما علمتنا انك أنت العليم الحكيم]

صدق الله العلي العظيم

سورة البقرة، الآية (32)

CERTIFICATION

We certify that this thesis titled "**Buckling and Post-Buckling Analysis of Stiffened Plates by Finite Element Method**", was prepared by "**Bahaa Husain Mohammad**" under our supervision as partial requirement for the degree of Master of Science in Civil Engineering (structures).

Signature:
Name: Prof. Dr. Husain Mohammad Husain
Date: / /2005

Signature:
Name: Asst. Prof. Dr. Haitham H. Al-Daami
Date: / /2005

CERTIFICATION

We certify that we have read this thesis, titled "**Buckling and Post-Buckling Analysis of Stiffened Plates by Finite Element Method**", and as examining committee examined the student **Bahaa Husain Mohammad** in contents and in what is connected with it, and that in our opinion it meets the standard of thesis for the Degree of Master of Science in Civil Engineering (Structures).

Signature:
Name:Asst.Prof.Dr. Mustafa B. Dawood
(Member)
Date: / /2005

Signature:
Name: Asst. Prof. Mr. Abdul Ridah Saleh
(Member)
Date: / /2005

Signature:
Name: Asst. Prof. Dr. Ihsan A. Al-Shaarbaf
(Chairman)
Date: / /2005

Signature:
Name: Prof. Dr. Husain M. Husain
(Supervisor)
Date: / /2005

Signature:
Name: Asst. Prof. Dr. Haitham H. Al-Daami
(Supervisor)
Date: / /2005

Approval of the Civil Engineering Department
Head of the Civil Engineering Department

Signature:
Name: Asst. Prof. Dr. Ammar Y. Ali
Date: / /2005

Approval of the Deanery of the College of Engineering

Signature:
Name: Asst. Prof. Dr. Haroun A. K. Shahad
Date: / /2005
Dean of the College of Engineering
University of Babylon
Date: / /2005

To My

PARENTS

With Respect

ACKNOWLEDGMENTS

First and foremost, I thank my supervisors **Prof. Dr. Husain Mohammad Husain and Asst. Prof. Dr. Haitham Hassan Al-Daami** for suggesting this topic and for their constant guidance, advice and support.

Thanks are to be given to the Dean of the College of Engineering and to the Head and Staff of the Department of Civil Engineering in the University of Babylon for their support to finish this work.

Great thanks to my family for their support to finish this work.

Also, I thank **Mr.Haidar K.Amash** for his help in this work.

Finally, I am indebted to all my friends, especially for **Hasanien**, **Salam, Ammar, Amir**, and **Muslim** for their support and encouragement.

Bahaa Husain Mohammad

2005

ABSTRACT

An investigation of the buckling and post-buckling behavior of stiffened plates is presented in this study. This work first addresses the validation of the nonlinear finite element analysis used to perform the simulation of the buckling and post-buckling behavior of stiffened plates. Different buckling failure modes and failure loads are observed in stiffened panels. In this work, failure modes and buckling loads of stiffened plates under uniaxial loading condition are investigated by using the nonlinear finite element analysis. The nonlinear finite element analysis was performed using ANSYS V5.4, a finite element analysis software package.

The analysis performed in this study includes both buckling and nonlinear post-buckling of stiffened plates. Linear buckling analysis was conducted by using both analytical and numerical finite element techniques and comparison is made between the two methods. The mean difference between the analytical method and present study for the 50 panels presented in these tables is 0.074 and 0.087 for the local and overall buckling stresses respectively and between the present study and Biswarup[(7)] [2003] the mean difference is 0.041.

Parametric studies were performed in order to investigate the effects of aspect ratio, slenderness ratio and (number, height) of stiffeners on buckling load and post-buckling compressive strength. Several plates were analyzed with aspect ratios (1.5,1.0,0.667,and0.5) and with different number of stiffeners (1,2,3,and 5) for a range of plates from stocky to slender plates having slenderness ratios (7.1,9.9,13.6,24.8).

It is concluded that the post-buckling behavior of stiffened plates is very sensitive to the magnitude of slenderness ratio, aspect ratio and the ratio of plate thickness to stiffener height. For the load and boundary conditions used in this study, the behavior of 3-stiffener model does not change when edge stiffeners are added (5-stiffener model) and only a small increase of in-plane stiffness is noticed and the best dimensions are noticed for plates having three intermediate stiffeners with 9.9 slenderness ratio (corresponding to $t/h_w = 0.3$) since they have absolute maximum strength-to-weight ratio.

الخلاصة

تقدم هذه الدراسة تحريا لسلوك الانبعاج وما بعد الانبعاج للصفائح المُجَسأة. انصب هذا العمل أولا على صلاحية التحليل اللاخطي بالعناصر المحددة المستخدم لإتمام سلوك الانبعاج وما بعد الانبعاج للصفائح المُجَسأة. وقد لوحظت أنماط وأحمال فشل مختلفة في الصفائح المُجَسأة. تم التحري في هذا العمل عن أنماط وأحمال الفشل تحت حمل ضغط محوري أحادي باستعمال التحليل اللاخطي للعناصر المحددة.

استعمل التحليل اللاخطي للعناصر المحددة باستخدام برنامج التحليل (ANSYS V5.4).

يتضمن التحليل في هذه الدراسة كلا الانبعاج وما بعد الانبعاج اللاخطي للصفائح المُجَسأة. دُرسَ تحليل الانبعاج الخطي باستخدام الطريقتين التحليلية والعددية ومن ثم المقارنة بينهما, وكان معدل الفرق بين الطريقة التحليلية والدراسة الحالية لخمسين صفيحة يساوي 0.074 و 0.087 لحملي الانبعاج الموضعي والإجمالي على التوالي وبين الدراسة الحالية والباحث [Biswarup] كان معدل الفرق 0.041 .

تمت دراسة تأثير المعاملات للتحري عن تأثير نسبة العرض إلى الطول, نسبة النحافة, و(عدد وارتفاع) المُجَسِئات على حمل الانبعاج وعلى مقاومة الانبعاج؛ لذلك تم تحليل عدة صفائح بنسب عرض إلى طول (1.5, 1.0, 0.667, و0.5) وبأعداد مختلفة من المُجَسِئات (1, 2, 3, و 5) لسلسلة من الصفائح تبدأ بصفائح مربوعة وتنتهي بصفائح نحيفة وبنسب نحافة(7.1, 9.9, 13.6, و 24.8).

استُنتِج بان تصرف الصفائح المُجَسأة لما بعد الانبعاج حساس جدا إلى قيمة نسبة النحافة ونسبة العرض إلى الطول ونسبة سمك الصفيحة إلى ارتفاع المُجَسِئ. ولظروف التحميل والتقييد المعتمدة في هذه الدراسة استنتج أن تصرف الصفائح بثلاثة مُجَسِئات لا يتغير عند إضافة مُجَسِئين في الحافات (صفائح بخمسة مُجَسِئات) وبزيادة قليلة في الجسائة وان الأبعاد الأفضل قد لوحظت لصفائح بثلاثة مُجَسِئات وبنسبة نحافة تساوي 9.9 (تقابل نسبة سمك الصفيحة إلى ارتفاع المُجَسِئ تساوي 0.3) طالما تمتلك أعظم نسبة مقاومة إلى الوزن.

LIST OF NOTATIONS

Symbol	Description
GEOMETRIC PROPERTIES	
a	Length of one-bay, spacing between two adjacent transverse frames
A_f	Sectional area of stiffener flange
A_p	Sectional area of plate in between adjacent stiffeners (=bt)
A_s	Sectional area of a single longitudinal stiffener
A_T	Sectional area of a single longitudinal stiffener plus effective plating
A_w	Sectional area of stiffener web
b	Spacing between two adjacent longitudinal stiffeners
B	Breadth of stiffened panel
b_f	Breadth of stiffener flange
h_w	Height of stiffener web
I_x, I_y	Moment of inertia of a single stiffener with attached plating
ns	Number of longitudinal stiffeners in a stiffened panel
t	Thickness of plate
t_f	Thickness of stiffener flange
t_w	Thickness of stiffener web

γ	Ratio of flexural rigidity of plate-stiffener combination to flexural rigidity of plating $\gamma = \frac{EI_X}{Db}$
λ	Slenderness ratio of stiffener with attached plating $\lambda^2 = 4\left(\frac{a}{b}\right)^2$
ρ	Radius of gyration of longitudinal stiffener with attached plating $\rho^2 = I_X / A_T$
MATERIALS PROPERTIES AND STRENGTH PARAMETERS	
D	Flexural rigidity of isotropic plate
E	Young's modulus
G	Shear modulus
J_x	Torsional rigidity of a longitudinal stiffener for continuous stiffening $J_X = \frac{1}{6}(h_w.t_w^3 + b_f.t_f^3)$
ζ	Ratio of torsional rigidity of stiffener to bending rigidity of attached plating
v	Poisson's ratio
σ_E	Euler column buckling stress
σ_{local}	Elastic local plate buckling stress
$\sigma_{ov,panel}$	Elastic overall panel buckling stress
σ_x	Applied longitudinal compressive stress
σ_y	Yield stress

Chapter One

INTRODUCTION

1.1 Exposition

Stiffened plates are extensively used in long span bridges, aircrafts, ships and other situations where the reduction of self-weight is an important design objective for satisfying the requirements of increased stiffness and reduced weight.

Stiffened plates have been considered for use in these weight-sensitive structures, where high strength-to-weight and stiffness-to-weight ratios are required. Besides their high strength and stiffness, stiffened plates are usually thin. Thus, buckling is a critical consideration for the optimum design of structures made of such plates**.** These plates are fabricated as an assembly of individual plates. This allows the designer to select the most effective disposition of material in the cross section to carry the specified loading.

To maximize the saving in self-weight, the component plates of cross section are designed to be of slender proportions. They will then have a low elastic critical load and will normally operate in the post-buckling range so that advantage must be taken of their post-buckling reversed strength [(44)]. Thus, the design of the stiffened panels is based on post-buckling compressive strength with consideration of buckling load. Therefore, it is necessary to study the post-buckling behavior of the stiffened panels besides their buckling behavior. The buckling characteristics of such panels are of crucial importance for the overall structural strength. The post-buckling behavior is especially important because of the reserved capacity which exists after the initial buckling.

However, looking at the deflection behavior of actual stiffened panels, it is clear that a column model does not provide the best representation of the real structural response. Usually, local deformations dominate, while lateral deflection in the global mode is less significant.

Previous works in this field have been restricted mostly to linearized buckling predictions, neglecting nonlinear geometrical effects in the large deflection region. Some work has been performed on the large deflection response of unstiffened plates [13]. In the present work, the coupled behavior of a plate with an attached stiffener is treated using large deflection theory for both the plate and the stiffener.

The compressive strength of stiffened plates is of primary concern to the designer. As a sequence, the evaluation of plate compressive strength has mainly been achieved through laboratory experiments in the past few decades. For a realistic assessment of the buckling and post-buckling behavior of stiffened plates, large deflection theory must be used because small deflection theory is of limited practical value for the analysis of stiffened plates at loads comparable to their ultimate loads. The large deflection mechanics of stiffened plates is a highly nonlinear problem whose solution relies on the use of a numerical technique such as the nonlinear finite element analysis.

Although the linear buckling loads provide a measure of the compressive load carrying capacity of the stiffened panels, the test results indicate that the panels can undergo substantial nonlinear transverse deformations prior to failure. Hence, it has been decided to perform a nonlinear analysis in order to understand the effects of stiffeners on post-buckling behavior.

Traditionally, such structures have been designed according to allowable stress principles so that a linear elastic analysis of the stress distribution was sufficient to be used by employing simplified linear numerical analysis such as the finite difference and the finite element methods. The improved nonlinear analysis is applicable to different plates with various stiffeners properties, which continue to operate in the post buckling range. It must be, therefore, taken into account the effects of geometric nonlinearity arising from the plate buckling.

1.2 Buckling Behavior

Stiffened plates are used in naval and aerospace applications, and in construction of certain civil structures and industrial buildings. These elements are subjected to normal and shearing forces acting in the plane of the plate, the most important phenomenon in such structures is the local or overall buckling of the constituent elements. The load producing this buckling is called the critical load. This critical load state characterizes the neutral equilibrium of an axially loaded plate. At this state, it is observed that the plate would keep the small out-of-plane perturbation and still remains stable. The importance of the critical load is the initiation of a deflection pattern, which leads, if the load is further increased, to very large lateral deflections and eventually to a complete failure of the plate. It is a dangerous condition which must be avoided [14].

1.3 Finite Element Method

In order to study the post-buckling behavior of stiffened plates for different boundary and load conditions, and because of the limitations on the boundary and load conditions imposed for the analytical methods, it is decided to use the finite element method.

The finite element method has proved to be a powerful method of analysis in many fields of engineering. Most of its early applications were to the solution of linear problems. However, for more than four decades, the applications of the finite element method to nonlinear problems have been under successful development.

The finite element method involves dividing the continuum into a finite number of elements connected only at nodal points. These elements have a simple shape (usually rectangular or triangular), and any complex structural shape can be approximately represented by a proper assemblage of these elements. Any difficulties due to complex loading conditions can be simplified by assuming that the loads are applied only at the nodes of the element. The accuracy of the method depends not only on the idealization of the continuum, but also on the properties of the shape functions assumed to represent the deformed shapes of the element.

The solution techniques for nonlinear problems in solid mechanics depend mainly on the form of the mathematical equations obtained. In nonlinear problems, the stiffness matrix is a function of the applied loads and the displacements. Thus, the stiffness matrix established for a particular system of loading is not valid for other loading systems.

1.4 Scope of This Study

This study is divided into two parts; first, an attempt is made for modeling a linear finite element method to analyze the eigen-value buckling of longitudinally stiffened steel plates. The effect of slenderness, aspect ratio, and stiffeners properties are considered.

The second part deals with a nonlinear post-buckling analysis of stiffened plates. The effect of slenderness, aspect ratio, stiffeners properties, and number of stiffeners are considered.

1.5 Outline of the Thesis

The present study is given through six chapters. Chapter one gives a general introduction. In chapter two, a brief review of early studies and more advanced studies on the subject are given with an interpretation of the results as possible. A linearized buckling analysis of plates with stiffeners is presented in chapter three. A nonlinear post-buckling behavior of stiffened plates is presented in chapter four. The applications and the presentation of the results with discussions are given in chapter five. Finally; chapter six gives the conclusions and recommendations for further studies.

Chapter Two

REVIEW OF LITERATURE

2.1 General

The review presented here aims at showing the most important developments and steps that have been taken on the path leading to the knowledge of today in this subject (buckling and post-buckling of plates stiffened plates).

In this chapter the literature survey is divided into three major scopes: -

1. Buckling Analysis
2. Post-buckling Analysis of Plates
3. Post-buckling Analysis of Stiffened Plates

2.2 Buckling Analysis

As cited in Ref. (4), **Salvadori** [50] **[1949]** introduced a numerical and a graphical computation of buckling loads by successive approximations. The finite difference method was used to solve the buckling problem. This solution is purely obtained by numerical computations, which is greatly enhanced by a simple method of extrapolation. This procedure was applied to various cases of buckling of beams, plates, and shells.

Chehil and **Dua** [15] **[1973]** employed a perturbation technique to determine the critical buckling stress of a simply supported rectangular plate with variable thickness cross section. The differential equation was derived for a general thickness variation in one direction. Their analysis

included a stiffened plate; the stiffener is fabricated from a factory. The major advantage of this analysis lies in the fact that the fabrication of these stiffened plates is very simple as compared to the manufacturing of plate which has a linear or exponential taper.

Kobayashi and **Sonoda** [31] **[1990]** used a power series method with the use of a co-ordinate transformation to solve analytically the buckling problem of uniaxially compressed rectangular plates with linearly tapered thickness. This solution was limited where the compressed edges were simply supported and the unloaded edges are (simply supported, clamped, or free). Their conclusion was that the buckling load is highly dependent on the thickness variation.

Chin, *et al* .[17] **[1993]** used the finite element method to predict the buckling capacity of arbitrary shaped thin-walled members under any general load and boundary conditions. The thin plate elements used in this method contained 30 degree of freedom (d.o.f): [14 d.o.f for the in-plane (membrane) action and 16 d.o.f for the out-of-plane (bending) action]. The linear and geometry stiffness matrices for the thin plate element were derived explicitly based on the principle of minimum total potential energy. This method was used for thin-walled structures involving distorsional and flexural-torsional buckling failure mode.

Ohga, *et al.* [43] **[1995]** used an analytical procedure for the elastic buckling problems of thin-walled members with variable thickness cross section by using the transfer matrix method. The transfer matrix was derived from the nonlinear differential equations for the plate panels with variable thickness by using the Fourier series expansion in the longitudinal direction and then applying a numerical integration in the lateral direction.

Husain, *et al.* [27] **[2002]** used the finite difference method to estimate the buckling factor of a rectangular thin plate with variable thickness cross section. Their results were presented graphically for the buckling coefficients for uniaxially compressed plates where the loaded edges were simply and clamped supported and where different plate aspect ratios, different tapering ratios, and different boundary conditions were considered. This study has shown that the value of the buckling load is very sensitive for tapering ratio.

2.3 Post-Buckling Analysis of Plates

Coan [18] **[1951]** solved Marguerre's equations to study the post-buckling behavior of plates by assuming the deflected shape of a rectangular simply supported plate as a double Fourier series and overcame the restriction of Levy's solution. Edge pull-in of three kinds was allowed for by adding further complementary functions to the expressions for the stress function (Φ). The theory was applied to a square plate with the central initial deflection (w_o=0.1t) and the results were compared with the experimental values.

Wah [63] **[1958]** introduced a closed form solution for the deflections, residual deflection, residual membrane tensions, and other quantities of engineering interest for infinitely long clamped rectangular plates with large deflections under uniform pressure. The analysis assumed infinite rigidity, in the plane of the plate and at the boundary supports. His formula is based on several idealizations which cannot be exactly duplicated in practice.

Yamaki [66] **[1959]** gave an extension of Levy and Coan's works by solving the problem with different boundary conditions, combining two kinds of loading conditions [**case (1)**, the edges are kept straight by the distribution of normal stresses, while in **case (2)**, the edges are free from stresses]. The solution of Marguerre's fundamental equations for large deflections of thin plates with slight initial curvature was presented in his study for the case of a rectangular plate subjected to edge compressive load by using double trigonometric series with coefficients to solve these equations. The conclusions from this study are: -

1. The deflection in **case (1)** is always smaller than the corresponding value in **case (2)**.
2. Under loads much greater than the critical, the net deflection for the initially deflected plate is smaller than that for the initially flat plate.

Stein [54] **[1960]** proposed a purely mathematical approach to explain the possibility of a change of buckling wave form. He investigated the post-buckling behavior of simply supported rectangular plates in end compressive load by solving the first few equations and presented non-dimensional load-shortening curves for plates with various length-width ratio ($m=a/b$ =1 to 5). These curves were obtained by using the values of (m), which intersect with these basic curves for the range plotted. The intersections of the load- shortening curves indicate possible changes in buckle pattern, as shown in Figure (2.1).

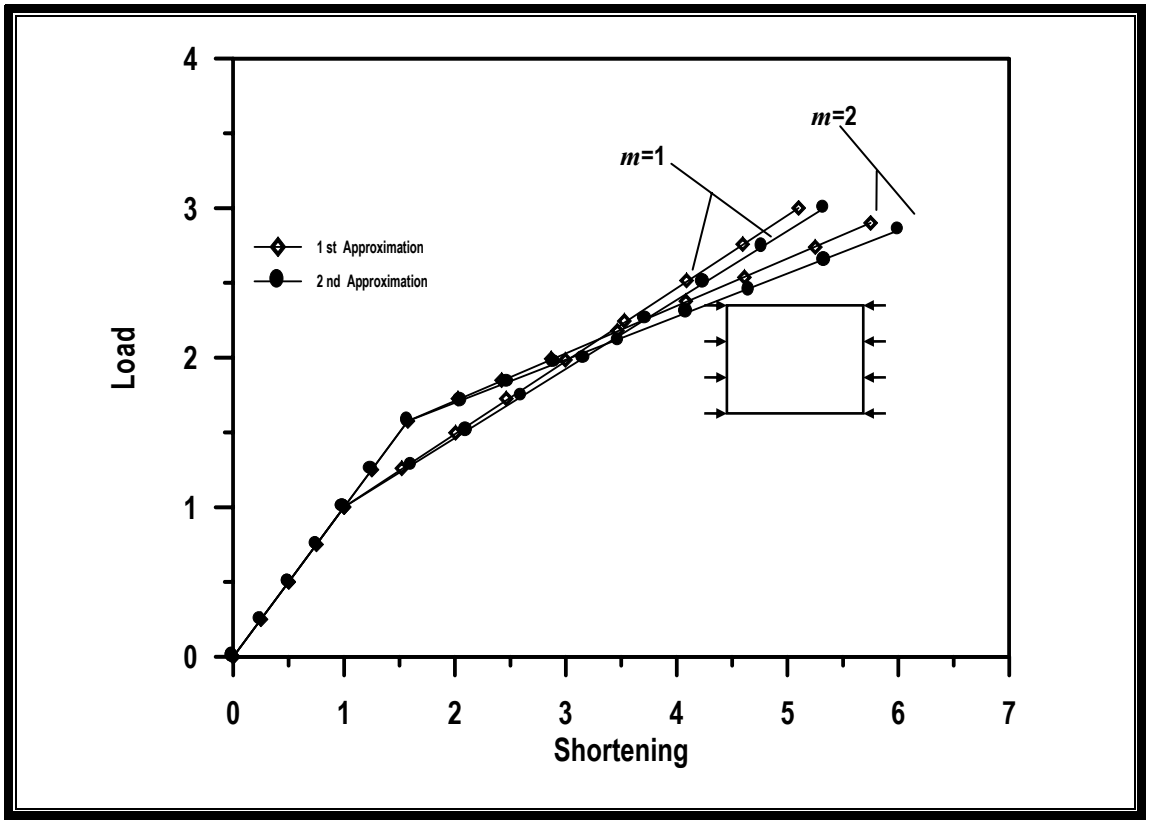

Fig. (2.1): Non-Dimensional Load-Shortening Curves of Rectangular Simply Supported Plates in Compression.

Basu and **Chapman** [6] **[1966]** used the finite difference method to investigate the large deflection behavior of transversely loaded rectangular orthotropic plates, having elastic flexural, extensional and shearing edge restraint. They derived the differential equations and boundary conditions and showed the effect of membrane action at a large displacement stage.

Abdel-Sayed [3] **[1969]** introduced a formula for the effective width of wide thin plates, under end compressive load in their planes by solving the Von-Karman governing differential equations. This solution was based on the assumption that the deflection form at the instant of buckling is preserved after loading exceeds the buckling limit. This formula was

used for plates with a small initial deflection or for plates with edges parallel to loading being free to move in the plane of the plate. This formula takes the following form: -

$$\frac{\lambda}{t}=\frac{1}{2}\left[1+\frac{n_{cr}\left(\frac{e}{e+e_o}\right)}{n_x}\right]\frac{b}{t} \qquad \textit{(2-1)}$$

to find the ratio $[e/(e+e_o)]$, the unknown magnitude of the deflection e, is calculated by the following equation: -

$$e.n_{cr}=(e+e_o)\left\{n_a+\frac{Et}{16}\pi^2\left[\left(\frac{a}{L}\right)^2+\left(\frac{a}{b}\right)^2\right]\frac{1}{b^2}\left(e^2+2e.e_o\right)\right\} \qquad \textit{(2-2)}$$

Here λ= effective width; n_{cr}= critical compressive force per unit width; b= width of plate; a= length of one buckled panel of plate; n_x= axial loading per unit length; n_a= average loading per unit width of plate; e= magnitude of deflection.

Aalami and **Chapman** [(1)] **[1969]** used the finite difference method for the large deflection behavior of rectangular orthotropic (including isotropic) plates under symmetrical or anti-symmetrical transverse loading and in-plane loading. The essential difference between solutions by **Basu** and **Chapman [1966]** and by **Aalami** and **Chapman [1969]** is that the last studied the behavior of plates under transverse and in-plane loading and with initial imperfection and rotational nodes and tangential boundary restraints.

Rushton [49] **[1969]** demonstrated the dynamic relaxation method to analyze the post-buckling behavior of plates with variable thickness and with edge restrained against lateral expansion. In this approach the plate at the nodes had been considered to have a constant thickness different from the thickness of the previous node. A variable thickness plate was considered in which the thickness is defined by:

$$t_x = t_o\, e^{\lambda x} \qquad (2\text{-}3)$$

with λ chosen so that at the thicker end $t = 2t_o$. He observed that the finite difference method tends to underestimate the initial buckling load by about 3% when compared with the exact solution.

As cited in Ref. (4), **Moxham** [42] **[1971]** used Ritz procedure to solve the large deflection in elasto-plastic behavior of plates with a small initial imperfection under in-plane compressive load. This study included plasticity through a volume integration in which the plate was divided into five layers through its thickness. His results were given for plates with different slender ratios (b/t= 30, 40, 55, and 80) and with a very small initial imperfection (w_o/t=0.05 and 0.08) and with the edges of the panel simply supported and free to pull-in.

Lin, *et al.* [36] **[1972]** introduced an analytical method for predicting the elasto-plastic bending of rectangular plates with large deflection. The effects of the plastic strain and the large deflection on plate deformation were shown to be the same as a set of applied external forces on the plate in the classical elastic small deflection theory. Their observation was that the deflection increased only slightly by plastic strain and the maximum extreme fiber stress relieved by plastic yielding.

Sherbourne and **Korol** [51] **[1972]** used experimental and theoretical investigations for the post-buckling behavior of axially compressed plates. They observed that the load predictions were overestimation to the real capacity of the plates and they also observed that when the imperfections were incorporated into the theoretical solution the scale-down values of the theoretical prediction accord more nearly with the experimental results.

Colville, *et al.* [19] **[1973]** used a general method for the solution of the Von-Karman plate equations by using a direct iterative finite element procedure. Their study included all applicable nonlinearity in the strain-displacement equations and the use of fully compatible finite element for both the in-plane and bending action and resulted in monotonic convergence to the theoretical solution by the structure idealization. This procedure gave minimum computational time.

Williams and **Walker** [65] **[1975]** derived an explicit expression for the load-deflection relationship for simply supported uniformly loaded square plate based on the perturbation approach. The results were presented for plates with a variety of geometries, boundary constraints and in-plane loading conditions. The accuracy of these results was sufficient for engineering design purposes.

Harding, *et al.* [26] **[1977]** introduced a finite difference formulation for the large deflection elasto-plastic analysis of initially imperfect thin rectangular plates subjected to in-plane loads. The elasto-plastic rigidities were calculated by using a rigorous multi-layer approach, and the governing equations were solved in an incremental

form by using dynamic relaxation. Their program was used to study the effects of both uniaxial and biaxial residual stresses due to welding and out-of-plane imperfection. The loading included tension and compression and their interaction with co-existing shear. Their conclusion was that the effect of initial imperfection on the ultimate collapse behavior by shear is small and a partially restrained panel (without transverse restraint on top and bottom edges) offers a considerable increase in design strength over the four edges under an unrestrained condition.

Little [37] **[1977]** used a simple formulation by a minimum energy principle for the analysis of plate collapse. This method is rigorous and yet economical in its use for the computer. His collapse analysis included a procedure which makes allowance for the effect of a large shortening increment where his results showed, surprisingly, that the predicted load-shortening response of a typical plate was only marginally dependent on the increment size. He presented results for biaxial in-plane compression and compared his results with previous theoretical work, both elastic and elasto-plastic analysis gave agreement.

Frieze, *et al.* [25] **[1978]** presented a theoretical treatment for the large deflection elasto-plastic analysis of plates by using a finite difference formulation with dynamic relaxation and iteration. Incremental form was used to the tangential elasto-plastic rigidities so that it can be used in the constitutive equations. The in-plane loading was applied by means of displacements. Their conclusion was that the dynamic relaxation is suitable to study plastic large deflection behavior of plates and that it probably offers both computer time and storage advantages for such analysis.

Colville and **Shye** [20] **[1979]** used the finite element method to investigate the post-buckling behavior of plates. In this study, the finite element solution procedure was employed for the large deflection problems based on the theory developed by Colville, who had shown that for post-buckling applications the uncoupled equilibrium equations may be written as: -

$$[K_w + K_N]\{w\} = q - [K_g]\{w\} \qquad \textit{(2-4)}$$

$$[\boldsymbol{K_u}]\{\boldsymbol{u}\} = \boldsymbol{f} - \boldsymbol{G_N} \qquad \textit{(2-5)}$$

In which $\boldsymbol{K_w}$ = bending stiffness of the undeformed plate; $\boldsymbol{K_g}$ = the geometric stiffness of the plate; $\boldsymbol{K_N}$ = the nonlinear stiffness matrix; $\boldsymbol{w}$= nodal bending displacements; $\boldsymbol{q}$ = applied bending loads; $\boldsymbol{K_u}$= in-plane stiffness of the undeformed plate; $\boldsymbol{G_N}$ = a nonlinear membrane correction force vector; $\boldsymbol{u}$= nodal in-plane displacements; $\boldsymbol{f}$ = applied in-plane loads.

As cited in Ref. (4), **Fok** [23] **[1980]** used the finite difference method to study the influence of imperfections in nonlinear behavior of rectangular plates. He analyzed the elastic post-buckling behavior of seventy-three isolated plates and confirmed his study by experimental work. The conclusion was that the post-buckling is very sensitive to the imperfections and the finite difference method gives results close to the experimental results.

Sridhran and **Graves-Smith** [53] **[1981]** used two versions of the finite strip method for the post-buckling behavior of prismatic plate structures under compressive load. Version I based on the classical approximation is found to be a powerful method for dealing with a variety of plate structures of practical interest. Version II which is

complementary to version I, is shown to be necessary when investigating the effect of corner displacements on the stiffness of the structures.

Rerkshanandana, *et al.* [48] **[1981]** applied a finite element method to study the elastic-plastic post-buckling behavior of initially deflected and eccentrically loaded steel plates and box sections. A computer program based on a finite element (rectangular element) incremental displacement method had been developed. The mathematical formulation was based on an incremental virtual Lagrangian formulation and used a modified Ilyusion yield criterion with the associated flow rule to incorporate in the analysis the plasticity effect of the plate material. Their proposition was that the empirical formula to predict the ultimate strength of eccentrically loaded plates whose unloaded edges are either simply supported-simply supported, clamped-clamped, or simply supported – clamped is to be based on an extensive numerical study.

Ueda and **Yao** [59] **[1982]** presented a new mechanism of plastic hinge based on the incremental theory of plasticity and derived the elastic-plastic and plastic stiffness matrices for one-dimensional members. Using this plastic hinge, a method of elastic-plastic analysis of space-framed structures was well developed including the effect of large deflection. This basic idea of plastic hinge method was developed for plates and solid bodies. The basic theory of the new method was based on using the ordinary finite element method (the stiffness method).

In this theory, the yield condition at the *i* th node of an element is described as follows: "the ***i*** th node becomes plastic when the resultant stresses at this node satisfy an appropriate plasticity condition and the plastic deformation is developed only at the nodes".

For the element, the relation between the increment of the nodal force, ***df***, and the nodal displacement, ***du***, is given in the following form:

$$df = k^p \; du \qquad \textbf{(2-6)}$$

In this equation $\boldsymbol{k^p}$ is either elastic-plastic or plastic stiffness matrix and was expressed in explicit form. When an element is subjected to constant strain, the element becomes plastic in the entire volume if the yield condition is satisfied at any point. Simultaneously, the plastic node is formed at every node of the element. Completely the same plastic stiffness matrix is obtained by either the ordinary finite element method or by the plastic node method. From these facts the accuracy of the solution by this method is anticipated to be of the same order as that by the ordinary finite element method when the element division increases.

Bradfield [10] **[1982]** presented a simplified elastic-plastic analysis for plates uniaxially compressed in their plane. Their assumption was that the plates are not initially flat and contain residual stresses due to welds at the longitudinal edges and the formulation were based on physical models and tested with other previous numerical solutions. These solutions based on full section yield criterion. A simple criterion was given for the plate shortening at which the maximum loads were carried by welded and unwelded plates. These lead to single calculations of plate strength.

Usami [61] **[1982]** used the finite element method to investigate the elastic-post-buckling behavior of rectangular plates in combined compression and bending. The analysis started with Marguerre compatibility and used the energy method to obtain the solution. An effective width formula was proposed to analyze the post-buckling

behavior of thin-walled steel members in bending or in combined compression and bending.

Fok [24] **[1984]** presented two numerical methods for correlating the experimental critical load and the initial imperfection of rectangular plates loaded in edge compression from recordings of load and deflection. The three points technique makes use of three sets of such readings to form a system of nonlinear simultaneous equations, the solution of which yields the critical load, where the initial imperfection and the constant curvature govern the load-deflection curve. The least square technique employs an applicable solution to the neutral bifurcation. Both of the two techniques were applied to various experimental results and it was found that the calculated values were very close to the experimental values. Galerkin method has been widely applied to both static and dynamic problems in the area of solid mechanics. The idea of the method is minimization of error by orthogonalizing the error with respect to a set of given (or basic) functions[12].

Paik and **Kim**[44] **[1989]** presented a new and simplified rectangular finite element having only four corner nodal points to analyze the elastic-plastic large deformation behavior up to the ultimate limit state of plates with initial imperfections. The finite element contains the geometric nonlinearity caused by both in-plane and out-of-plane large deformation because for very thin plates the influence of the former is not negligible. A simple matrix operation was derived for the elastic-plastic large deflection to treat the expanded plastic zone in the plate thickness direction of the element based upon the concept of plastic node method.

Paik, *et al.* [45] **[1992]** introduced a new buckling formula for all edge supported plate panels subjected to combined in-plane and lateral loads. This formula included the effect of welding residual stress and edge condition effects. Their conclusion was that by using this formula, about 15% of the critical plate buckling strength is additionally admitted at the severe case and the plate buckling strength is very much dependent on the edge conditions as well as the plate thickness.

Usami[62] **[1993]** proposed a formula based on extensive numerical results of elastic-plastic large deflection analysis of simply supported imperfect plates in compression as well as in combined compression and bending. This formula was expressed as functions of the magnitudes of compressive residual stress and initial out-of-flatness and used to compute the ultimate strength of welded built up beam-column segments.

Mirambell, *et al.* [39] **[1994]** presented experimental investigations and numerical solutions to the behavior of steel plates under pure compression. The measurements are concentrated on the strains at several characteristic points of the panel displacements. A numerical model was developed for the analysis of the geometrical and material nonlinearities of steel plate structures, based on the finite element method. Their study showed that the numerical and experimental stress values were close.

Lam [32] **[1998]** used a computational procedure for the post-buckling behavior of a strut with initial imperfection and under progressive end shortening. A polynomial expression was used to simulate the actual initial imperfection, while the deformations were expressed by a suitable trigonometric series. The nonlinear equilibrium

equations were solved by the Newton-Raphson procedure. His results were compared with other solutions and with experimental results.

Lee and **Yoo** [34] **[1999]** introduced an experimental study on the ultimate shear strength of web panels. In this study, 10 scaled plate girder models were tested to investigate the shear behavior of web panels up to failure. The following conclusions are obtained with regard to the behavior of the plate girder web panels:

1. The boundary condition at the flange-web juncture in practical design is much closer to the fixity.
2. In all existing failure mechanisms, the results that the through–thickness bending stress affects the ultimate shear strength are neglected; however, it has been found that very high bending stresses are developed at failure.
3. An anchoring system, such as flanges, is not needed for the development of the post-buckling strength.

Recently, **Paik, *et al.*** [46] **[2000]** presented a study on five subjects theoretically, numerically, and experimentally: modeling of post-weld initial imperfections (i.e. initial deflections and residual stresses) and their effects, influence of rotational rigidity of support members on the plate buckling strength, ultimate strength design equations under combined loads including biaxial compression/tension, edge shear and lateral pressure loads, and dynamic collapse strength characteristics under dynamic axial compressive loads or slamming-induced impact lateral pressure loading. Their proposition was a new design formula for more advanced buckling and ultimate strength of ship plating.

Bjelajac [8] **[2000]** used the finite difference method for the post-buckling behavior of thin elastic plates subjected to in-plane loading. This method was used to analyze plates with initial curvature and with variable boundary conditions. He derived equations from the minimum potential energy in a potential force field in a manner, which does not involve additional nodal displacements. This study considered that the unloaded edges are kept straight and fixed (u_x=0). His results were compared with other methods.

Mirambell and **Zarate** [40] **[2000]** used the finite element method to investigate the post-buckling behavior of plates with variable depth under in-plane shear loading. Their conclusion was that the post-buckling and the strength reserve tend to diminish by increasing the slope of the bottom face; this is due to the decrease in the vertical component of the tension field.

In 2000, Sun, ***et al.*** [56] proposed a procedure to analyze the post-buckling behavior of isotropic prismatic plate assemblies. The perturbation method combined with the variable separation method was used to obtain the perturbation equations of first and second order. The first order problem is a transcendental eigen-value problem and it is solved analytically by using Wittrick-William's algorithm. The second order problem is solved analytically to obtain displacement functions corresponding to axially constant and axially harmonic problems.

Jayachandran, ***et al.*** [28] **[2001]** derived incremental matrices for thin initially imperfect plates with small out-of-flatness by using the minimum potential energy principles. Explicit coefficients of the displacement gradient tensor had been evaluated. These matrices were

used in combination with any thin plate element. The formulations were incorporated in a software plot-code.

Mohammed [41] **[2001]** studied the buckling and post-buckling behavior by finite element method of rectangular isolated steel plates under in-plane shear load. This study considered the effect of initial imperfection and boundary conditions on the total behavior of the plate. His study was divided into two parts, the first included analysis of isolated plates under in-plane shear load with different values of initial shapes. The second part included analysis of isolated plates under in-plane shear load with different cases of support conditions. His conclusion was that the behavior of a thin-walled structure is usually sensitive to the nature and magnitude of initial imperfection.

Turvey and **Salehi**[57] **[2001]** introduced a finite difference formulation with the dynamic relaxation algorithm to solve the governing equations of an elasto-plastic large deflection analysis of pressure loaded sector plate, based on the Ilyusion full- section yield criterion and the flow theory of plasticity. This study showed that the effect of the in-plane edge restraint is more significant in changing the post-yielding response of slender simply supported plates with substantial stiffness increase accompanying the presence of full in-plane restraint. It showed that for slender sector plates the development of plasticity within the plate is quite complicated. At the maximum pressure applied, a plastic membrane state is approached in slender sector plates under simply supported in-plane fixed edge conditions, whereas in the case of clamped in-plane fixed edge plates a residual interior elastic zone remains.

Shnan [52] **[2001]** used a finite element method to analyze isolated steel plates. This study was divided into two parts: plate under shear load

was analyzed in the first part. In the second part, he analyzed isolated steel plates under compressive loads. He also studied the factors affecting the behavior of the plate such as initial imperfection, slenderness ratio (***b***/***t***) equal to 226,256,289, and 316,and aspect ratio (***a***/***b***) equal to 0.75,1.0,1.5, and 2.0.

His conclusion was that the stresses produced increase with an increase of both slenderness and aspect ratios especially on the long edges. Plastic mode mechanism was used in the prediction of the ultimate load capacity of plate structures.

Zou and **Qiao** [67] **[2002]** presented a higher order finite strip method for the post-buckling behavior of imperfect composite plates subjected to progressive end shortening. The arbitrary nature of the initial geometric imperfection induced during manufacturing was accounted for in the analysis. The nonlinear equilibrium equations were solved by the Newton-Raphson method. This study showed that the post-buckling behavior of an imperfect composite plate depends not only on the material lay-up, snap-to-thickness and anisotropy of the laminate, but also on the direction of induced out-of-plane imperfection.

Amash [4] **[2003]** used the finite difference method to analyze the post-buckling and post-yielding of imperfect thin plates. His study considered the effects of initial imperfections, boundary conditions, direction of loading, and tapering ratios. It has concluded that the post-buckling behavior of a thin plate is very sensitive to the magnitude of initial imperfection and magnitude of tapering ratio.

2.4 Post-Buckling Analysis of Stiffened Plates

Over the past four decades, a lot of research has been focused on the post buckling behavior of stiffened plates. The recent years have seen an increasing tendency to design large structural members as in welded steel stiffened plate systems. The geometries used in many heavy structures fail in compressive load by a combination of yielding and buckling. Analysis of strength of plates in such structures is complicated by the nonlinearities caused by the large out-of-plane displacements and by yielding of parts of the plate. The obvious significance of initial out-of-flatness was shown in many simplified analyses.

Crisfield [21] **[1975]** used a finite element formulation for the large deflection elasto-plastic analysis of thin mild steel plates subjected to in-plane compressive load. This method was used to trace the behavior of imperfect steel panels over the full load range, including the unloading stage following collapse. A series of simply supported thin plates under uniaxial compression were analyzed to study different in-plane boundary conditions, levels of geometric imperfection and residual stress. The load-shortening curves to predict the behavior of wide eccentricity stiffened plates subjected to uniaxial compression had been derived. He obtained good correlation with experimental results and showed that the imposition of straight edge constraint to the unloaded edges had no influence on the behavior of moderately stocky plates whereas an increase in the collapse load of (5-10%) was achieved for thinner plates.

Ueda, *et al.* [60] **[1987]** studied the large deflection behavior of a rectangular plate by an efficient semi-analytical method. An incremental

form of the governing differential equations of plates and stiffened plates with initial deflection had been derived. For each load increment, these equations were solved by the Galerkin method with especial consideration of simply supported boundaries. These equations take the following form: -

$$D\nabla^4(\Delta w)=\left(\begin{array}{l}\dfrac{\partial^2\Phi_{i-1}}{\partial y^2}\dfrac{\partial^2(\Delta w)}{\partial x^2}+\dfrac{\partial^2(\Delta\Phi)}{\partial y^2}\dfrac{\partial^2 w^t_{i-1}}{\partial x^2}\\ +\dfrac{\partial^2\Phi_{i-1}}{\partial x^2}\dfrac{\partial^2(\Delta w)}{\partial y^2}+\dfrac{\partial^2(\Delta\Phi)}{\partial x^2}\dfrac{\partial^2 w^t_{i-1}}{\partial y^2}\\ -2\dfrac{\partial^2\Phi_{i-1}}{\partial x\partial y}\dfrac{\partial^2(\Delta w)}{\partial x\partial y}-2\dfrac{\partial^2(\Delta\Phi)}{\partial x\partial y}\dfrac{\partial^2 w^t_{i-1}}{\partial x\partial y}\\ +\dfrac{\Delta q}{t}\end{array}\right) \qquad (2\text{-}7)$$

$$\nabla^4(\Delta\Phi)=Et\left(2\frac{\partial^2 w^t_{i-1}}{\partial x\partial y}\frac{\partial^2(\Delta w)}{\partial x\partial y}-\frac{\partial^2 w^t_{i-1}}{\partial x^2}\frac{\partial^2(\Delta w)}{\partial y^2}\frac{\partial^2 w^t_{i-1}}{\partial y^2}\frac{\partial^2(\Delta w)}{\partial x^2}\right) \qquad (2\text{-}8)$$

where w_{i-1}= total deflection at the end of the load increment (i-1), Φ_{i-1}= stress function at the end load increment (i-1), Δw_i= increment of deflection through current load increment, $\Delta\Phi_i$= increment of stress function through current load increment. A procedure of equilibrium correction at intermediate load steps must maintain that good accuracy of the solution may be maintained with larger load steps because the small quantities of higher order of (Δw, and $\Delta\Phi$) are neglected.

Sun and **Williams**[55] **[1997]** employed Koiter's theory to analyze the initial post-buckling behavior of prismatic plate assemblies which are composed of isotropic materials and subjected only to longitudinal compressive load. The post-buckling equations were solved exactly and the post-buckling coefficients were obtained by exact integration for all

component plates. Their conclusion was that the post-buckling characteristics of the stiffened plate are influenced significantly by the height of the stiffener.

Mathlum [38] **[1997]** presented a large deflection elasto-plastic analysis by the finite element method to analyze rectangular thin plates under compressive and shear load as well as the ultimate strength of plate girders with longitudinal and diaphragm stiffeners. His study was divided into three parts, the first, included the analysis of isolated plates under compression load. The second included the analysis of isolated plates under shear load. The last part contained the analysis of ultimate load of plate girders with transverse and longitudinal stiffeners. His conclusion was that the plate girder without stiffener gives low strength and the plate girder with transverse stiffener has a larger strength more than the plate with longitudinal stiffener.

Lee and **Yoo** [33] **[1998]** introduced a nonlinear analysis based on three dimensional finite element models to transversely stiffened plate girder web panels (without longitudinal stiffeners) subjected to pure shear, including the effects of initial out-of-flatness. This study showed that the design for shear in plate girder web panels in (**AASHTO**) and (**AISC**) specifications accounts for both elastic shear buckling strength and post-buckling strength separately and combine these resisting capacities which are based on the aspect ratio of the web panel. Although, equations in these specifications predict the overall shear strength with reasonable accuracy, they often underestimate the elastic shear buckling strength, due to an underestimation of the rigidity at the flange-web juncture and often overestimate the post-buckling strength of certain web panels, as a result of excluding the effect of out-of-plane bending stresses.

The first conclusion based on the assumption that the boundary condition at the flange-web juncture is simply supported gives too much conservative shear strength for many plate girder web panels and the second conclusion based on the flange rigidity appears to have little effect on the post-buckling strength of web panels.

Byklum and **Amdahl** [13] **[2002]** derived a computational model for the analysis of local buckling and post-buckling of stiffened panels. They used energy principles and perturbation theory to derive all energy formulation analytically, while a numerical method is used for solving the resulting set of equations, and for incrementation of the solution.

More recently, **Chen** [16] **[2003]** introduced an efficient beam-column approach, using an improved step-by-step numerical method for studying the ultimate strength analysis of stiffened panels. A fine mesh finite element ultimate strength analysis is carried out with 107 three-bay stiffened panels, covering a wide range of panel length, plate thickness, and stiffener sizes and properties. He concluded that the three-bay simply supported model is sufficiently general to apply to any panel with three or more bays.

Biswarup[7] **[2003]** used the improved expressions for elastic local plate buckling and overall panel buckling of uniaxially compressed T-stiffened panels and used it to solve the eigen-value buckling analysis of 55 panels of a wide range of typical panel geometries. These two expressions are equated to derive a new expression for the rigidity ratio $(EI_x / Db)_{co}$ that uniquely identifies 'crossover' panels -- those for which local and overall buckling stresses are the same . Collapse pattern, for the

crossover panels are also studied and classified from Von Mises stress distribution at collapse.

In the present study, the effect of slenderness and aspect ratios, number of stiffeners and the effect of stiffener cross section on the buckling and post-buckling behavior of stiffened plates will be investigated based on the finite element idealization.

BUCKLING ANALYSIS OF STIFFENED PLATES

3.1 General

The evaluation of linear critical stress has been well documented in contemporary literature. This critical stress state characterizes the neutral equilibrium of an axially loaded stiffened plate. At this state, it is observed that the plate would keep the small out-of-plane perturbations and still remain stable. In the case of slender columns, an increase in the axial load beyond such a critical state would produce a disproportionate lateral deflection resulting in an unstable state.

Nevertheless, edge supported plates do not undergo such unstable deformations immediately after attaining the critical buckling stress, i.e., in the vicinity of the neutral equilibrium, the fibers parallel to the edges in compression shorten because of elastic strain and bowing effect. The latter causes fiber lengthening in the direction perpendicular to the axial compression. This membrane effect tends to stabilize equilibrium of the plate and results in a possible increase in strength, which is termed as the post-buckling strength. In other words, the plate continues to carry an axial load up to a certain level, even beyond the critical stress, and presents a stable equilibrium.

The strength of a bare plate simply supported at the edges is strongly affected by its width to length ratio. As this ratio increases the strength diminishes rapidly and, therefore, it is structurally advantageous to subdivide the width by welding stiffeners onto the plate. Thus, by

judicious addition of a small proportion of structural weight the strength of the panel is greatly increased. The cross section of a single plate-stiffener combination is shown in Fig. 3.1.

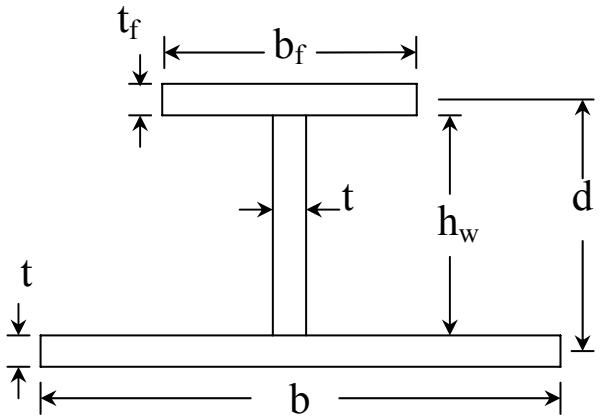

Fig. (3.1): Cross-Section of a Single Plate-Stiffener Combination

Based on Ref. [46], the buckling modes of a stiffened panel can be artificially subdivided into the following categories:

- Mode I: Overall buckling of the plating and stiffeners as a unit
- Mode II: Buckling due to predominantly transverse compression
- Mode III: Beam-column buckling of the stiffeners
- Mode IV: Local buckling of the stiffener web
- Mode V: flexural-torsional buckling or "tripping" of the stiffeners

These modes as shown in Figs. 3.2 to 3.6 are neither mutually exclusive nor independent. However, stiffeners with good proportions can prevent the last two buckling modes cited above. Some local bending of the stiffener web could still interact with the other modes in otherwise practical panel dimensions.

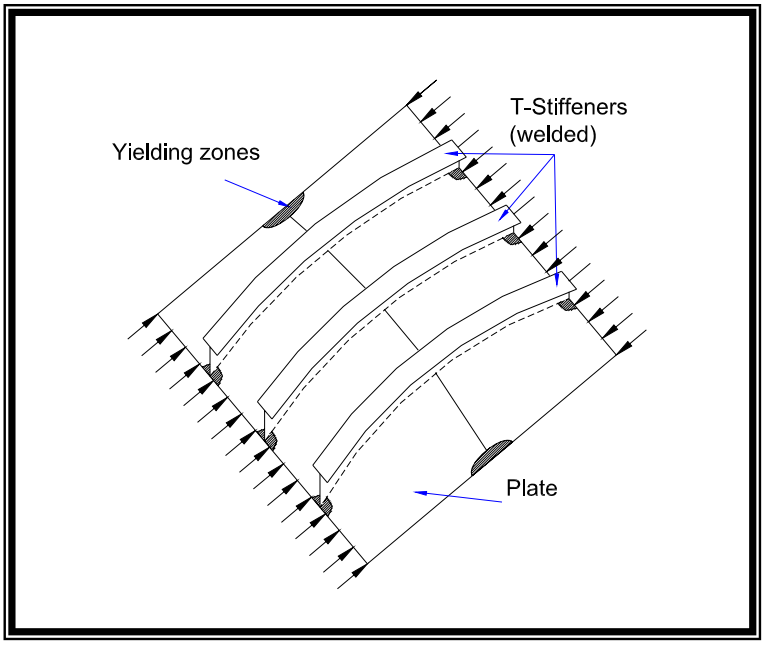

Fig. (3.2): Overall Buckling of the Plating and Stiffeners as a Unit [46]

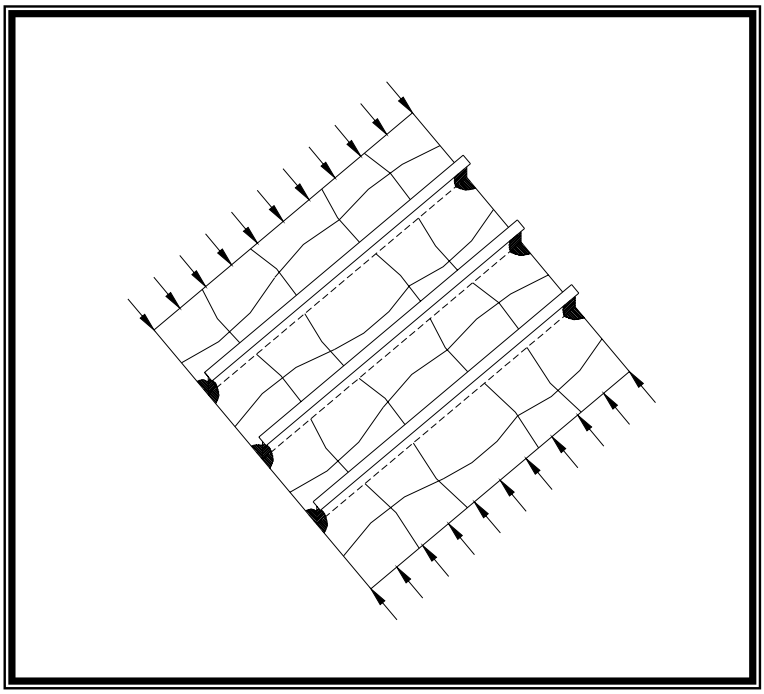

Fig. (3.3): Buckling Due to Predominantly Transverse Compression [46]

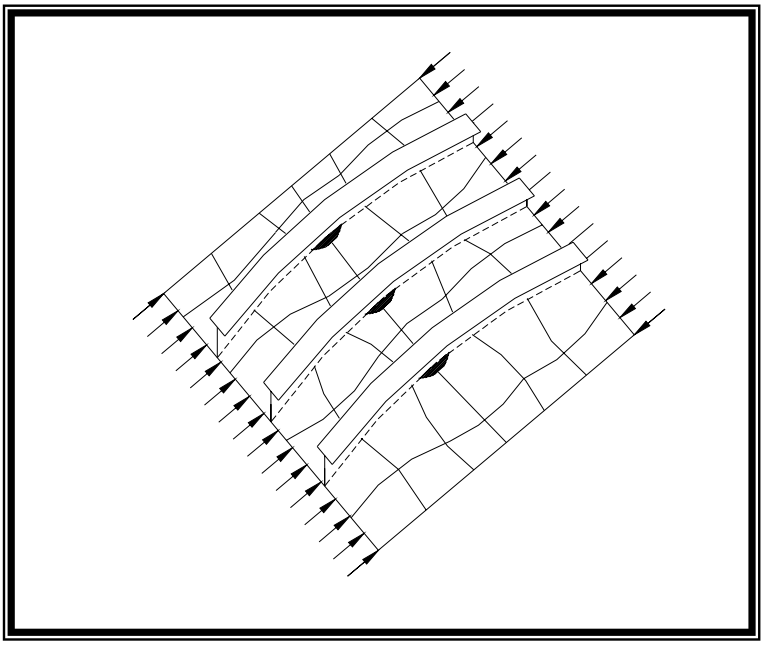

Fig. (3.4): Beam-Column Buckling of the Stiffeners [46]

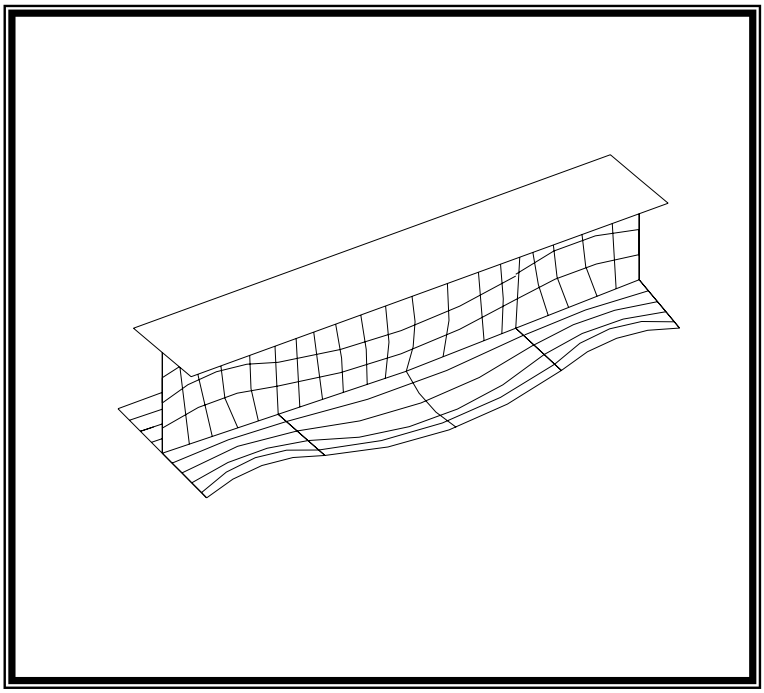

Fig. (3.5): Local Buckling of the Stiffener Web [46]

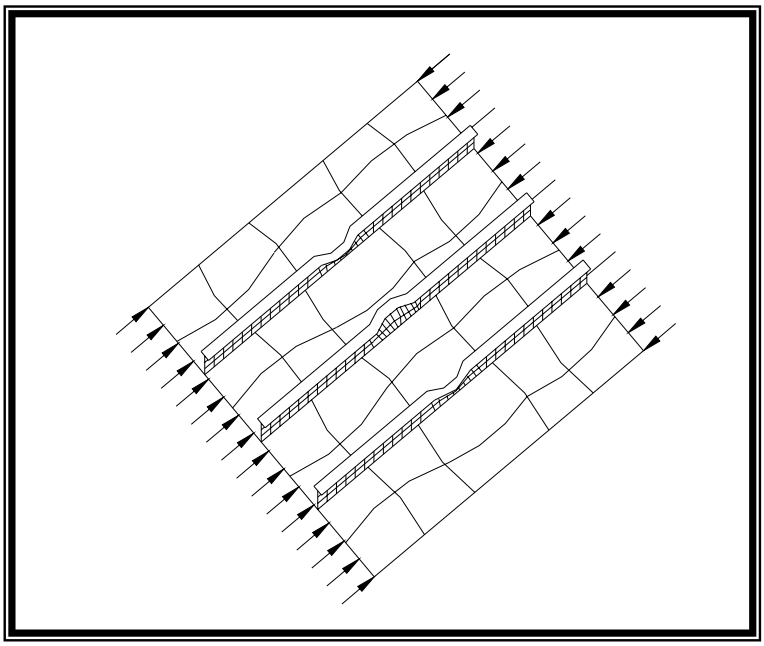

Fig. (3.6): Flexural-Torsional Buckling (Tripping) of the Stiffeners [46]

Figure 3.7 shows a simplified design graph with only two design variables, plate thickness and height of the stiffener web. The axis normal to the page is the weight of the stiffened panel and the contours are those of constant weight per unit width. The figure shows the constraints against local plate buckling and overall panel buckling, and it is evident that the optimum design would be at the junction of these two constraints. Such an optimum panel would have the highest bifurcation buckling stress in its class of panels of equal weight per unit width [7]. This can be explained by arguing that if the plate thickness is increased by taking material from the stiffeners and adding it to the plate, the critical stress for local plate buckling would increase and the critical stress for overall

panel buckling would decrease for most practical combinations of other parameters. Thus, the panel with the highest critical bifurcation buckling stress would have simultaneous buckling modes.

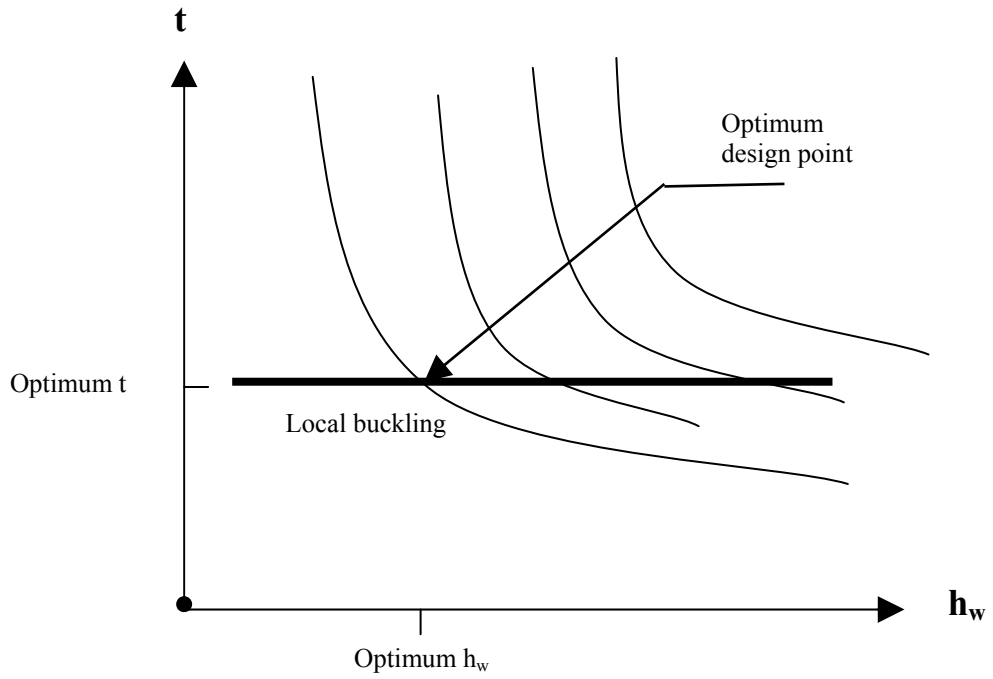

Fig. (3.7): Simplified Design Graph for Optimum Stiffened Panel Design

It is useful to have a structural parameter by which one can determine which mode of buckling would occur first in a given panel. Bleich [9] [1952], introduced the following flexural rigidity ratio which is commonly used for this purpose $\gamma=\frac{E I_X}{Db}$

where E is the young's modulus, I_X is the moment of inertia of a single stiffener with attached plating, D is the flexural rigidity of isotropic plate, and b is the spacing between two adjacent longitudinal stiffeners.

3.2. Local Plate Buckling Stress

The equation for buckling of a simply supported bare plate was derived by Bryan [12] [1891]. In terms of a buckling coefficient *k*, Bryan's equation is:

$$\sigma_{local} = \frac{\Pi^2 D}{b^2 t} k \tag{3-1}$$

The expression for the buckling coefficient *k* depends on the type of boundary support, and for long simply supported plates, it is usually assumed that *k* = 4. In one-bay panels under consideration the bare plating in between the stiffeners is simply supported on the loaded edges and is elastically restrained by the stiffeners along the longitudinal edges. Paik and Thayamballi [46] [2000], obtained an exact solution for the elastic buckling coefficient that allows for the rotational restraint given to the plating by the stiffeners. They also presented a set of more convenient and sufficiently accurate approximate expressions obtained by curve fitting as follows:

$$k = \begin{cases} 4 + 0.396\zeta^3 - 1.974\zeta^2 + 3.565\zeta & for\ 0 \le \zeta \le 2 \\ 6.951 - \dfrac{0.881}{\zeta - 0.4} & for\ 2 \le \zeta \le 20 \\ 7.025 & for\ \zeta \ge 20 \end{cases} \tag{3-2}$$

in which $\zeta = \frac{G J_X}{D b}$ is a non-dimensional parameter involving the St.Venant torsional stiffness J_x of the stiffener. Equation (3.2) is based on the assumption that the stiffeners remain straight until the plating in between them buckles. But if the stiffener web is slender (either tall or thin) then there will be bending of the stiffener web and the stiffeners will not provide the full theoretical rotational restraint along their line of

attachment. Paik and Thayamballi [46] [2000], proposed a correction factor C_L to the original torsional rigidity as follows:

$$\zeta_L = C_L \zeta$$

However, they found that the expression for C_L gave a value of 1.0 for $\zeta < 2$, which is a range within which many practical panels lie. Therefore, an alternative correction factor C_r for web bending is proposed as follows:

$$\zeta_{Cr} = C_r \zeta \tag{3-3}$$

where

$$C_r = \frac{1}{1 + 3.6\left(\frac{t}{t_w}\right)^3 \frac{d}{b}} \tag{3-4}$$

An expression is obtained for local plate buckling which allows not only for rotational restraint by the stiffeners but also for possible web bending in the stiffeners [7]:

$$\sigma_{local} = \frac{\Pi^2 D}{b^2 t} k_{Cr} \tag{3-5}$$

where

$$k_{Cr} = \begin{cases} 4 + 0.396\zeta_{Cr}^{\ 3} - 1.974\zeta_{Cr}^{\ 2} + 3.565\zeta_{Cr} \ for \ 0 \le \zeta_{Cr} \le 2 \\ 6.951 - \dfrac{0.881}{\zeta_{Cr} - 0.4} \ for \ 2 \le \zeta_{Cr} \le 20 \\ 7.025 \ for \ \zeta_{Cr} \ge 20 \end{cases} \tag{3.6}$$

3.3. Overall Panel Buckling Stress

The Euler buckling stress for a column is:

$$\sigma_E = \frac{\pi^2 E}{\left(\frac{a}{\rho}\right)^2} \tag{3-7}$$

As shown by Timoshenko [1936], in a column under axial compressive load there is some transverse shear Q due to the slope; that is $Q = \mathrm{P}\, w'(\mathrm{x})$ as in Fig. 3.8.

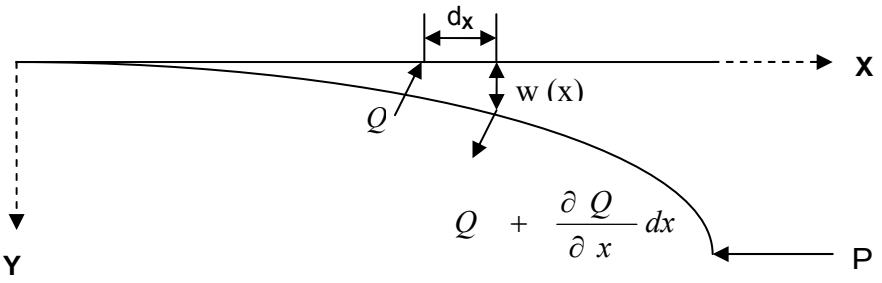

Fig. (3.8): Transverse Shear in an Axially Loaded Column

The resulting shear strain causes an additional deflection, and the effect is to reduce the overall (Euler) buckling stress by the factor $A_W G/(A_W G + A_T \sigma_E)$. For an ordinary column the effect is negligible but for a stiffener-column the web area A_w is a small fraction of the total area A_T and the factor can be significant[7]. Therefore, the corrected overall buckling stress for a stiffener-column is given by:

$$\sigma_{ov} = \sigma_E \left(\frac{A_W G}{A_W G + A_T \sigma_E} \right) \tag{3-8}$$

3.4. The Crossover Parameter γ_{Co}

The structural parameter $\gamma = \frac{E\, I_X}{D\, b}$ is the ratio of the flexural rigidity of a plate-stiffener combination to the flexural rigidity of the plating.

3.4.1. Klitchieff Equation for γ_{Co}

By transformation of a system of equations established by Timoshenko [1936], to determine the critical compressive load of a longitudinally stiffened panel Klitchieff, 1951, derived an expression for γ_{Co} assuming the plating in between the stiffeners to have buckled in one half-sine wave in the transverse direction and ignoring the rotational restraint given by the stiffeners(7). His expression is:

$$\gamma_{Co,K} = (n_s + 1)\left[\frac{4a\lambda}{\pi BC} + \lambda^2\left(\frac{A_S}{Bt}\right)\right] \tag{3-9}$$

where

$$\lambda^2 = 4\left(\frac{a}{b}\right)^2 \tag{3-10}$$

and

$$C = -\frac{1}{\sqrt{\lambda-1}}\frac{SIN\frac{\sqrt{\lambda-1}}{a/b}\pi}{COS\frac{\sqrt{\lambda-1}}{a/b}\pi - COS\frac{\pi}{ns+1}} + \frac{1}{\sqrt{\lambda-1}}\frac{SINH\frac{\sqrt{\lambda+1}}{a/b}\pi}{COSH\frac{\sqrt{\lambda+1}}{a/b}\pi - COS\frac{\pi}{ns+1}} \tag{3-11}$$

3.4.2. Improved Equation for γ_{Co}

Since a crossover panel undergoes simultaneous local and overall buckling [7], an expression can be obtained for γ_{Co} by equating eqs. (3.5) and (3.8):

$$\frac{\pi^2 D}{b^2 t} k_{cr} = \sigma_E \left(\frac{A_W G}{A_W G + AT \sigma_E} \right)$$

Substituting $\sigma_E = \frac{\pi^2 E}{\left(\frac{a}{\rho}\right)^2}$ and $\rho^2 = \frac{I_X}{AT}$

$$\frac{\pi^2 D}{b^2 t} k_{cr} = \frac{\pi^2 E I_X}{a^2 A_T} \left(\frac{A_W G}{A_W G + A_T \sigma_E} \right)$$

from which

$$\gamma_{Co,new} = \frac{E I_X}{D b} = \frac{a^2 A_T}{b^3 t} \left[\frac{k_{cr}}{\left(\frac{A_W G}{A_W G + A_T \sigma_E} \right)} \right] \qquad (3\text{-}12)$$

where *kcr* has been defined earlier.

FINITE ELEMENT FORMULATION

4.1 General

Those concepts behind the Finite Element Method, which are useful in applying the basic theory to the post-buckling analysis of stiffened panels, will be briefly outlined in this chapter. However, no attempt will be made to present in detail the Finite Element Method or the fundamental equations of the nonlinear theory of elasticity. This material can be found in several references[11, 17..ect.].

First, the large deflection problem is intrinsically different from the small deflection problem. This is so, not because large deflections necessarily occur in a literal sense, but rather because stresses exist which, in the presence of certain displacements, exert a significant influence on structural deformations. The beam column problem illustrates this typical, large deflection behavior. The existence of axial loading in the presence of bending displacements does affect the stiffness of the member. In fact, if the loading is compressive and approaches the critical value, the bending stiffness tends towards zero. Consequently, the need for an "initial stress stiffness matrix" becomes evident. Two sources of nonlinearity exist for the large deflection problem. The first is connected with the strain-displacement equations. Even if strains remain small in the conventional sense, rotation of the element adds nonlinear terms to the strain-displacement equations. As will be seen in the derivation of the shell element, if these nonlinear rotational terms are omitted, the derivation becomes incapable of giving the nonlinear

stiffness matrix. The second source of nonlinearity exists with respect to the equilibrium equations. It is necessary to keep the deformed geometry in mind when writing the equilibrium equations. This in turn, causes these equations to become nonlinear. In the Finite Element Method, this is taken into account at the start of each step. In this manner a close approximation to the actual behavior can be maintained. It is therefore seen that the Finite Element method accounts for both sources of nonlinearity in the large deflection problem. Entering into the derivation of the stiffness matrices through the strain-displacement equations is sufficient for stability analyses [22]. By using the stiffness matrices so derived, in conjunction with the incremental step procedure, corrections in the equilibrium equations due to structural deformation can be taken into account. This makes it possible to carry out a detailed analysis of the large deflection problem. In this chapter, a start is made by introducing the variational equations of equilibrium along with the derived element equilibrium equations. Then the stiffness formulation for 4-node, 6-degree-of freedom per node flat shell element is presented. Finally, a short introduction to the frontal solution technique used in this study is presented.

4.2 Variational Equation of Equilibrium

The total potential energy π of a deformed plate with initial deflection of the order of magnitude of the thickness of the plate and with additional bending deflection of the same order, is defined as

$$\Pi = U - W \tag{4.1}$$

where U is the potential energy of deformation and W is the potential of the external loading. The state of equilibrium of a deformed plate can be

characterized as that for which the first variation of the total potential energy of the system is equal to zero, or:

$$\delta\Pi=\delta U-\delta W \tag{4.2}$$

The potential of the external load is:

$$W = \mathrm{P}_i . q_i \tag{4.3}$$

in which the repeated indices imply summation, p_i is the external load, and q_i is the displacement. Thus, if the displacements are defined by a finite number of nodal parameters a, the variation in the potential of the external load is:

$$\delta W = f' da \tag{4.4}$$

where f' is a vector of generalized external forces.

The variation in the potential energy of deformation for a plate element with large deflection can be written as

$$\delta U = \left(\int_V \left[\bar{B}\right]^T \sigma dv \right) da \tag{4.5}$$

where [B] is defined from the strain definition as

$$d\bar{\varepsilon}=\left[\bar{\mathrm{B}}\right] \overline{da} \tag{4.6}$$

The bar suffix has been added as, if displacements are large, the strains depend nonlinearly on displacements, while the matrix [B] depends on $\bar{a}$, conveniently writing $[\bar{B}]$ as:

$$\left[\bar{B}\right]=[B_o]+[B_L(a)] \tag{4.7}$$

in which $[\mathrm{B_o}]$ is the same matrix as in the linear infinitesimal strain analysis and only $[\mathrm{B_L}]$ depends on the displacement. In general $[\mathrm{B_L}]$ is found to be a linear function of the displacements.

Substituting Equations (4.5) and (4.4) into Equation (4.2) to get the equilibrium equations which can be written as:

$$\overline{\Psi}\left(\overline{a}\right)=\int_V \left[\overline{B}\right]^T \overline{\sigma}\, dV - \overline{f} = 0 \tag{4.8}$$

where $\overline{\Psi}$ represents the sum of external and internal generalized forces.

Clearly, solution of Equation (4.8) will have to be approached iteratively. In order to use an incremental solution procedure, the relation between $\mathrm{d}\overline{a}$ and $\mathrm{d}\overline{\Psi}$ must be found. Thus, taking appropriate variation of Equation (4.8) with respect to $\mathrm{d}\overline{a}$, then:

$$d\overline{\Psi}=\int_V d\left[\overline{B}\right]^T \overline{\sigma}\, dV + \int_V \left[\overline{B}\right]^T d\overline{\sigma}\, dV = \left[K_T\right] d\overline{a} \tag{4.9}$$

$[K_T]$ being the total tangential stiffness matrix. If strains are reasonably small, we can write the general elastic relation as:

$$\overline{\sigma} = [D]\,\overline{\varepsilon} \tag{4.10}$$

in which $[D]$ is the usual set of elastic constants. Thus using Equations (4.10) and (4.6), then

$$d\overline{\sigma} = [D]\, d\overline{\varepsilon} = [D][\overline{B}]\, d\overline{a} \tag{4.11}$$

and if (4.7) is valid

$$d\,[\overline{B}] = d\,[B_L] \tag{4.12}$$

therefore

$$d\overline{\Psi}=\int_V d\left[B_L\right]^T \overline{\sigma}\, dV + \left[\overline{K}\right] d\overline{a} \tag{4.13}$$

where

$$[\overline{K}] = \int_V [\overline{B}]^T\, [D][\overline{B}]\, dV = [K_O] + [K_L] \tag{4.14}$$

In this expression $[K_O]$ represents the usual, small displacement stiffness matrix, i.e.

$$[K_O] \;=\; \int_V [B_O]^T\, [D][B_O]\, dV \tag{4.15}$$

The matrix $[K_L]$ is due to large displacements and is given by

$$[K_L] = \int_V \left([B_O]^T [D] [B_L] + [B_L]^T [D] [B_L] + [B_L]^T [D] [B_O] \right) dV \quad (4.16)$$

$[K_L]$ is alternatively known as the initial displacement matrix or large displacement matrix, and it contains only terms that are linear and quadratic in a.

The first term of Equation (4.13) can be written as

$$\int_V d[B_L]^T \bar{\sigma}\, dV = [K_\sigma]\, d\bar{a} \quad (4.17)$$

where $[K_\sigma]$ is a symmetric matrix dependent on the stress level. This matrix is known as initial stress matrix or geometric matrix. Thus,

$$d\bar{\Psi} = ([K_O] + [K_\sigma] + [K_L])\, d\bar{a} = [K_T]\, d\bar{a} \quad (4.18)$$

with $[K_T]$ being the total, tangential stiffness matrix.

In the next section, the tangential stiffness matrix for a (SHELL43) element is derived in terms of the element shape functions and nodal displacements.

4.3 Stiffness Formulation

The nonlinear stiffness formulation for large deflection analysis of stiffened plates is formulated for this typical flat shell finite element (zero initial curvature). The element is shown in Figure (4.1) with six degrees of freedom at each nodal point. These are: two in-plane displacements u and v in the x and y directions, respectively; one transverse deflection w; two rotations $W_{,X}$ and $W_{,Y}$ about y and x axes, respectively, and a generalized twist $W_{,XY}$.

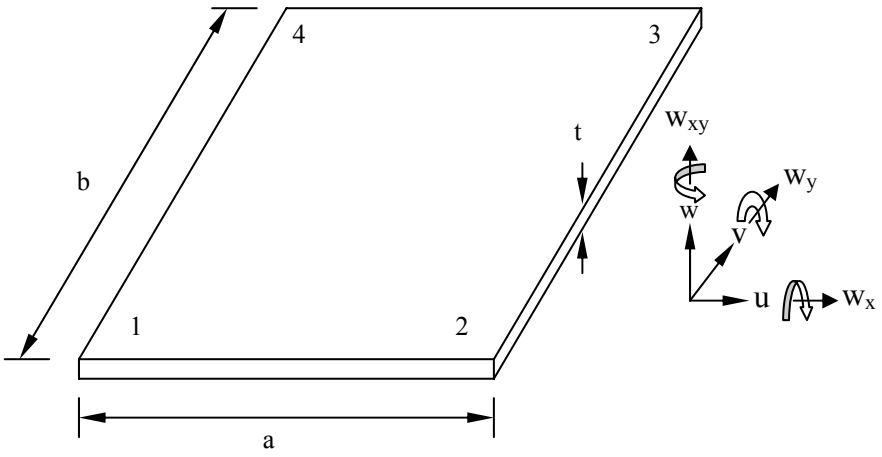

Fig. (4.1): Shell Element Geometry and Nodal Degrees of Freedom

The present element is based on Kirchhoff hypothesis [64] which neglects transverse shear deformation by assuming that straight lines normal to the mid-surface before deformation remain straight and normal to the mid-surface after deformation.

Knowing that the panels in this study have a large width-to-thickness ratio, it is thus clear that the transverse shear deformation effects can be neglected without any significant loss in accuracy. The displacement model used in the formulation is thus given as [64]

$$\begin{aligned} u &= u_o - z\frac{\partial w}{\partial x} \\ v &= v_o - z\frac{\partial w}{\partial y} \\ w &= w_o \end{aligned} \tag{4.19}$$

where u_o , v_o ,w_o are the mid-plane displacements in x, y and z-direction, respectively. Figure (4.2) shows the plate configuration before and after deformation. It is clear from Equations (4.19) that the displacement at any point inside the plate can be expressed in terms of five unknown quantities; u_o , v_o ,w_o , $w_{,x}$, $w_{,Y}$. However, the joint twist derivatives $W_{,XY}$ are adopted as extra degrees of freedom to assure inclusion of the strain due to simple twist.

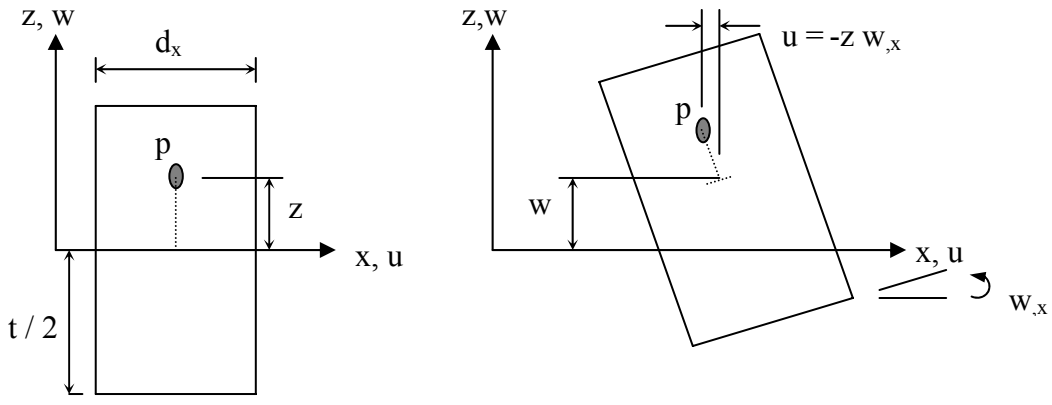

Fig. (4.2): Kirchhoff Deformation Model

4.3.1 Strain-Displacement Relations

The plate strains can be written in terms of the middle surface deflections as [22]

$$\varepsilon_X = \frac{\partial u}{\partial x} + \frac{1}{2}\frac{\partial w}{\partial x}\left(\frac{\partial w}{\partial x}\right) - z\,\frac{\partial^2 w}{\partial x^2}$$

$$\varepsilon_y = \frac{\partial v}{\partial y} + \frac{1}{2}\frac{\partial w}{\partial y}\left(\frac{\partial w}{\partial y}\right) - z\,\frac{\partial^2 w}{\partial y^2} \qquad (4.20)$$

$$\gamma_{xy} = \frac{\partial u}{\partial y} + \frac{\partial v}{\partial x} + \frac{\partial w}{\partial x}\left(\frac{\partial w}{\partial y}\right) + 2\,z\,\frac{\partial^2 w}{\partial x\,\partial y}$$

or in a more compact form

$$\{\varepsilon\} = \begin{Bmatrix} u_{,x} \\ v_{,y} \\ u_{,y} + v_{,x} \end{Bmatrix} + z \begin{Bmatrix} -w_{,xx} \\ -w_{,yy} \\ 2w_{,xy} \end{Bmatrix} + \frac{1}{2}\begin{Bmatrix} w^2{}_{,x} \\ w^2{}_{,y} \\ 2w_{,x}\ w_{,y} \end{Bmatrix} \qquad (4.21a)$$

or

$$\{\varepsilon\} = \{\varepsilon_o{}^{\mathrm{p}}\} + z\ \{\varepsilon_o{}^{b}\} + \{\varepsilon_L{}^{\mathrm{p}}\} \qquad (4.21b)$$

$\{\varepsilon_o{}^{\mathrm{p}}\}$ are the linear strains due to in-plane deformation

$\{\varepsilon_o{}^{b}\}$ are the linear strains due to bending deformation.

$\{\varepsilon_L{}^{\mathrm{p}}\}$ are the nonlinear plane strains due to out-of-plane deformation.

4.3.2 Stress-Strain Relations

Each orthotropic layer of the plate has known elastic constants. The stress-strain relation of any particular layer, with one of the axes of orthotropy coinciding with one of the principal axes, is given by

$$\begin{Bmatrix} \sigma_x \\ \sigma_y \\ \sigma_z \\ \tau_{xy} \\ \tau_{xz} \\ \tau_{yz} \end{Bmatrix} = \begin{bmatrix} C_{11} & C_{12} & C_{13} & C_{14} & 0 & 0 \\ C_{21} & C_{22} & C_{23} & C_{24} & 0 & 0 \\ C_{31} & C_{32} & C_{33} & C_{34} & 0 & 0 \\ C_{41} & C_{42} & C_{43} & C_{44} & 0 & 0 \\ 0 & 0 & 0 & 0 & C_{55} & C_{56} \\ 0 & 0 & 0 & 0 & C_{65} & C_{66} \end{bmatrix} \begin{Bmatrix} \varepsilon_x \\ \varepsilon_y \\ \varepsilon_z \\ \gamma_{xy} \\ \gamma_{xz} \\ \gamma_{yz} \end{Bmatrix} \tag{4.22}$$

Since normal stress σ_z is small, it can be neglected. The corresponding strain ε_z can be eliminated from Equations (4.22) by putting σ_z equal to zero. Also τ_{xz} and τ_{yz} will be omitted from Equations (4.22) since transverse shear effects are not considered in this study. This results in a reduced stress-strain relationship as

$$\begin{Bmatrix} \sigma_x \\ \sigma_y \\ \tau_{xy} \end{Bmatrix} = \begin{bmatrix} C'_{11} & C'_{12} & C'_{13} \\ C'_{21} & C'_{22} & C'_{23} \\ C'_{31} & C'_{32} & C'_{33} \end{bmatrix} \begin{Bmatrix} \varepsilon_x \\ \varepsilon_y \\ \gamma_{xy} \end{Bmatrix} \tag{4.23}$$

where

$$C'_{ij} = C_{ij} - C_{i3}\, C_{j3} / C_{33} \qquad \text{for i ,j = 1,2,3.}$$

For a particular case where fibers are oriented at an angle θ with the x-axis, the transformed stress-strain relation for a lamina will be [22]

$$\begin{Bmatrix} \sigma_x \\ \sigma_y \\ \tau_{xy} \end{Bmatrix} = \begin{bmatrix} Q_{11} & Q_{12} & Q_{13} \\ Q_{21} & Q_{22} & Q_{23} \\ Q_{31} & Q_{32} & Q_{33} \end{bmatrix} \begin{Bmatrix} \varepsilon_x \\ \varepsilon_y \\ \gamma_{xy} \end{Bmatrix} \tag{4.24}$$

where

$$
\begin{aligned}
Q_{11} &= C'_{11}\cos^4\theta + 2\left(C'_{12} + 2C'_{33}\right)\cos^2\theta\sin^2\theta + C'_{22}\sin^4\theta \\
Q_{12} &= \left(C'_{11} + C'_{22} - 4C'_{33}\right)\cos^2\theta\sin^2\theta + C'_{12}\left(\cos^4\theta + \sin^4\theta\right) \\
Q_{22} &= C'_{11}\sin^4\theta + 2\left(C'_{12} + 2C'_{33}\right)\cos^2\theta\sin^2\theta + C'_{22}\cos^4\theta \\
Q_{33} &= \left(C'_{11} + C'_{22} - 2C'_{12} - 2C'_{33}\right)\cos^2\theta\sin^2\theta + C'_{33}\left(\cos^4\theta + \sin^4\theta\right) \\
Q_{13} &= \left(C'_{11} - 2\,C'_{33} - C'_{12}\right)\cos^3\theta\sin\theta + \left(C'_{12} - C'_{22} + 2\,C'_{33}\right)\cos\theta\sin^3\theta \\
Q_{23} &= \left(C'_{11} - 2\,C'_{33} - C'_{12}\right)\cos\theta\sin^3\theta + \left(C'_{12} - C'_{22} + 2\,C'_{33}\right)\cos^3\theta\sin\theta
\end{aligned}
\qquad (4.25)
$$

4.3.3 Stress Resultant-Strain Relation

The linear strain terms in Equation (4.21) will be considered. Combining these strain terms with the laminate constitutive equations given by Equations (4.24) and integrating layer-by-layer over the thickness, one obtains the following relations of stress resultants as

$$
\begin{aligned}
N_x, M_x &= \int_{-t/2}^{t/2} \sigma_x(1, z)\, dz \\
N_y, M_y &= \int_{-t/2}^{t/2} \sigma_y(1, z)\, dz \\
N_{xy}, M_{xy} &= \int_{-t/2}^{t/2} \tau_{xy}(1, z)\, dz
\end{aligned}
\qquad (4.26)
$$

The above equations can be cast in matrix form as

$$\begin{Bmatrix} N_x \\ N_y \\ N_{xy} \\ M_x \\ M_y \\ M_{xy} \end{Bmatrix} = \begin{bmatrix} A_{11} & A_{12} & A_{13} & B_{11} & B_{12} & B_{13} \\ & A_{22} & A_{23} & B_{21} & B_{22} & B_{23} \\ & & A_{33} & B_{31} & B_{32} & B_{33} \\ & & & D_{11} & D_{12} & D_{13} \\ & sym & & & D_{22} & D_{23} \\ & & & & & D_{33} \end{bmatrix} \begin{Bmatrix} \varepsilon^o_x \\ \varepsilon^o_y \\ \gamma^o_{xy} \\ k_x \\ k_y \\ k_{xy} \end{Bmatrix} \tag{4.27}$$

where k_x, k_y, k_{xy} are the linear strains due to bending deformation.Or in compact notation

$$\{N\} = [D]\{\varepsilon^o\} \tag{4.28}$$

Elements of membrane stiffness matrix [A], membrane-bending coupling matrix [B], bending stiffness matrix [D] are

$$(A_{ij}, B_{ij}, D_{ij}) = \int_{-t/2}^{t/2} Q_{ij}\,(1, z, z^2)\,dz \tag{4.29}$$

4.3.4 Finite Element Formulation

Based on the theory just exposed, a finite element is developed using a bilinear isoparametric rectangular element. Each node of the element has six degrees of freedom given as

$\{ u , v , w , w_x , w_y , w_{xy} \}$

Within the element, displacements can be interpolated in terms of the nodal degrees of freedom by adopting:

a) Bilinear interpolation functions for the in-plane displacements u and v given by

$$u = \sum_i N_i\, u_i \qquad and \qquad v = \sum_i N_i\, v_i \qquad (i=1,..,4)$$

where u and v are the displacements in the x and y-directions, respectively, at any point in the element and u_i , v_i are their values at node i of that particular element. N_i is the interpolation function, which in the local coordinate system shown in Figure (4.3) is

$N_i = (1+ r\, r_i)\,(1+ s\, s_i)\,/4$ (4.30)

where i is the function number and r_i = -1,1,1,-1; s_i =-1,-1,1,1 for i=1,..,4 respectively.

b) The transverse displacement w is interpolated using Hermite Cubic interpolation functions, which can be given in explicit form [22]:

$$w(x,y)=\begin{bmatrix} f_1 & g_1 & h_1 & k_1 & \cdots & \cdots & f_4 & g_4 & h_4 & k_4 \end{bmatrix} \begin{Bmatrix} w_1 \\ w_{,x1} \\ w_{,y1} \\ w_{,xy1} \\ \vdots \\ \vdots \\ w_4 \\ w_{,x4} \\ w_{,y4} \\ w_{,xy4} \end{Bmatrix} \quad (4.31a)$$

where for i=1,..,4 :

$$f_i = \frac{1}{16}(r + r_i)^2\,(r\, r_i - 2)\,(s + s_i)^2\,(s\, s_i - 2)$$

$$g_i = \frac{-a}{32} r_i\,(r + r_i)^2\,(r\, r_i - 1)\,(s + s_i)^2\,(s\, s_i - 2) \quad (4.31b)$$

$$h_i = \frac{-b}{32}(r + r_i)^2\,(r\, r_i - 2)\, s_i\,(s + s_i)^2\,(s\, s_i - 1)$$

$$k_i = \frac{a\, b}{64} r_i\,(r + r_i)^2\,(r\, r_i - 1)\, s_i\,(s + s_i)^2\,(s\, s_i - 1)$$

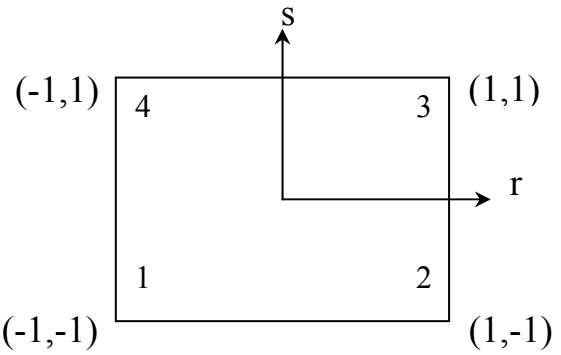

Fig. (4.3): Element Local Coordinate System and Node Numbering

Thus, one can express the displacement in terms of nodal degrees of freedom and using the previously defined shape functions. For instance,

$$\begin{Bmatrix} u \\ v \\ w \end{Bmatrix} = [N]\bar{a}^e \tag{4.32}$$

where $\bar{a}^e$ is the element nodal displacement vector and [N] is the matrix of shape functions. For convenience, the element nodal displacement vector $\bar{a}^e$ will be divided into those which influence in-plane and those which influence bending deformation respectively.

$$\bar{a}_i^e = \begin{Bmatrix} \bar{a}_i^p \\ \bar{a}_i^b \end{Bmatrix} \quad with \quad \bar{a}_i^p = \begin{Bmatrix} u_i \\ v_i \end{Bmatrix} \quad and \quad \bar{a}_i^b = \begin{Bmatrix} w_i \\ \dfrac{\partial w}{\partial x_i} \\ \dfrac{\partial w}{\partial y_i} \\ \dfrac{\partial^2 w}{\partial x_i \partial y_i} \end{Bmatrix} \tag{4.33}$$

Thus the shape functions can also be subdivided as

$$[N_i] = \begin{bmatrix} N_i^p & \\ & N_i^b \end{bmatrix} \tag{4.34}$$

4.3.5 Evaluation of the Linear Stiffness Matrix $[K_o]$

Substituting Equations (4.30) and (4.31) into the linear strain components of Equation (4.21), then

$$\begin{Bmatrix} \varepsilon_x^o \\ \varepsilon_y^o \\ \gamma_{xy}^o \\ k_x \\ k_y \\ k_{xy} \end{Bmatrix} = \begin{bmatrix} N_{1,x} & 0 & N_{2,x} & 0 & N_{3,x} & 0 & N_{4,x} & 0 & & & & & & & & & & & & \\ & N_{1,y} & & N_{2,y} & & N_{3,y} & & N_{4,y} & & & & & & 0 & & & & & & \\ N_{1,y} & N_{1,x} & N_{2,y} & N_{2,x} & N_{3,y} & N_{3,x} & N_{4,y} & N_{4,x} & & & & & & & & & & & & \\ & & & & & & & & -f_{1,xx} & -g_{1,xx} & -h_{1,xx} & -k_{1,xx} & \cdots & \cdots & -k_{4,xx} \\ & & & 0 & & & & & -f_{1,yy} & -g_{1,yy} & -h_{1,yy} & -k_{1,yy} & \cdots & \cdots & -k_{4,yy} \\ & & & & & & & & 2f_{1,xy} & 2g_{1,xy} & 2h_{1,xy} & 2k_{1,xy} & \cdots & \cdots & 2k_{4,xy} \end{bmatrix} \begin{Bmatrix} u_1 \\ v_1 \\ \vdots \\ \vdots \\ v_4 \\ w_1 \\ w_{,x1} \\ w_{,y1} \\ w_{,xy1} \\ \vdots \\ \vdots \\ w_{,xy4} \end{Bmatrix}$$

……(4.35)

In a short form:

$$\{\varepsilon^o\} = [B_O]\{\bar{a}^e\} \tag{4.36}$$

Internal strain energy (due to linear strains only) can now be determined by integrating the products of strains and stress resultants over the area of the element, i.e.

$$\pi = \frac{1}{2}\int_A \{\varepsilon\}^T \{N\}\, dA \tag{4.37}$$

where $\{\varepsilon\}$ includes all linear strains and $\{N\}$ is the vector of stress resultants defined in Equations (4.27). Substituting Equations (4.28) and (4.36) for $\{\varepsilon\}$ and $\{N\}$ into (4.37) we get

$$\pi = \frac{1}{2}\int_A \{\bar{a}^e\}[B_0]^T [D][B_O]\{\bar{a}^e\}\, dA \tag{4.38}$$

In a concise form:

$$\pi = \frac{1}{2} \left\{ \bar{a}^{e} \right\}^{T} \left[K_0 \right] \left\{ \bar{a}^{e} \right\} \tag{4.39}$$

where

$$\left[K_O \right] = \int_A \left[B_0 \right]^T \left[D \right] \left[B_O \right] \, dA \tag{4.40}$$

is the linear stiffness matrix for the element.

4.3.6 Evaluation of the Large Displacement Matrix $\left[K_L \right]$

In order to be able to evaluate the element large displacement stiffness matrix $\left[K_L \right]$, it will be necessary to establish an expression for $\left[\bar{B} \right]$. First, it is noted that

$$\left[\bar{B} \right] = \left[B_o \right] + \left[B_L \right] \tag{4.41}$$

where

$$\left[B_o \right] = \begin{bmatrix} B_{\mathrm{o}}^{\mathrm{p}} & 0 \\ 0 & B_{\mathrm{o}}^{\mathrm{b}} \end{bmatrix} \quad and \quad \left[B_L \right] = \begin{bmatrix} 0 & B_{\mathrm{L}}^{\mathrm{b}} \\ 0 & 0 \end{bmatrix}$$

where $\left[B_o \right]$ is defined in Equation (4.36) and $[\, B_{\mathrm{L}}^{\mathrm{b}} \,]$ is found by taking the variation of the nonlinear strain components $\left\{ \varepsilon_L^{\mathrm{p}} . \right\}$with respect to the parameters $\left\{ \bar{a}^{b} \right\}$. This nonlinear strain component of Equation (4.21) can be written in a more convenient form as:

$$\left\{\varepsilon_L^{\,\mathrm{p}}\right\}=\begin{Bmatrix}\frac{1}{2}\left(\frac{\partial w}{\partial x}\right)^2\\ \frac{1}{2}\left(\frac{\partial w}{\partial y}\right)^2\\ \left(\frac{\partial w}{\partial x}\right)\left(\frac{\partial w}{\partial y}\right)\end{Bmatrix}=\frac{1}{2}\begin{bmatrix}\frac{\partial w}{\partial x} & 0\\ 0 & \frac{\partial w}{\partial y}\\ \frac{\partial w}{\partial y} & \frac{\partial w}{\partial x}\end{bmatrix}\begin{Bmatrix}\frac{\partial w}{\partial x}\\ \frac{\partial w}{\partial y}\end{Bmatrix}=\frac{1}{2}[A]\{\theta\} \tag{4.42}$$

The derivatives (slopes) of w can be related to the nodal parameters $\{\bar{a}^b\}$ as

$$\{\theta\}=\begin{Bmatrix}\frac{\partial w}{\partial x}\\ \\ \frac{\partial w}{\partial x}\end{Bmatrix}=[G]\left\{\bar{a}^{\,b}\right\} \tag{4.43}$$

in which we have

$$[G]=\begin{bmatrix}f_{1,x} & g_{1,x} & h_{1,x} & k_{1,x} & \cdots & \cdots & k_{4,x}\\ f_{1,y} & g_{1,y} & h_{1,y} & k_{1,y} & \cdots & \cdots & k_{4,y}\end{bmatrix} \tag{4.44}$$

Taking the variation of Equation (4.42), then

$$d\left\{\varepsilon_{\mathrm{L}}^{\mathrm{p}}\right\}=\frac{1}{2}d[A]\{\theta\}+\frac{1}{2}[A]d\{\theta\}=[A]d\{\theta\}=[A][G]d\left\{\bar{a}^{\,b}\right\} \tag{4.45}$$

and hence immediately, by definition:

$$\left[B_L^b\right]=[A][G] \tag{4.46}$$

The nonlinear stiffness matrix $[K_L]$ as defined in Equation (4.16) can now be calculated as:

$$[K_L] = \int_A \left([B_O]^T [D] [B_L] + [B_L]^T [D] [B_L] + [B_L]^T [D] [B_O] \right) dA \tag{4.47}$$

4.3.7 Evaluation of the Linear Stress Stiffness Matrix $[K_\sigma]$

Finally, the linear stress stiffness matrix has to be found using the definition of Equation (4.17). By taking the variation of Equation (4.41), then:

$$d[B_L]^T = \begin{bmatrix} 0 & 0 \\ d[B_L^b]^T & \end{bmatrix} \tag{4.48}$$

which on substitution into Equations (4.17) and (4.46) gives

$$[K_\sigma] d\bar{a} = \int_A \begin{bmatrix} 0 & 0 \\ [G]^T d[A]^T & 0 \end{bmatrix} \begin{Bmatrix} N_x \\ N_y \\ N_{xy} \\ M_x \\ M_y \\ M_{xy} \end{Bmatrix} dA \tag{4.49}$$

However, using the mathematical properties of the matrix [A], then [64]:

$$d[A]^T \begin{Bmatrix} N_x \\ N_y \\ N_{xy} \end{Bmatrix} = \begin{bmatrix} N_x & N_{xy} \\ N_{xy} & N_y \end{bmatrix} [G] d\bar{a}^b$$

and finally

$$[K_\sigma] = \begin{bmatrix} 0 & 0 \\ 0 & [K_\sigma^b] \end{bmatrix} \tag{4.50}$$

with

$$[K_\sigma^b] = \int_A [G]^T \begin{bmatrix} N_x & N_{xy} \\ N_{xy} & N_y \end{bmatrix} [G] dA \tag{4.51}$$

Recall that the stress resultants are defined in terms of the element strains and thus in terms of the element displacements and shape functions through Equations (4.27) and (4.21).

4.4 The Frontal Equation Solution Technique

At any load step (i) during the incremental solution of the nonlinear problem, it is required to solve a system of linear equations in the nodal degrees of freedom in the form

$$\left[K_T^{i-1}\right]\Delta\overline{u}^{\,i} = \Delta\overline{f}^{\,i} \tag{4.52}$$

where $\left[K_T^{i-1}\right]$ is the tangent stiffness matrix evaluated at the previous load step, $\Delta\overline{f}^{\,i}$ is the load increment and $\Delta\overline{u}^{\,i}$ is the resulting displacement increment. The method adopted to solve this system of equations is a major factor influencing the efficiency of the ANSYS finite element program. In this study a direct elimination process will be employed and in particular the frontal method of equation assembly and reduction.

The frontal method can be considered as a particular technique for first assembling the finite elements stiffnesses and nodal forces into a global stiffness matrix and load vector and then solving for the unknown displacements by means of Gaussian elimination and back substitution process. It is designed to minimize core storage requirements, and the number of arithmetic operations.

No attempt will be made here to give a full detailed description of the frontal technique. Such detailed presentation can be found in ref.[5]. The frontal technique as described in this study is applicable only to the solution of symmetric systems of linear stiffness equations. The tangent stiffness matrix which has been derived previously from a variational principle is symmetric by definition. Furthermore, even though the

problem is nonlinear by nature, an incremental approach is used where the system is transformed into a series of linearized systems of equations at each load increment. This enables the use of the frontal technique at each load step.

The main idea of the frontal solver solution is to assemble the equations and eliminate the variables at the same time. As soon as the coefficients of an equation are completely assembled from the contributions of all relevant elements, the corresponding variable can be eliminated. Therefore, the complete structural stiffness matrix is never formed as such, since after elimination the reduced equation is immediately transferred to back-up disc storage.

The core contains, at any given instant, the upper triangular part of a square matrix containing the equations which are being formed at that particular time. These equations, their corresponding nodes and degrees of freedom are termed the front. The number of unknowns in the front is the frontwidth; this length generally changes continually during the assembly/reduction process. The maximum size of the problem that can be solved is governed by the maximum frontwidth. The equations, nodes and degrees of freedom belonging to the front are termed active; those which are yet to be considered are inactive; those which have passed through the front and have been eliminated are said to be deactivated.

During the assembly/elimination process the elements are considered each in turn according to a prescribed order. Whenever a new element is called in, its stiffness coefficients are read from a file and summed either into existing equations, if the nodes are already active, or into new equations, which have to be included in the front if the nodes are being activated for the first time. If some nodes are appearing for the last time, the corresponding equations can be eliminated and stored away in a file

and are thus deactivated. In so doing they free the space in the front which can be employed during assembly of the next element [5].

APPLICATION AND DISCUSSIONS OF RESULTS

5.1 General

To study the effect of different parameters such as: slenderness ratio, aspect ratio, number of stiffeners and stiffener's height on buckling and post-buckling behavior of stiffened plates, several plates are analyzed using the Finite Element Method expounded in this study.

The analysis is made into two stages:

- Studying the eigen-value buckling analysis with various aspect ratios, slenderness ratios and different values of stiffener's height.
- Studying the post-buckling behavior of the plates under in-plane compressive load with various aspect ratios, number of stiffeners, stiffener's height, and slenderness ratio.

Non-dimensional relationships of load-deflection are given to show the post-buckling behavior of these plates.

The results obtained are compared with the available analytical and numerical techniques.

5.2-Eigen-Value Buckling

For eigen-value buckling analysis, a series of 3-bay panels with three or five equally spaced longitudinal T-stiffeners was modeled and analyzed using ANSYS (V5.4). A 3-stiffener model is shown in Fig. (5.1). The stiffened panel is discretized into a sufficient number of elements to allow

for free development of the buckling modes. The use of four-node shell elements (SHELL43) allows for finite rotations and membrane strains. Uniaxial compressive load is applied on both the left and right hand sides of the model.

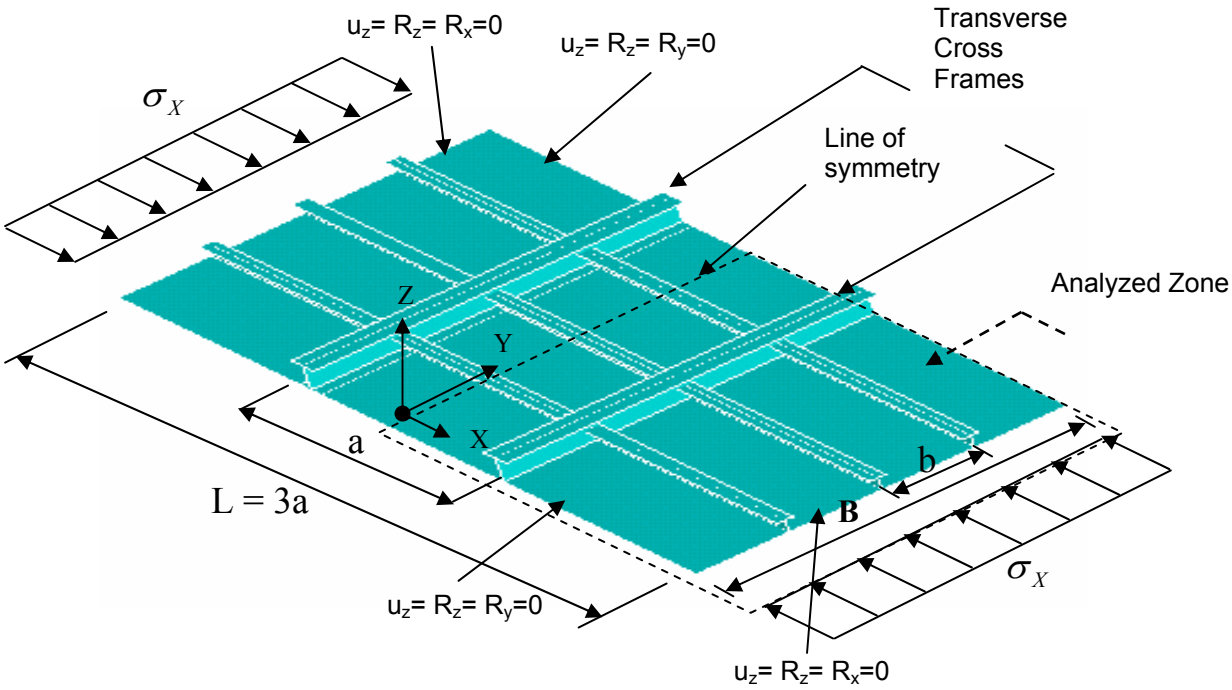

Fig. (5.1.a): Typical 3-Stiffener Model

5.2.1 Comparison with Other Studies

Tables 5.1 and 5.2 list the scantlings of the crossover panels with 3 stiffeners and 5 stiffeners respectively. All the panels are within practical proportions from a design point of view. The width B as shown in Fig. 5.1 is 3600 mm for all panels. In Tables 5.1and 5.2 the ANSYS eigen-values corresponding to local and overall buckling modes are recorded as one critical buckling stress value. The local and overall buckling stresses calculated using eq. (3.5) and eq. (3.8) is normalized by σ_{cr}. and the mean for the 50 panels presented in these tables is 0.926 and 0.913 respectively and between the present study and **Biswarup**[7] [2003] the mean is 0.959 .

Table (5.1): Comparison of Elastic Buckling Stresses (3-Stiffener Model)

a (mm)	t (mm)	h_w (mm)	t_w (mm)	b_f (mm)	t_f (mm)	*Analytical Results (MPa)*		*Biswarup Ref (7) (MPa)*	*Present Study (MPa)*
						σ_{local}	$\sigma_{ov.}$	$\sigma_{cr.}$	$\sigma_{cr.}$
1800	21	50	20	200	30	511.2	547.8	494	541.4
1800	21	84	12	100	15	409.6	455.1	428	456.5
1800	21	50	10	200	30	445.8	470.7	445	430
1800	16	36	20	200	30	350.2	395.5	367	400.1
1800	16	56	12	100	15	245.2	276.5	257	280.6
1800	16	81	5	60	10	235.4	231.7	239	289.6
1800	16	31	10	200	30	318.9	297.7	276	300.6
1800	10	28	12	100	15	111.1	125.6	109	111.1
1800	10	41	5	60	10	93.4	100.3	96	107.9
2640	21	80	20	200	30	506.5	524.6	502	564.3
2640	21	123	12	100	15	409.2	433.4	432	505.8
2640	21	75	10	200	30	438.4	440.3	442	521.2
2640	16	58	20	200	30	349.7	359.3	365	435.6
2640	16	84	12	100	15	244.8	259.4	262	310.9
2640	16	53	10	200	30	309.4	300.6	308	370.7
2640	10	45	12	100	15	111.7	118.5	112	124.4
2640	10	62	5	60	10	93.1	95.8	97	115.4
3600	21	112	20	200	30	502.2	490.3	501	601.4
3600	21	166	12	100	15	408.9	420.5	432	521.4
3600	21	106	10	200	30	432.3	428.5	440	530.7
3600	16	83	20	200	30	349.3	333.7	369	479.3
3600	16	120	12	100	15	244.4	268.7	266	309.3
3600	16	76	10	200	30	301.5	285.2	299	368.2
3600	10	65	12	100	15	112.4	116.9	115	132.9
3600	10	86	5	60	10	93.0	94.9	97	116.5

Table (5.2): Comparison of Elastic Buckling Stresses (5-Stiffener Model)

a (mm)	t (mm)	h_w (mm)	t_w (mm)	b_f (mm)	t_f (mm)	*Analytical Results (MPa)*		*Biswarup Ref (7) (MPa)*	*Present Study (MPa)*
						σ_{local}	$\sigma_{ov.}$	$\sigma_{cr.}$	$\sigma_{cr.}$
1800	21	84	20	200	30	1186.8	1271.7	1248	1265.1
1800	21	116	12	100	15	921.7	1031.6	1012	1027.1
1800	21	93	10	160	20	930.4	1012.5	1005	1014.0
1800	21	77	10	200	30	990.4	982.5	1017	1005.0
1800	16	60	20	200	30	817.8	840.7	813	832.15
1800	16	82	12	100	15	555.2	663.7	653	663.65
1800	16	54	10	200	30	715.1	660.8	666	668.7
1800	10	31	20	200	30	351.5	375.2	359	372.4
1800	10	45	12	100	15	265.8	312.7	308	315.65
2640	10	56	5	60	10	210.1	110.3	229	174.95
2640	21	126	20	200	30	1166.8	1191.2	1229	1215.4
2640	21	168	12	100	15	920.6	998.2	1001	1004.9
2640	21	136	10	160	20	926.2	973.4	989	986.5
2640	21	116	10	200	30	972.4	978.8	1000	994.7
2640	16	93	20	200	30	815.3	784.1	804	799.4
2640	16	120	12	100	15	553.4	625.4	641	638.5
2640	16	82	10	200	30	689.4	625.1	642	638.9
3600	10	52	20	200	30	351.6	189.9	358	279.3
3600	10	68	12	100	15	267.0	157.8	311	239.7
3600	10	84	5	60	10	209.4	123.9	230	182.3
3600	21	174	20	200	30	1149.1	1126.8	1197	1167.2
3600	21	223	12	100	15	919.8	952.0	984	973.3
3600	21	185	10	160	20	923.4	942.4	975	964
3600	21	159	10	200	30	960.3	946.9	988	972.8
3600	16	131	20	200	30	812.6	742.4	791	772

5.3-Post-Buckling Analysis

In order to study the effect of slenderness ratio, aspect ratio, size and number of stiffeners on the geometric nonlinear behavior of plates under compressive load, several plates are analyzed.

5.3.1 Mesh Effect

The rate of convergence of this type of analysis depends mainly on the mesh size. The mesh effect has been investigated for a 3-stiffener model . Table (5-3) gives a measure of convergence as a function of mesh size. It can be seen that (735-element) mesh for this problem gives accurate and economic solution.

Fig. (5.1.b): Finite Element Mesh

Table (5.3) : Finite Element Solution for A Simply Supported Rectangular Plate with Three Stiffeners Under Applied In-Plane Stress of 0.8 Yield Stress.

No.of Elements in Mesh	Maximum Deflection (mm)
39	3.009
102	4.167
294	4.904
621	5.254
735	5.602
855	5.676

5.3.2 Comparison with Available Results

The accuracy of the present study in the analysis of practical panels is compared with the finite element results obtained by **Biswarup**[7] [2003] on simply supported panels. The properties of the panels are as follows: width of the panels B =3600 mm, E=205800 MPa, υ = 0.3, and yield stress σ_y = 352.8 MPa. Good agreement is obtained with 2% difference in load and clear difference in deflection due to a very small initial imperfection used by **Biswarup**[7] [2003] while the present analysis was started without applying any initial imperfection.

5.3.2.1 Comparison for 3-Stiffener Model

Figures (5.2) and (5.3) show the load-shortening curve and the distribution of Von-Mises stresses on the deflected shape of plates under uniform compressive load.The results of the present study are compared with the results obtained by **Biswarup**[7] .

5.3.2.2 Comparison for 5-Stiffener Model

Figures (5.4) and (5.5) show the load-shortening curve and the distribution of Von-Mises stresses on the deflected shape of plates under uniform compressive load. The results of the present study are compared with the results of **Biswarup**[7] .

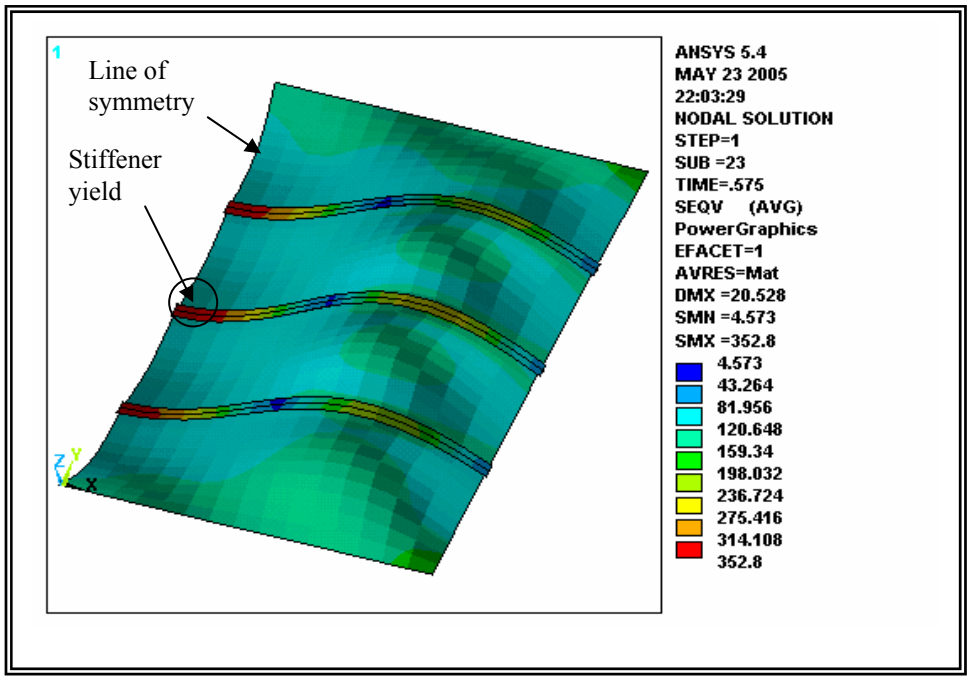

Von-Mises Stress Distribution

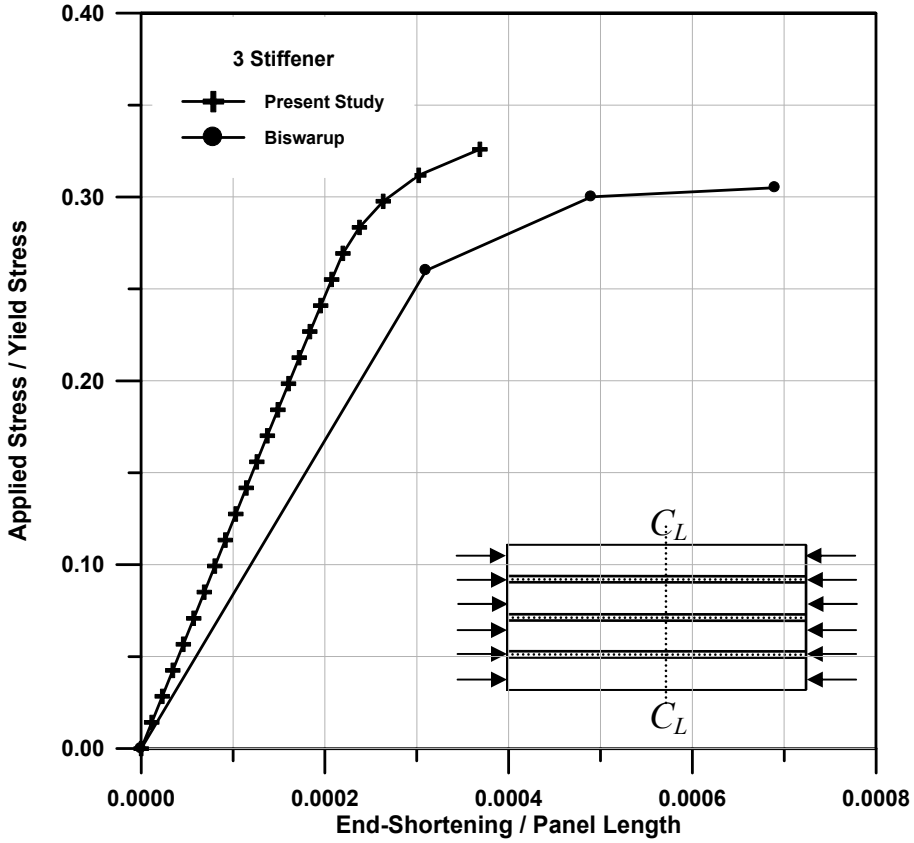

Fig. (5.2): Load-Shortening Curve (B/L=0.667, t=10, h_w=28, t_w=12, b_f=100, and t_f=15)

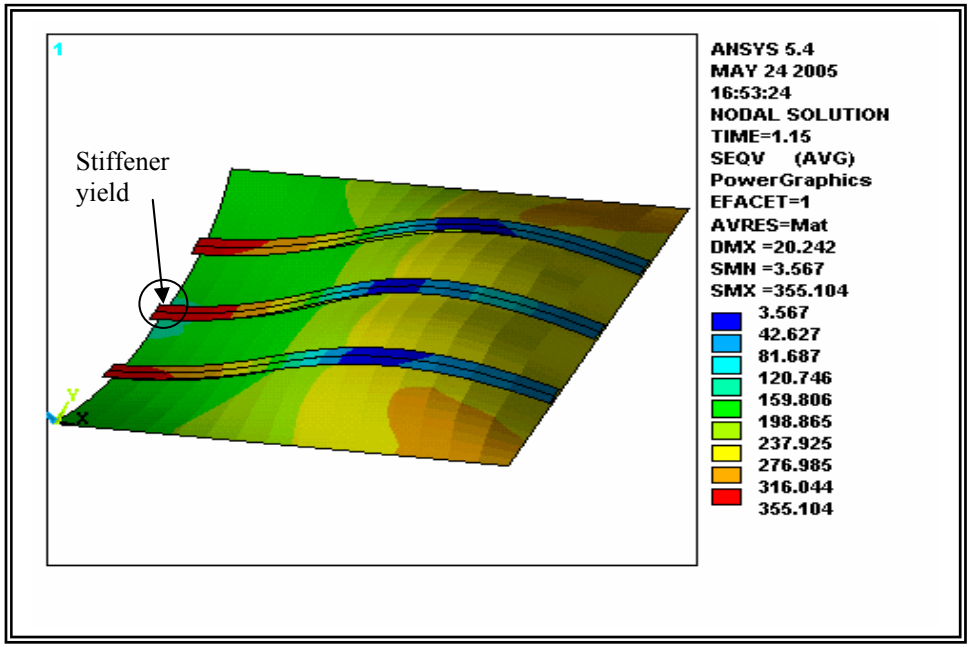

Von-Mises Stress Distribution

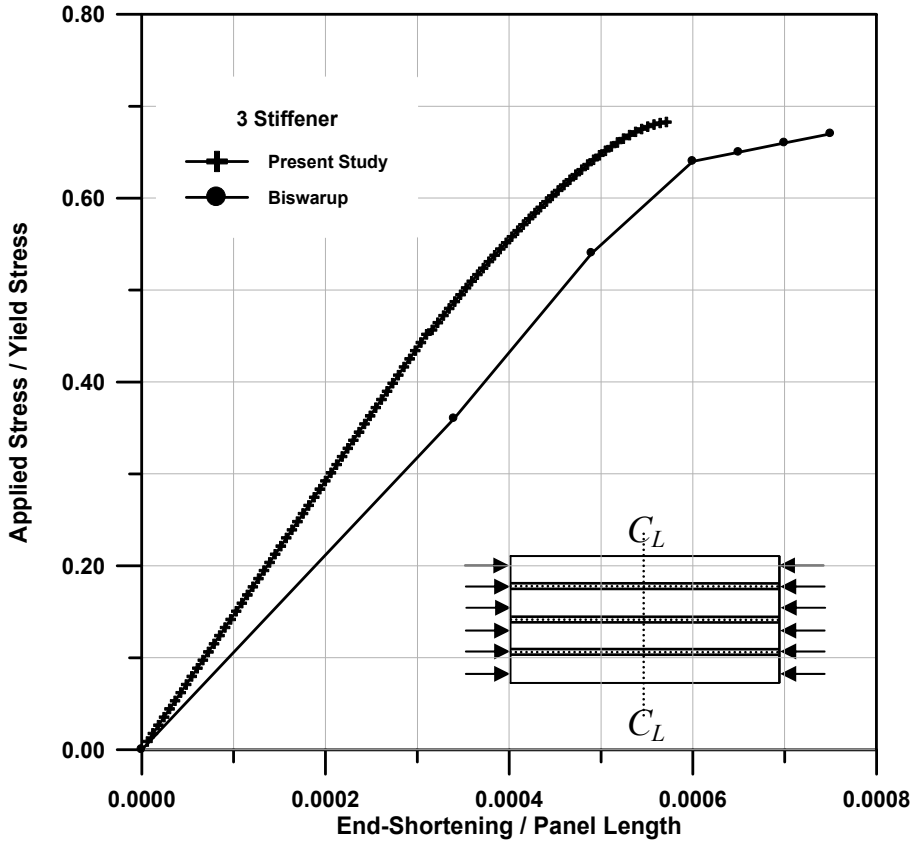

Fig. (5.3): Load-Shortening Curve (B/L=0.333, t=16, h_w=83, t_w=20, b_f=200, and t_f=30)

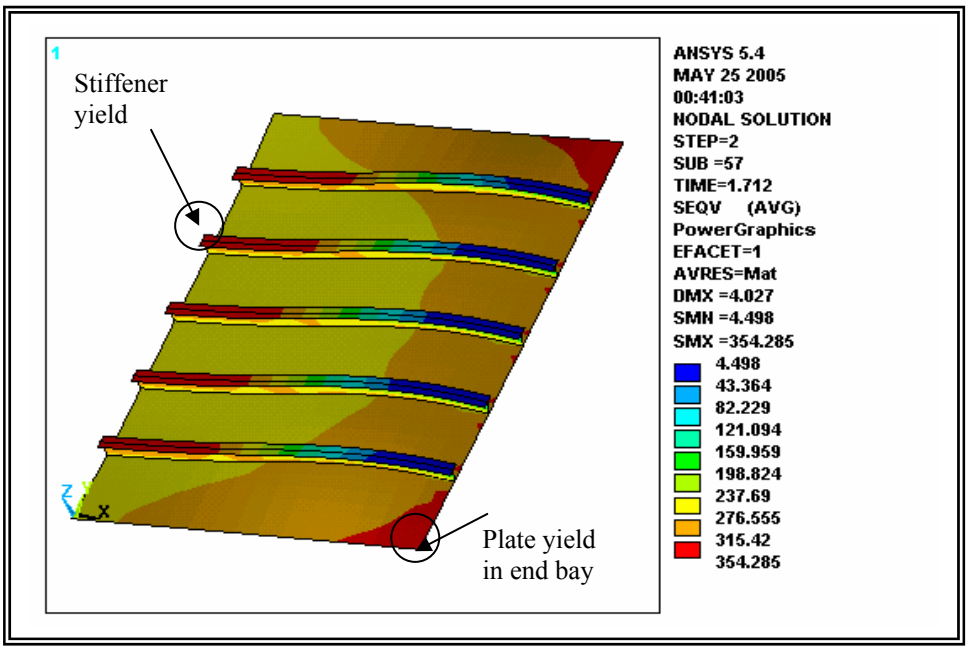

Von-Mises Stress Distribution

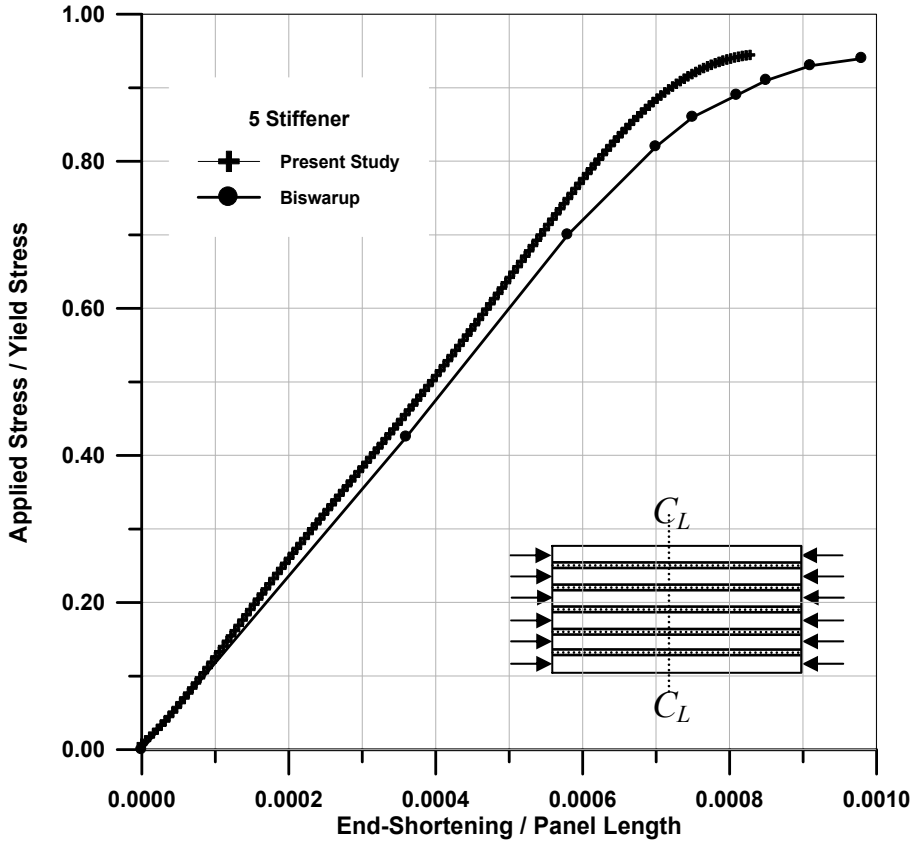

Fig. (5.4): Load-Shortening Curve (B/L=0.667, t=21, h_w=116, t_w=12, b_f=100, and t_f=15)

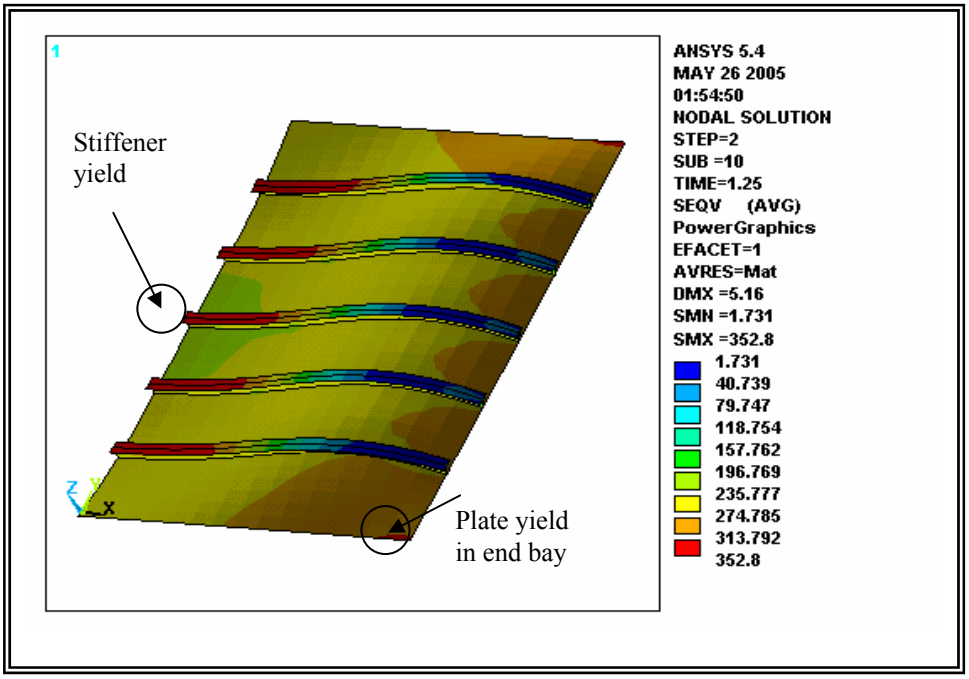

Von-Mises Stress Distribution

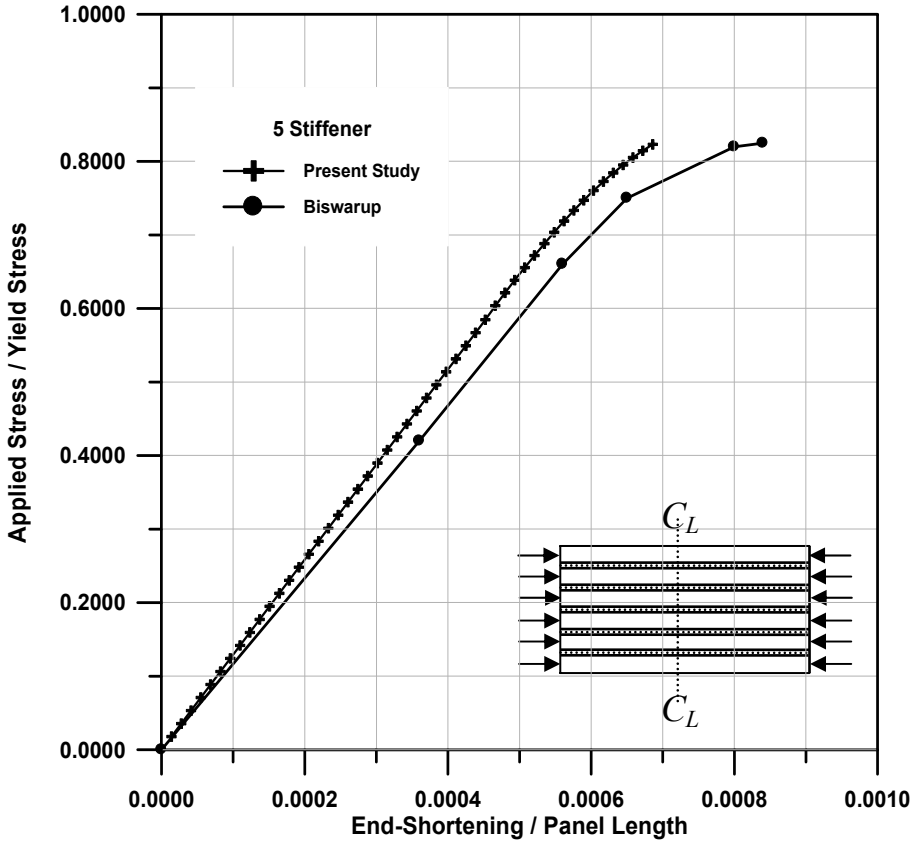

Fig. (5.5): Load-Shortening Curve (B/L=0.667, t=16, h_w=82, t_w=12, b_f=100, and t_f=15)

5.4 - Parametric Study

The effect of aspect ratio, number of stiffeners, slenderness ratio, and plate thickness to stiffener's height ratio(t/h_w) on the post-buckling behavior are considered. Four plates are selected to study the effect of aspect ratio and number of stiffeners, first having (t/h_w)=0.42 which represents a stocky plate, the last plate represents as a slender plate (t/h_w)=0.12 and the other between them (t/h_w=0.30 and 0.22).

5.4.1 Plate Dimensions and Properties

The plate width B is taken as [B=3600 mm] and the length is varied to give a different aspect ratio (B/L) of (1.5, 1.0, 0.667, 0.5). The effect of aspect ratio will be discussed in section (5.4.5). Different numbers of stiffeners were selected with and without edge stiffeners and different plate thickness were selected to give (t/h_w) ratios of (0.42, 0.3, 0.22, 0.12) so that a range from the stocky plate to slender plate was considered. The plate was loaded by the imposition of an in-plane compressive load.

5.4.2 Material Properties

In this study the idealized 'elastic-perfectly plastic' stress-strain curve as shown in Fig.5.6 was adopted .

Material : steel

Young's modulus : 205800 MPa

Poisson's ratio : 0.3

Yield stress : 352.8 MPa

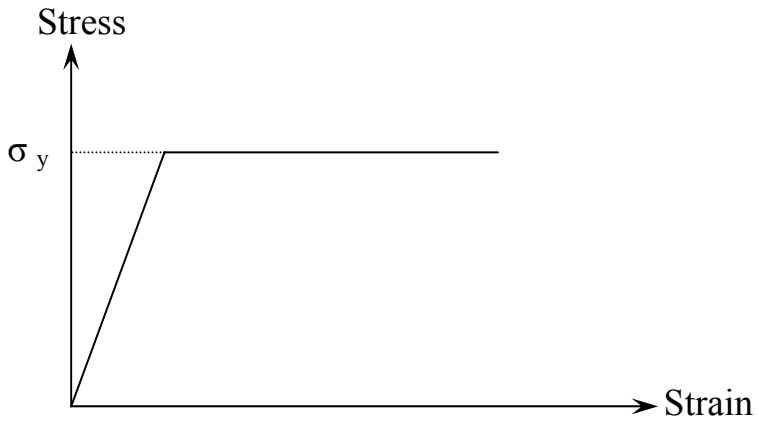

Fig. (5.6): Idealized Elastic-Perfectly Plastic Stress-Strain Curve

5.4.3 Finite Elements Mesh

No. of elements in plate : 42 x 15 for 2-stiffener model

40 x 15 for other models

No. of elements in web : 1 x 15 per stiffener

No. of elements in flange : 2 x 15 per stiffener

5.4.4 Boundary Conditions

Let "0" on T [x, y, z] denote translation constraints and on R [x, y, z] denote rotational constraints about the x, y and z-coordinates. Let "1" denote no constraint.

- The mid-width node in each of the two transverse edges has T [1, 0, 1] to prevent rigid body motion in the y direction.
- The longitudinal edges are simply supported with T [1, 1, 0] and R [1, 0, 0].

- The transverse edge on the left hand side, which is the mid-length of the mid-bay of the full 3-bay has symmetric boundary conditions. This is simulated with T [0, 1, 1] and R [1, 0, 1].
- The transverse edge on the right hand side, which is the loaded edge, is simply supported with T [1, 1, 0] and R [0, 1, 0].
- The transverse cross frame is not modeled, but it is simulated with T [1, 1,0].

5.4.5 Effect of Aspect Ratio

The effect of aspect ratio on the post-buckling behavior is considered in the present study. The values of aspect ratio (B/L) are taken to be (1.5,1.0,0.667,and 0.5). Figures (5.7) to (5.16) present the load-deflection curves for plates under uniaxial load in longitudinal direction. These figures show a comparison between the plates having aspect ratios of (1.5,1.0,0.667 and 0.5); the curves are ploted for different slenderness ratio and number of stiffeners, only in case of 5-stiffener, edge stiffeners are used to investigate the effect of these stiffeners on the behavior of plates with and without these stiffeners.

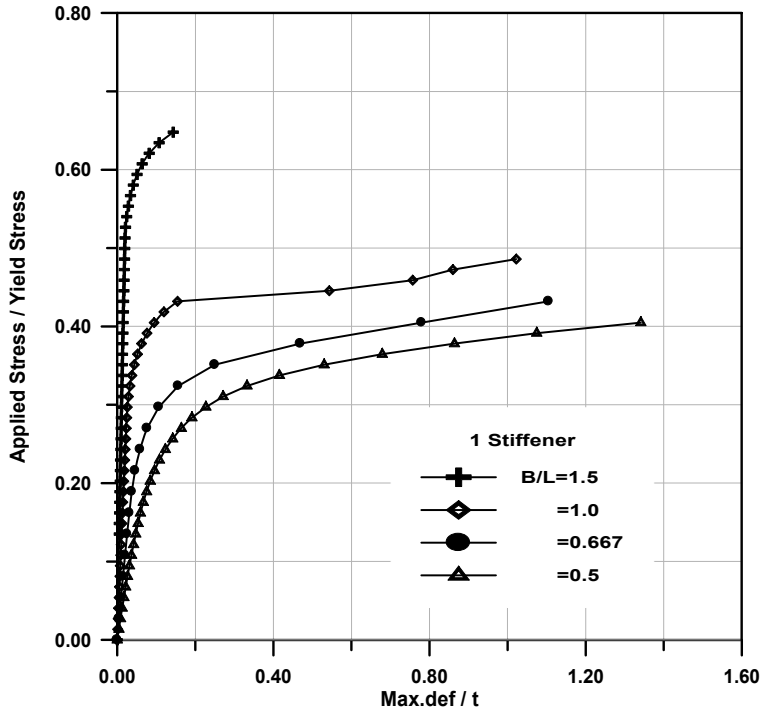

Fig. (5.7): Effect of Plate Aspect Ratio (B=3600, b_w=20, hw=50, tf=30, b_f=200, and t/h_w=0.42, ns=1)

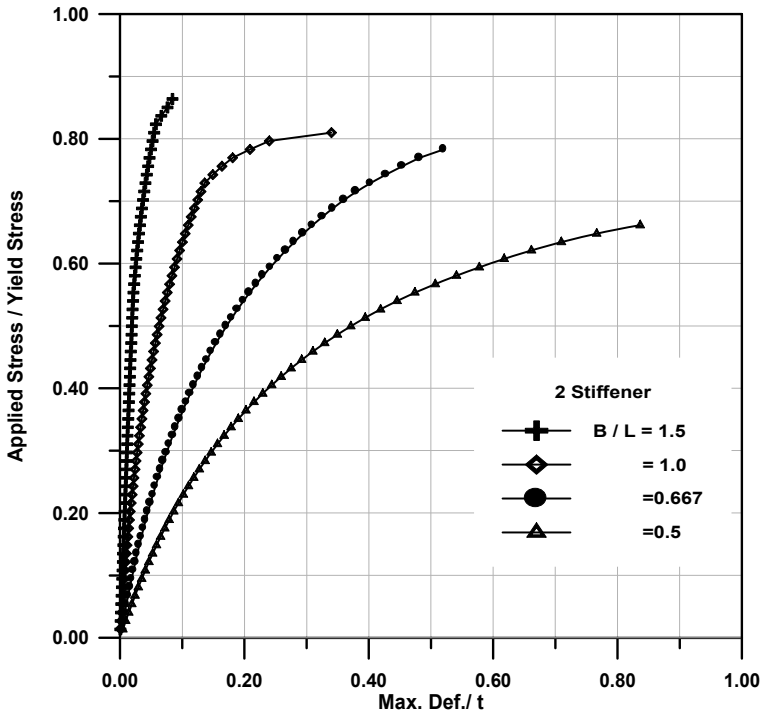

Fig. (5.8): Effect of Plate Aspect Ratio (B=3600, b_w=20, hw=50, tf=30, b_f=200, and t/h_w=0.42, ns=2)

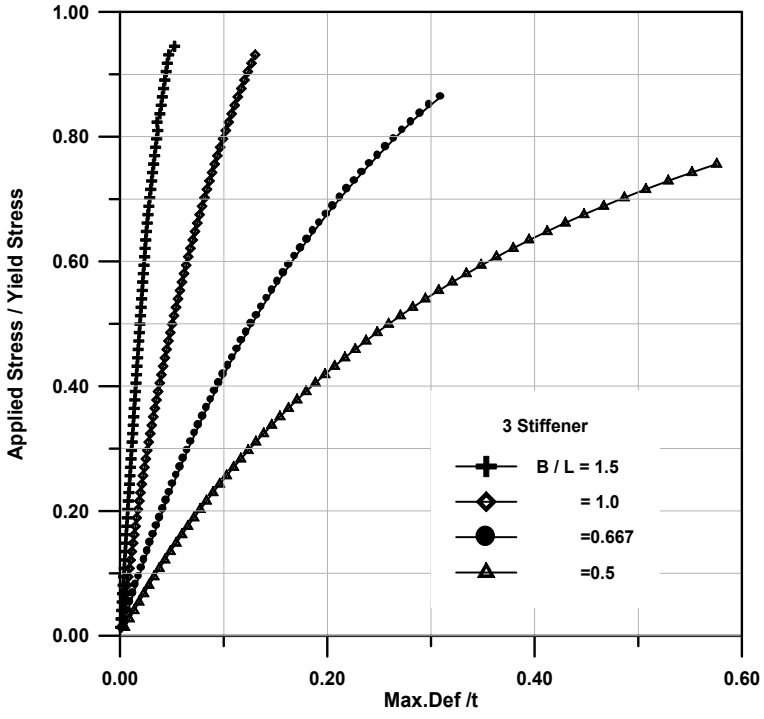

Fig.(5.9): Effect of Plate Aspect Ratio (B=3600, b_w=20, hw=50, tf=30, b_f=200, and t/h_w=0.42, ns=3)

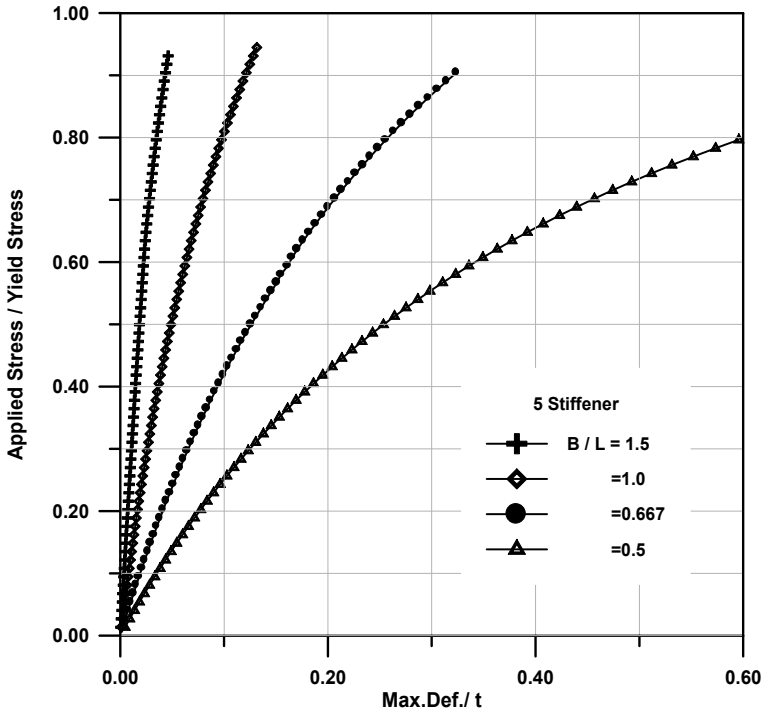

Fig.(5.10): Effect of Plate Aspect Ratio (B=3600, b_w=20, hw=50, tf=30, b_f=200, and t/h_w=0.42, ns=5)

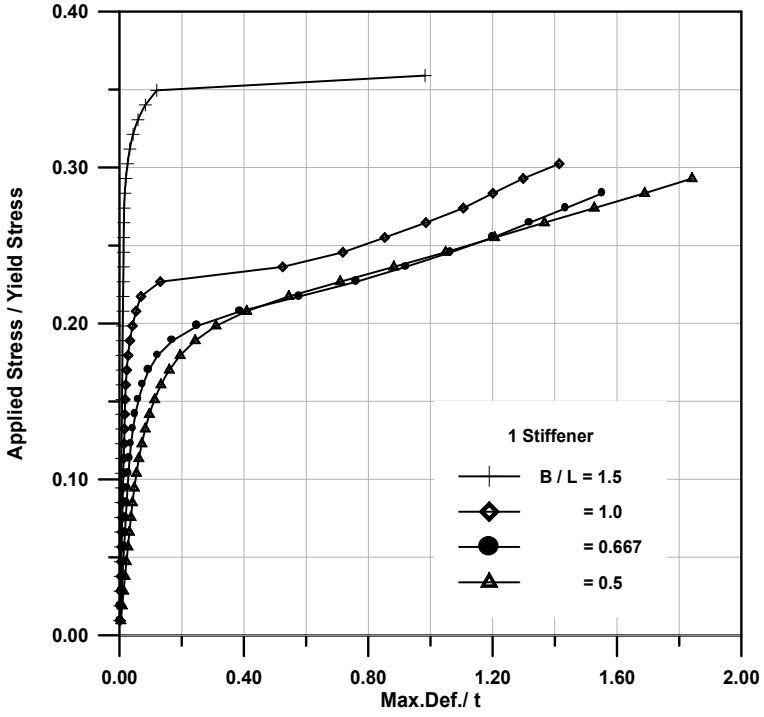

Fig.(5.11): Effect of Plate Aspect Ratio (B=3600, b_w=20, hw=50, tf=30, b_f=200, and t/h_w=0.3, ns=1)

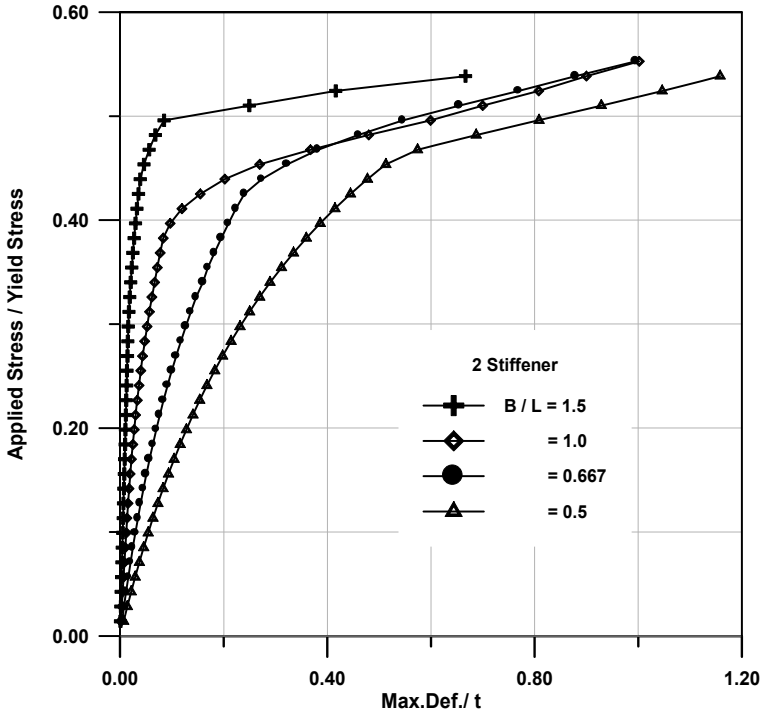

Fig.(5.12): Effect of Plate Aspect Ratio (B=3600, b_w=20, hw=50, tf=30, b_f=200, and t/h_w=0.3, ns=2)

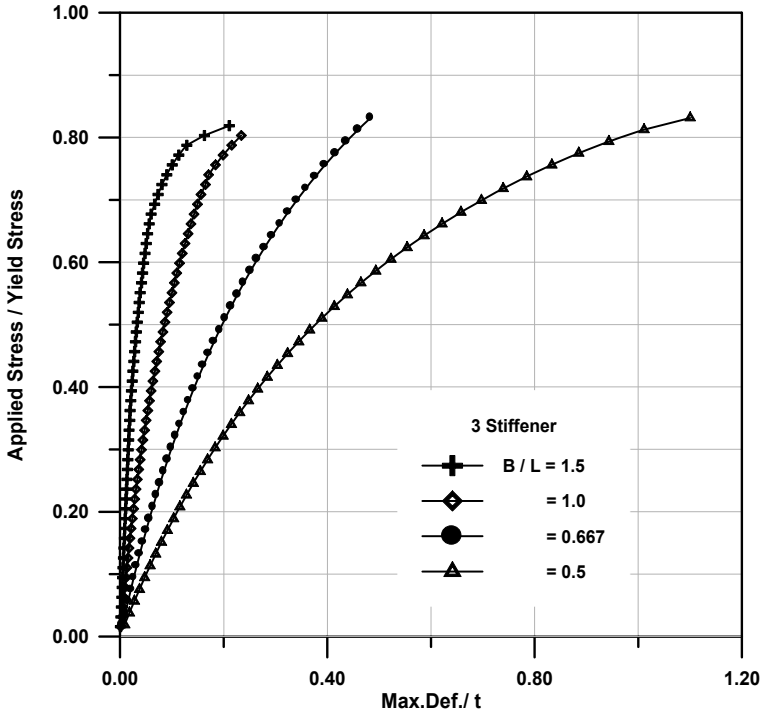

Fig.(5.13): Effect of Plate Aspect Ratio (B=3600, b_w=20, hw=50, tf=30, b_f=200, and t/h_w=0.3, ns=3)

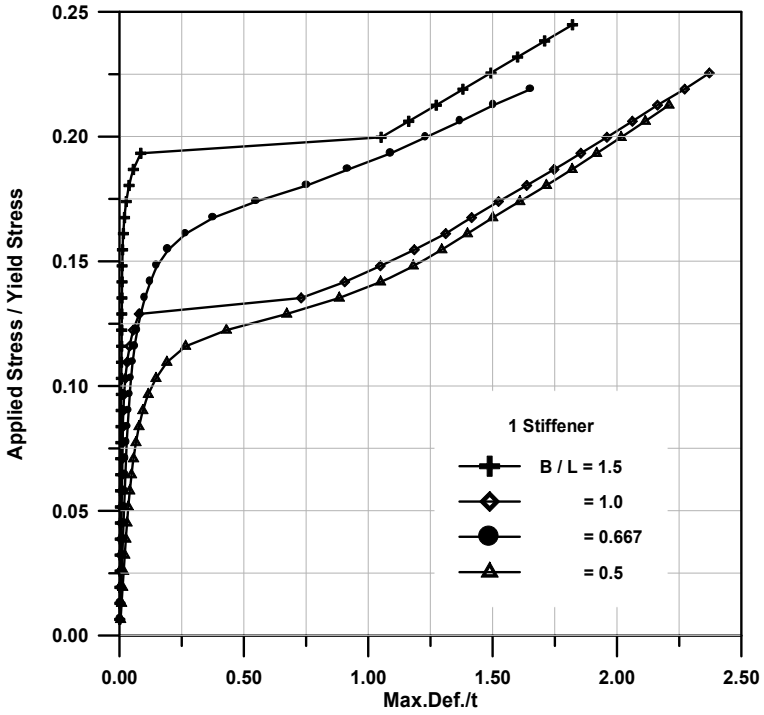

Fig.(5.14): Effect of Plate Aspect Ratio (B=3600, b_w=20, hw=50, tf=30, b_f=200, and t/h_w=0.22, ns=1)

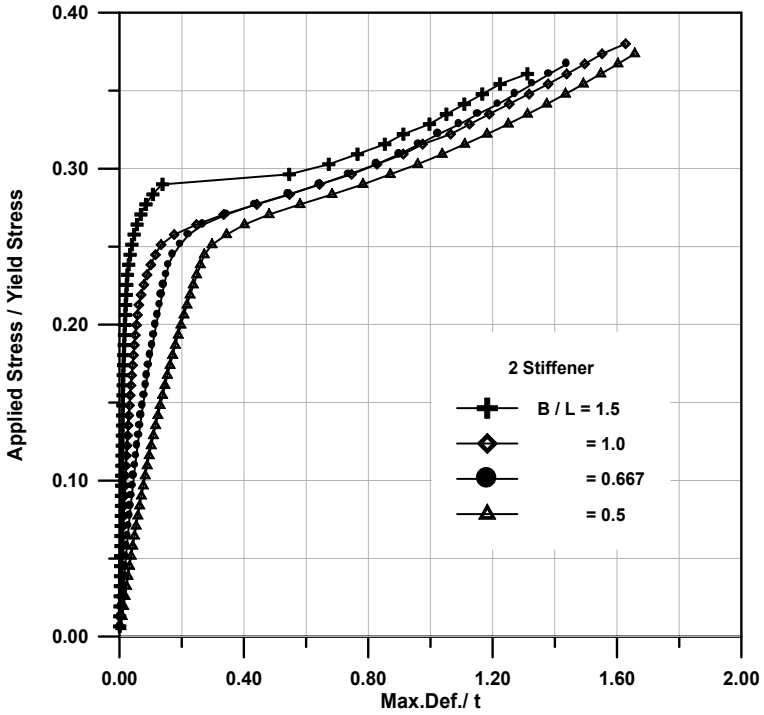

Fig.(5.15): Effect of Plate Aspect Ratio (B=3600, b_w=20, hw=50, tf=30, b_f=200, and t/h_w=0.22, ns=2)

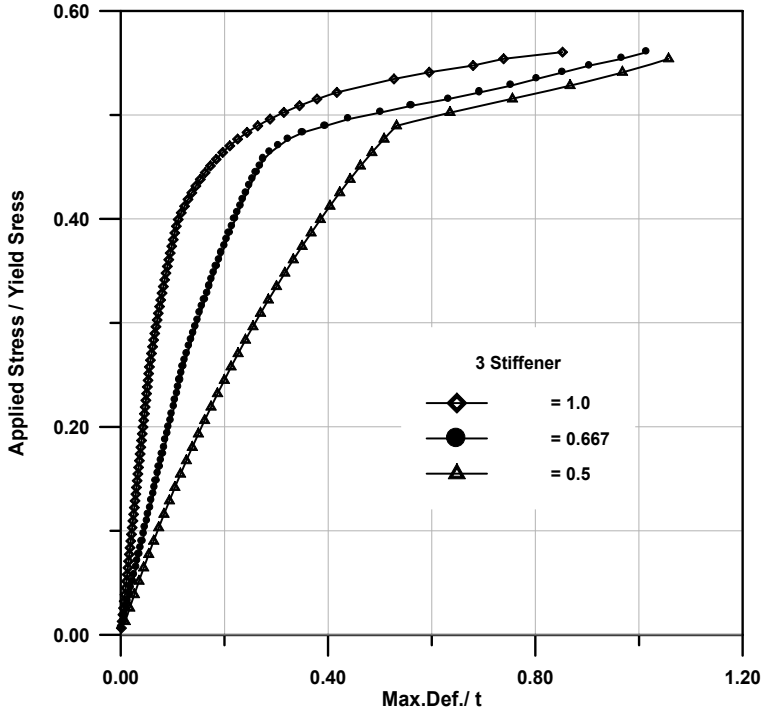

Fig.(5.16): Effect of Plate Aspect Ratio (B=3600, b_w=20, hw=50, tf=30, b_f=200, and t/h_w=0.22, ns=3)

From these figures, it can be noticed that:

1. By increasing the aspect ratio, the in-plane stiffeness of the plate increases and large amount of strength is obtained.
2. For 1-stiffener model, the increase in the in-plane stiffeness due to the increase of the aspect ratio by 0.5 (from 0.5 to 1.0) is (8 , 1, 1.3%)of yield stress for the plates having (t / h_w =0.42, 0.3, 0.22).
3. The maximum increase in strength due to increasing the aspect ratio by 0.5 is shown for plate having (t / h_w =0.42) for all stiffener model.
4. The absolute maximum increase in strength due to increasing the aspect ratio by 0.5 is shown to be for 3-stiffener model with (t / h_w =0.42).

5. For 5-stiffener model (three intermediate stiffeners and two edge stiffeners), the increase of the aspect ratio by 0.5 causes an increase in the in-plane stiffeness and the strength by approximately (15%)of yield stress for (t / h_w) equal (0.42).

5.4.6 Effect of Number of Stiffeners

The effect of number of stiffeners on the post-buckling behavior for different aspect ratios and slenderness ratios is considered in the present study. Also the effect of edge stiffeners is studied in this section. The number of stiffeners are one, two, three, and five. Different values of aspect ratio are used to obtain load-deflection curves for plates under uniaxial load. The aspect ratio (B/L) is taken to be (1.5, 1.0, 0.667, and 0.5), figures (5.17) to (5.31) show a comparison between a plate with (1,2,3 and 5) stiffeners. Only the case of 5-stiffener model edge stiffeners are used to investigate the effect of these edge stiffeners on the behavior of the plates with respect to a plate without these edge stiffeners.

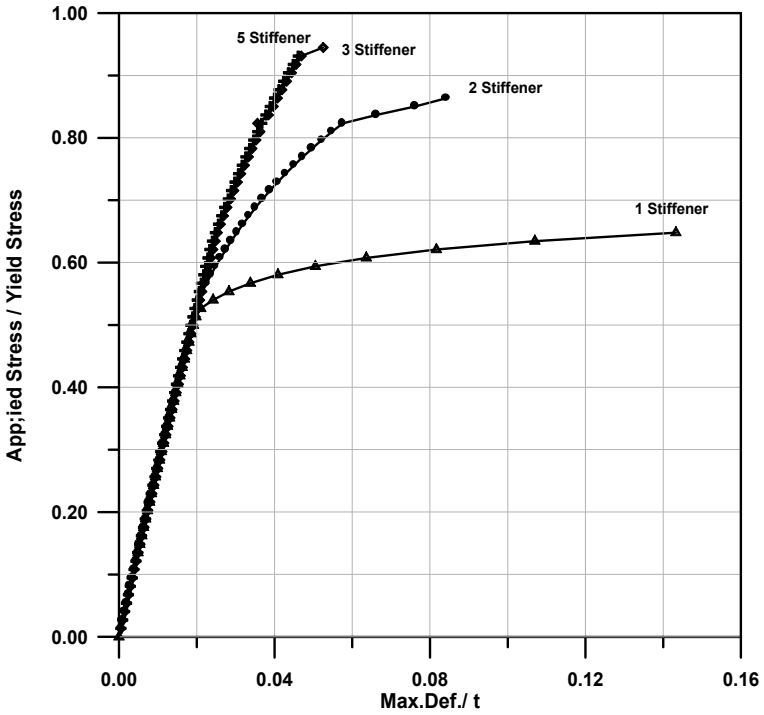

Fig.(5.17): Effect of No. of Stiffeners (B=3600, b_w=20, hw=50, tf=30, b_f=200, t/h_w=0.42, and aspect ratio = 1.5)

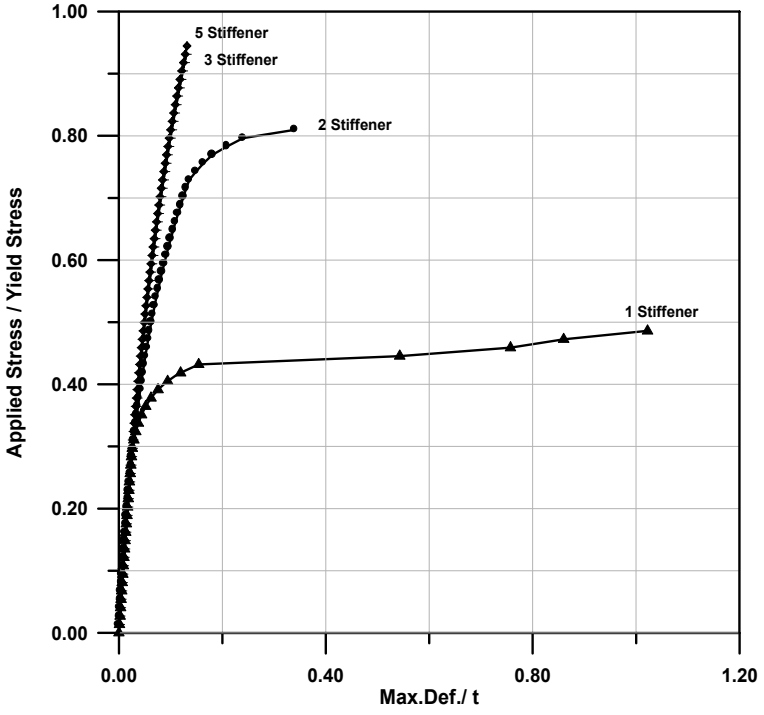

Fig.(5.18): Effect of No. of Stiffeners (B=3600, b_w=20, hw=50, tf=30, b_f=200, t/h_w=0.42, and aspect ratio = 1.0)

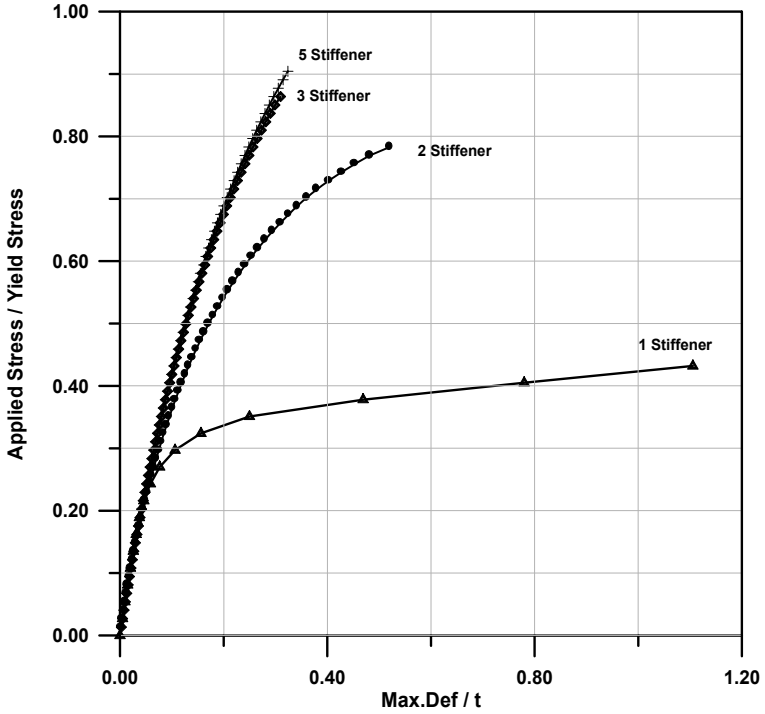

Fig.(5.19): Effect of No. of Stiffeners (B=3600, b_w=20, hw=50, tf=30, b_f=200, t/h_w=0.42, and aspect ratio = 0.667)

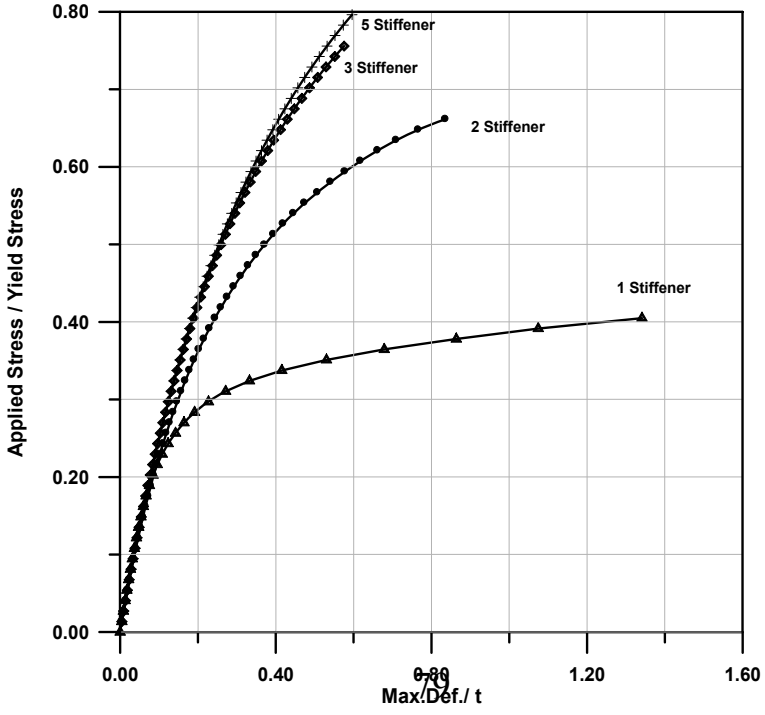

Fig.(5.20): Effect of No. of Stiffeners (B=3600, b_w=20, hw=50, tf=30, b_f=200, t/h_w=0.42, and aspect ratio = 0.5)

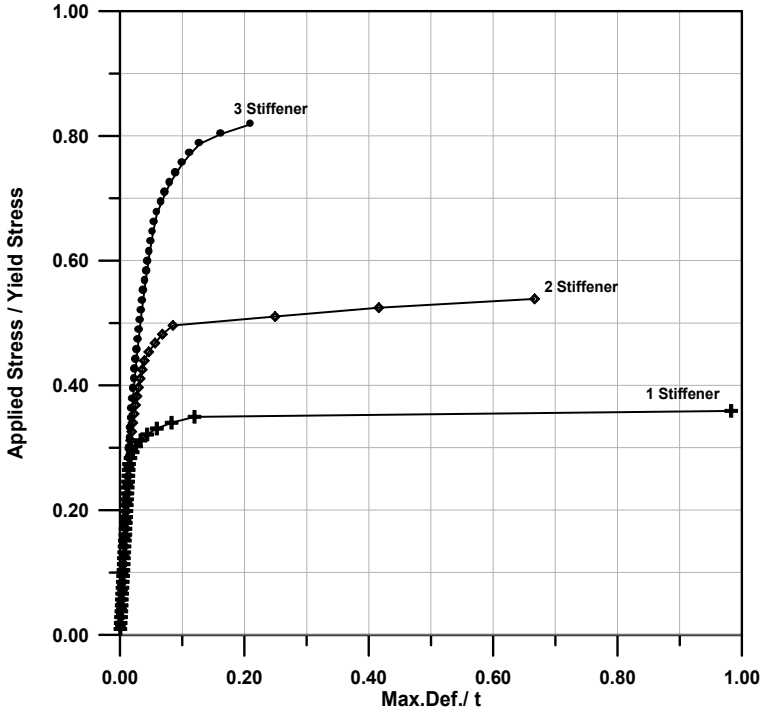

Fig.(5.21): Effect of No. of Stiffeners (B=3600, b_w=20, hw=50, tf=30, b_f=200, t/h_w=0.30, and aspect ratio = 1.5)

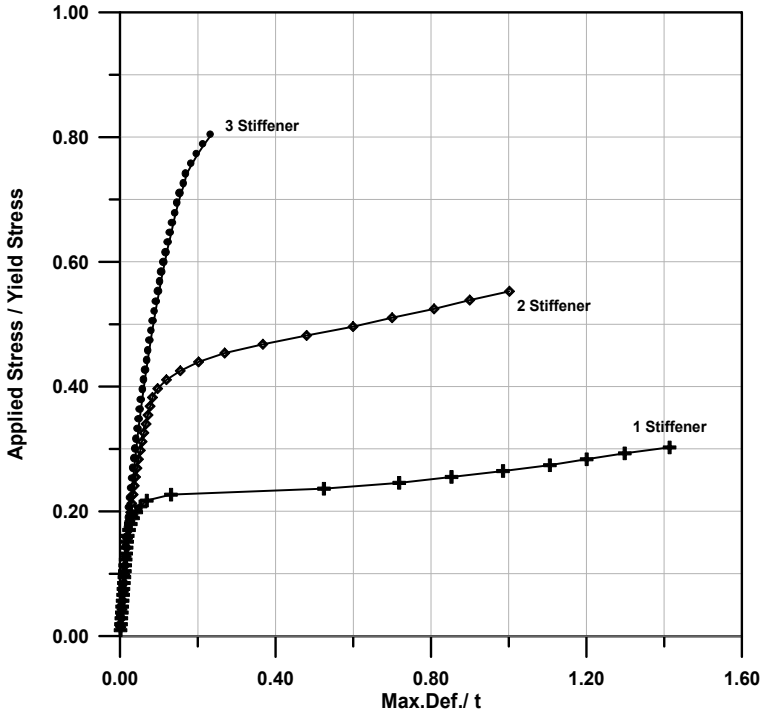

Fig.(5.22): Effect of No. of Stiffeners (B=3600, b_w=20, hw=50, tf=30, b_f=200, t/h_w=0.30, and aspect ratio = 1.0)

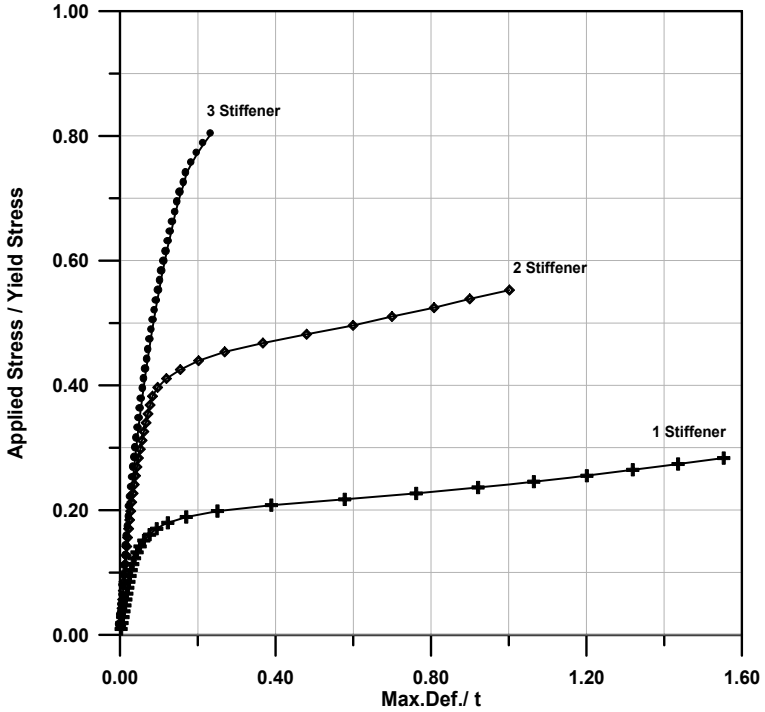

Fig.(5.23): Effect of No. of Stiffeners (B=3600, b_w=20, hw=50, tf=30, b_f=200, t/h_w=0.30, and aspect ratio = 0.667)

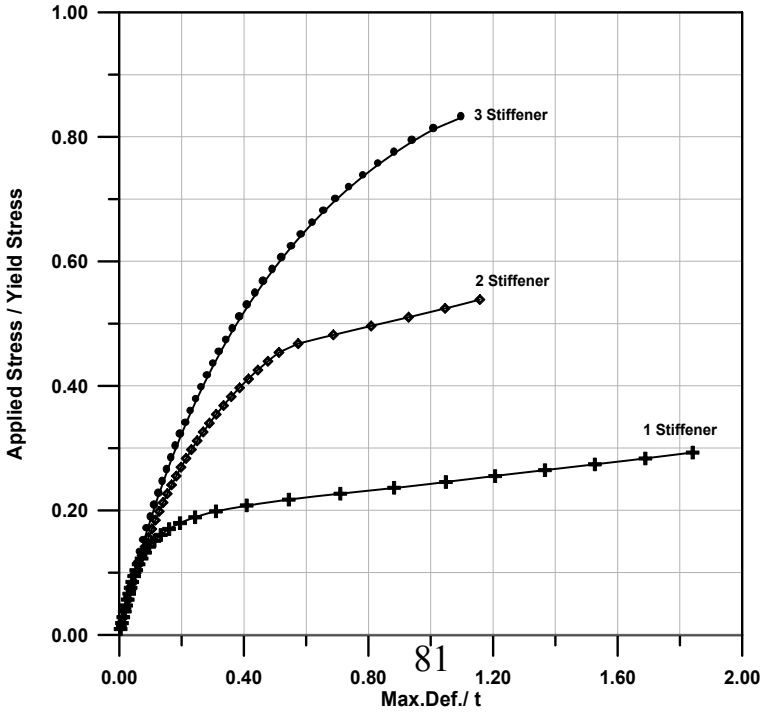

Fig.(5.24): Effect of No. of Stiffeners (B=3600, b_w=20, hw=50, tf=30, b_f=200, t/h_w=0.30, and aspect ratio = 0.5)

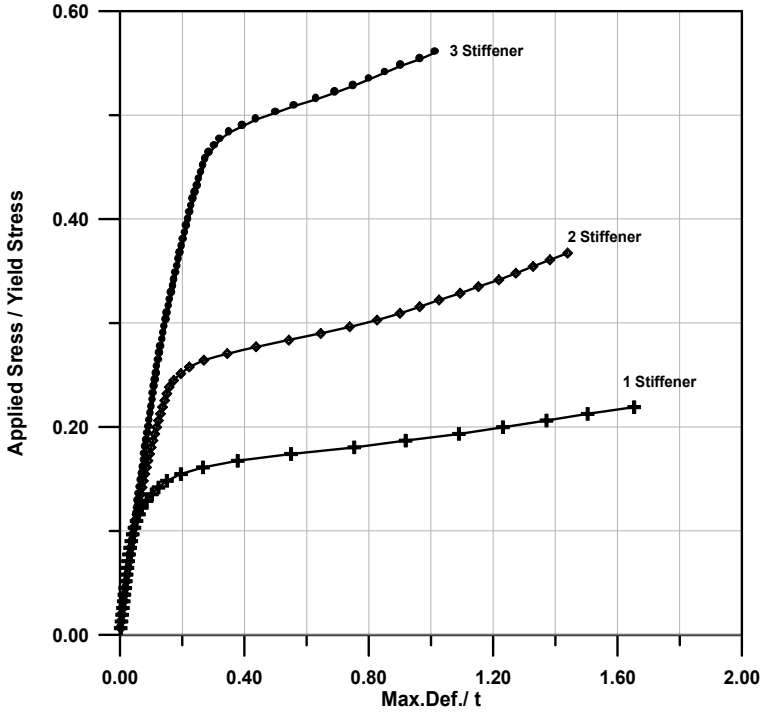

Fig.(5.25): Effect of No. of Stiffeners (B=3600, b_w=20, hw=50, tf=30, b_f=200, t/h_w=0.22, and aspect ratio = 1.5)

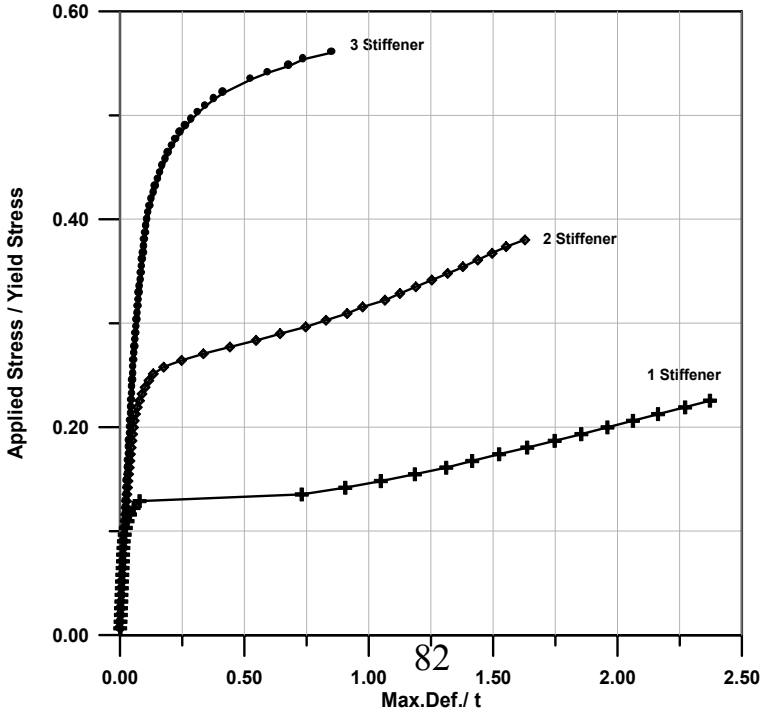

Fig.(5.26): Effect of No. of Stiffeners (B=3600, b_w=20, hw=50, tf=30, b_f=200, t/h_w=0.22, and aspect ratio = 1.0)

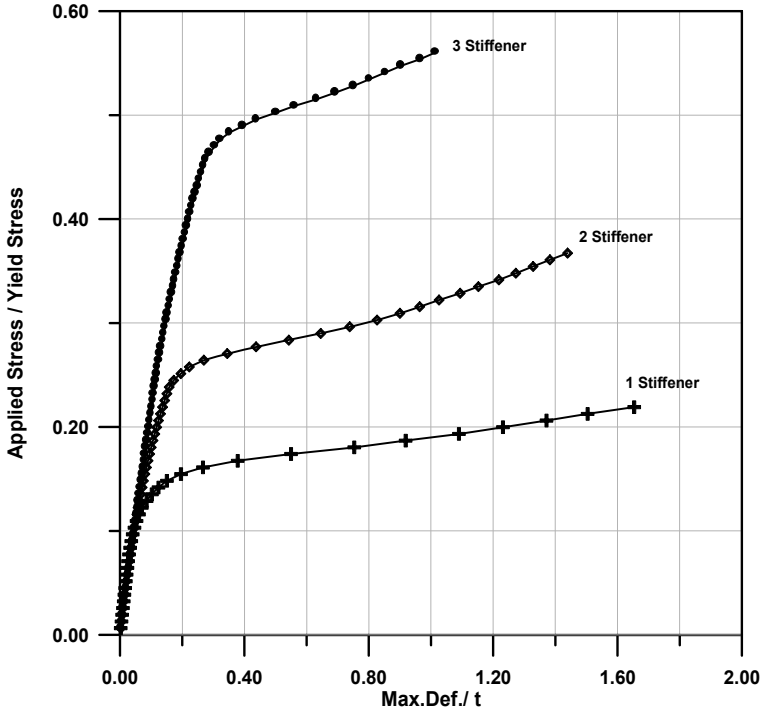

Fig.(5.27): Effect of No. of Stiffeners (B=3600, b_w=20, hw=50, tf=30, b_f=200, t/h_w=0.22, and aspect ratio = 0.667)

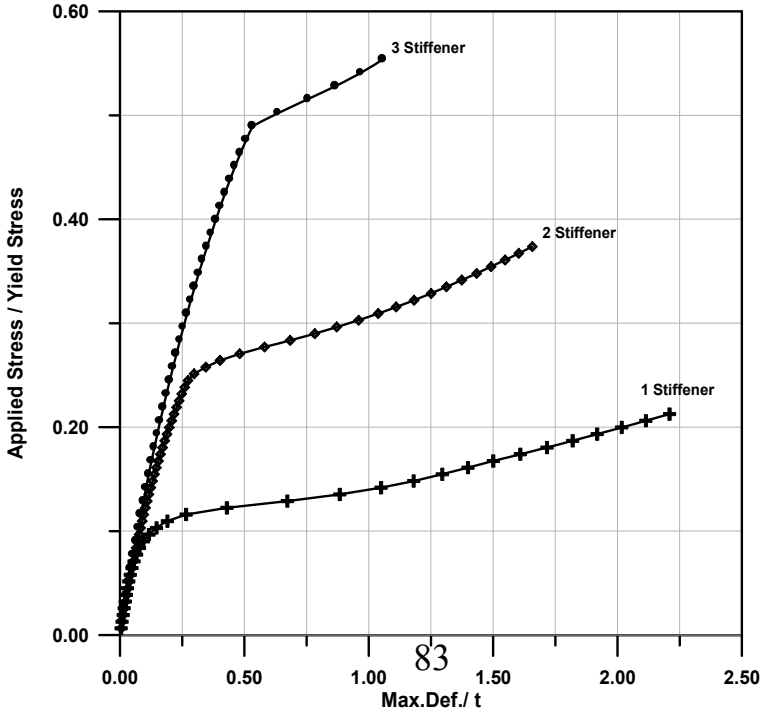

Fig.(5.28): Effect of No. of Stiffeners (B=3600, b_w=20, hw=50, tf=30, b_f=200, t/h_w=0.22, and aspect ratio = 0.5)

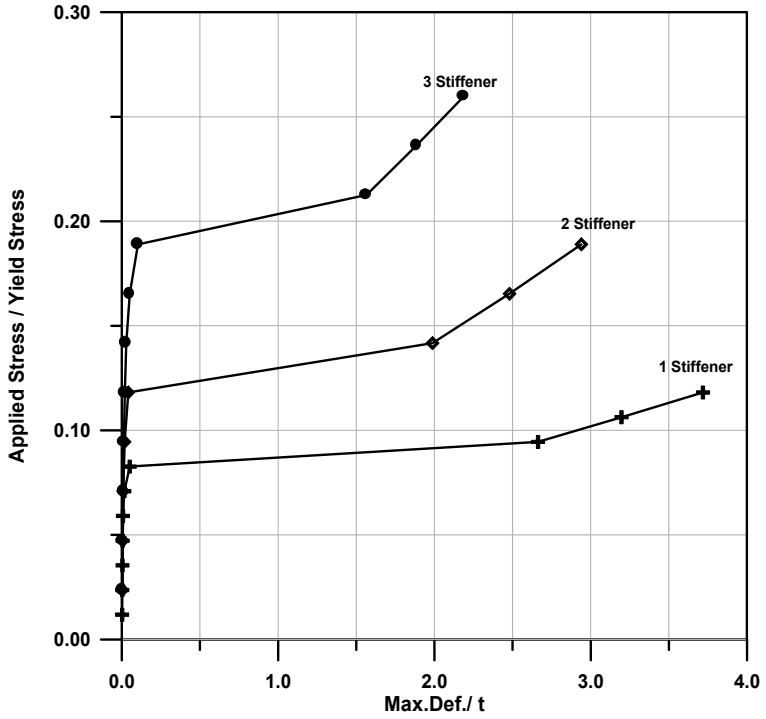

Fig.(5.29): Effect of No. of Stiffeners (B=3600, b_w=20, hw=50, tf=30, b_f=200, t/h_w=0.12, and aspect ratio = 1.5)

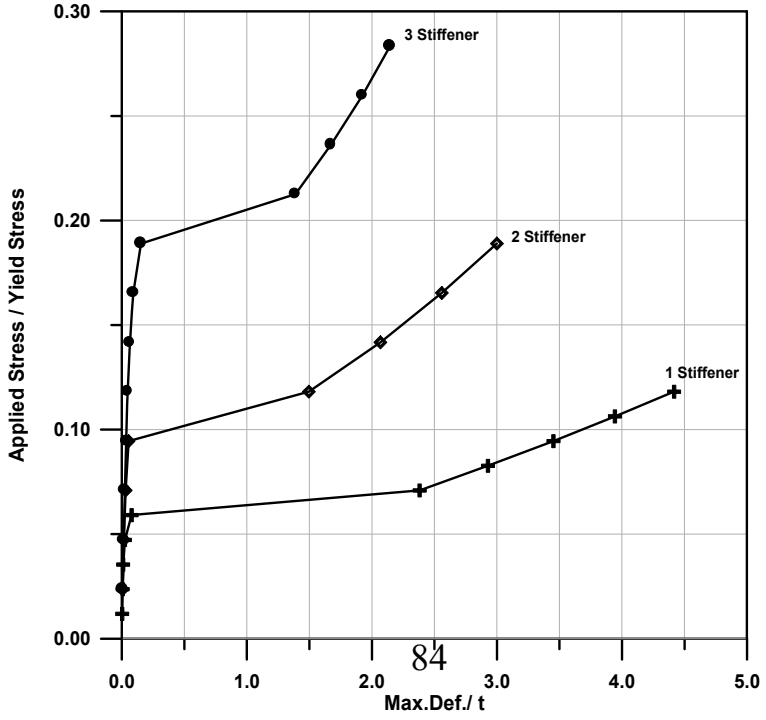

Fig.(5.30): Effect of No. of Stiffeners (B=3600, b_w=20, hw=50, tf=30, b_f=200, t/h_w=0.12, and aspect ratio = 1.0)

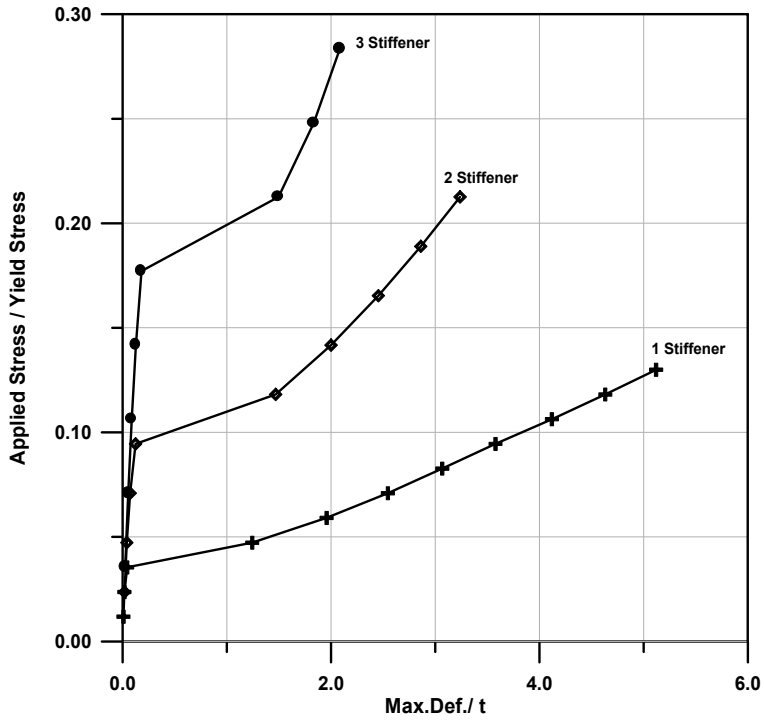

Fig.(5.31): Effect of No. of Stiffeners (B=3600, b_w=20, hw=50, tf=30, b_f=200, t/h_w=0.12, and aspect ratio = 0.667).

From these figures, it can be noticed that:

1. By the increase of number of stiffeners, the in-plane stiffeness of the plate increases and large amount of strength is obtained.
2. In case of a stocky plate, the increase in strength due to icreasing the number of stiffeners from one stiffener to two stiffeners is more than that for the number of stiffeners increasing from two to three, and contrariwise for the case of other plates.
3. Using two stiffeners instead of one stiffener causes a gradual increase in strength from a slender plate to a stocky plate.

4. Using three stiffeners instead of two causes a non-uniform increase in strength reaching a maximum magnitude for plates having (t / h_w) equal 0.3 .
5. The absolute maximum increase in strength is due to increasing the number of stiffeners from two to three for a plate having ($t / h_w = 0.3$) and aspect ratio 0.5.

5.4.7 Effect of Slenderness Ratio

In this section the effect of slenderness ratio ($B/t\sqrt{\sigma_y / E}$) and plate thickness to stiffener height ratio ($t / h_{w)}$ will be investigated for plates having different aspect ratios (1.5, 1.0, 0.667, and 0.5) and different number of stiffeners. The width B=3600 mm and the stiffener's height h_w = 50 mm will not be changed. Only the thickness of the plate will be taken (21,15,11,and 6 mm) to give slenderness ratios equal to (7.1,9.9,13.6,and 24.8) corresponding to thickness of the plate to stiffener's height ratios (t / h_w= 0.42,0.3,0.22,and 0.12) respectively.

Figures (5.32) to (5.43) give the load-deflection curves for plates under uniaxial load in longitudinal direction. These figures show a comparison between the plates with (0.42, 0.3, 0.22, and 0.12) plate thickness to stiffener's height ratios to investigate the effect of slenderness ratio and plate thickness to height of stiffener ratio on the post-buckling behavior of stiffened plates.

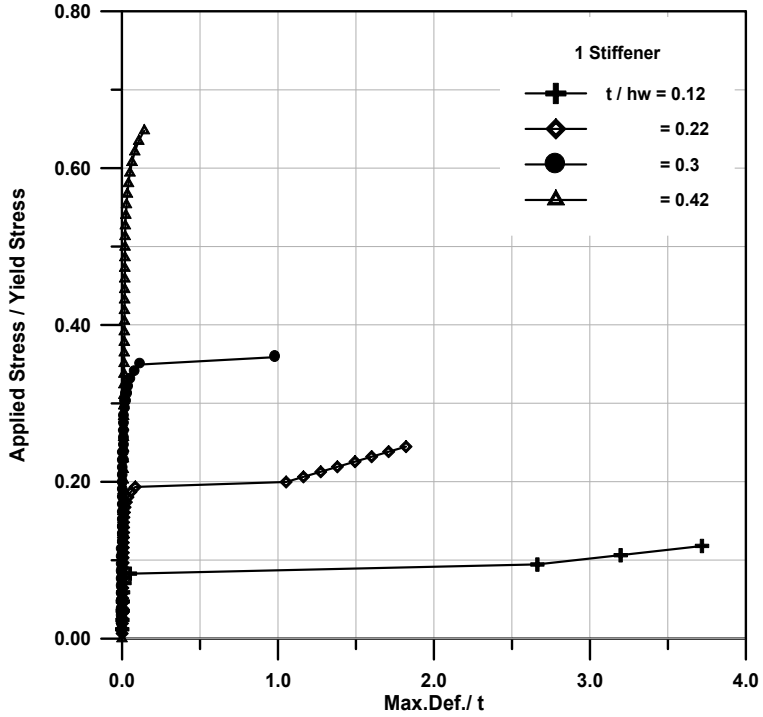

Fig.(5.32): Effect of Slenderness Ratio (b=3600, b_w=20, hw=50, tf=30, b_f=200, and aspect ratio = 1.5)

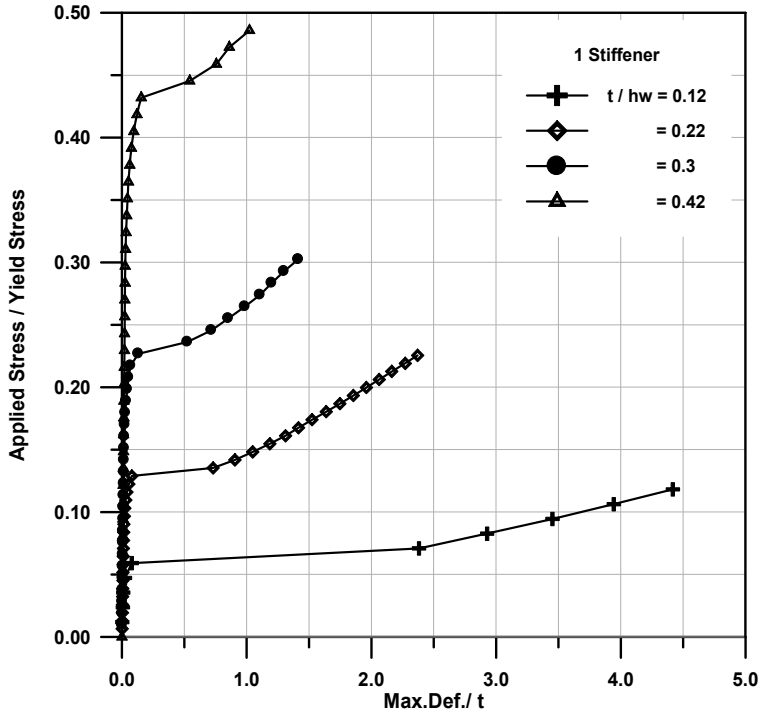

Fig.(5.33): Effect of Slenderness Ratio (B=3600, b_w=20, hw=50, tf=30, b_f=200, and aspect ratio = 1.0)

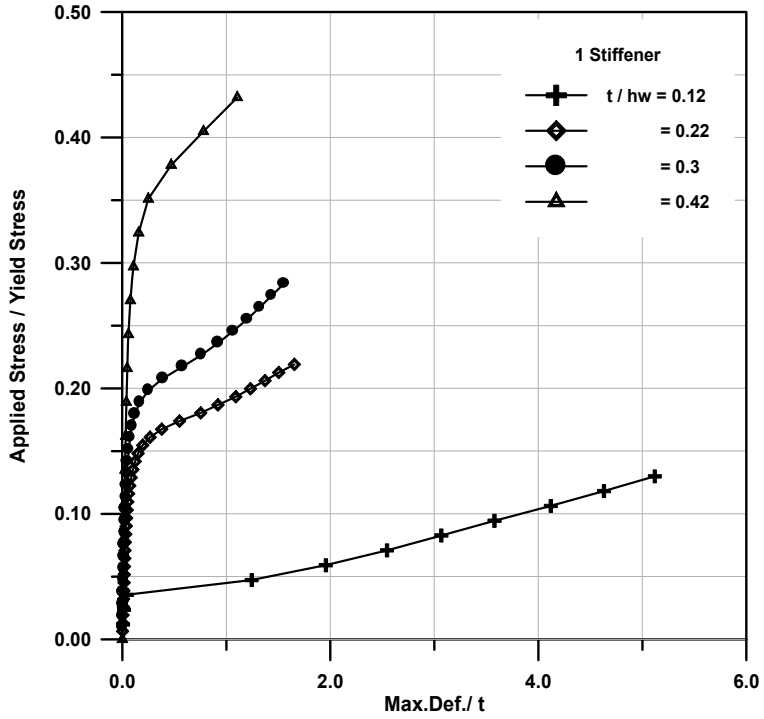

Fig.(5.34): Effect of Slenderness Ratio (B=3600, b_w=20, hw=50, tf=30, b_f=200, and aspect ratio = 0.667)

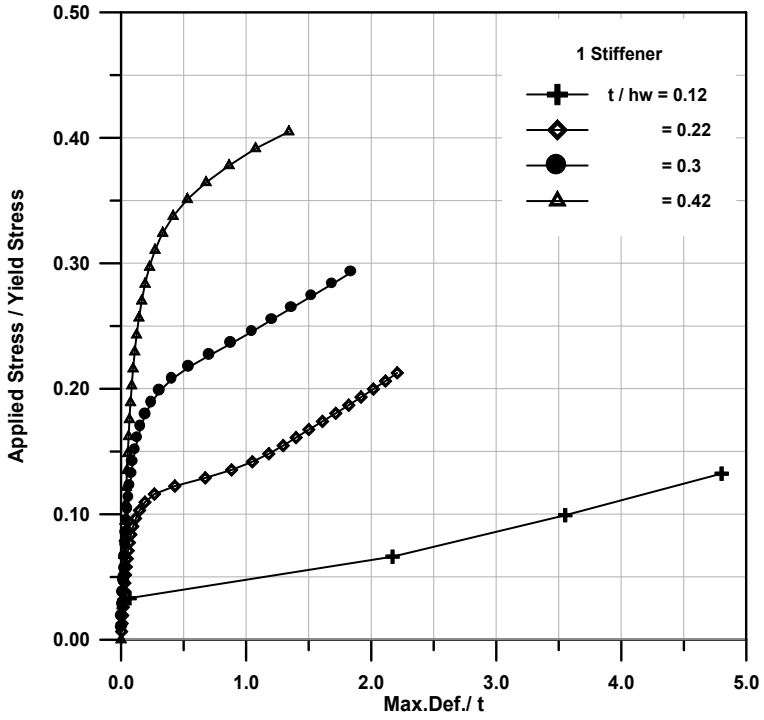

Fig.(5.35): Effect of Slenderness Ratio (B=3600, b_w=20, hw=50, tf=30, b_f=200, and aspect ratio = 0.5)

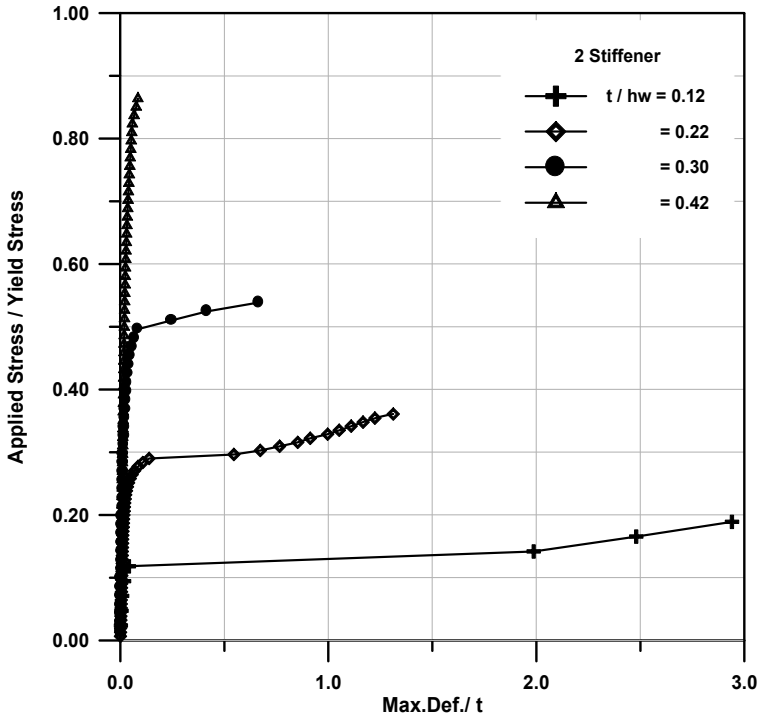

Fig.(5.36): Effect of Slenderness Ratio (B=3600, b_w=20, hw=50, tf=30, b_f=200, and aspect ratio = 1.5)

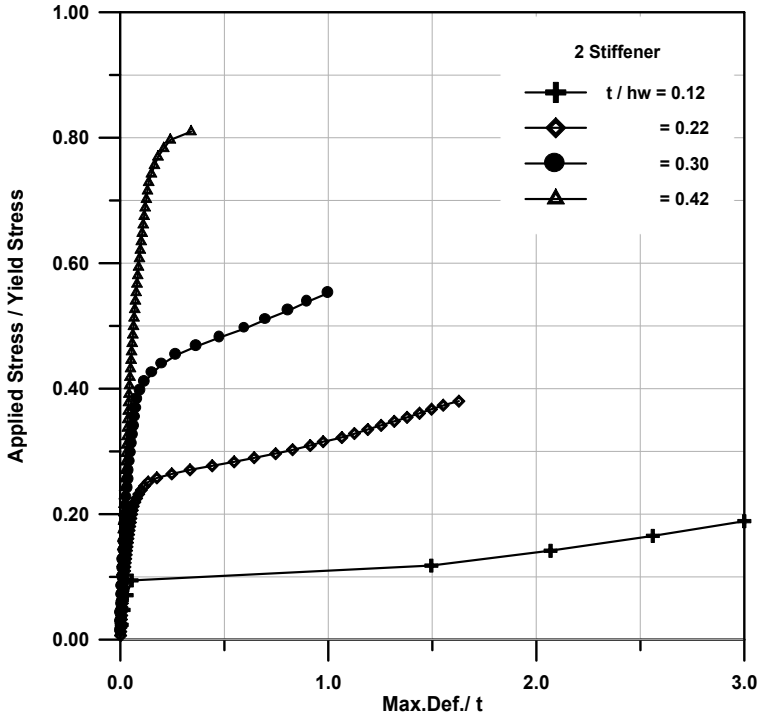

Fig.(5.37): Effect of Slenderness Ratio (B=3600, b_w=20, hw=50, tf=30, b_f=200, and aspect ratio = 1.0)

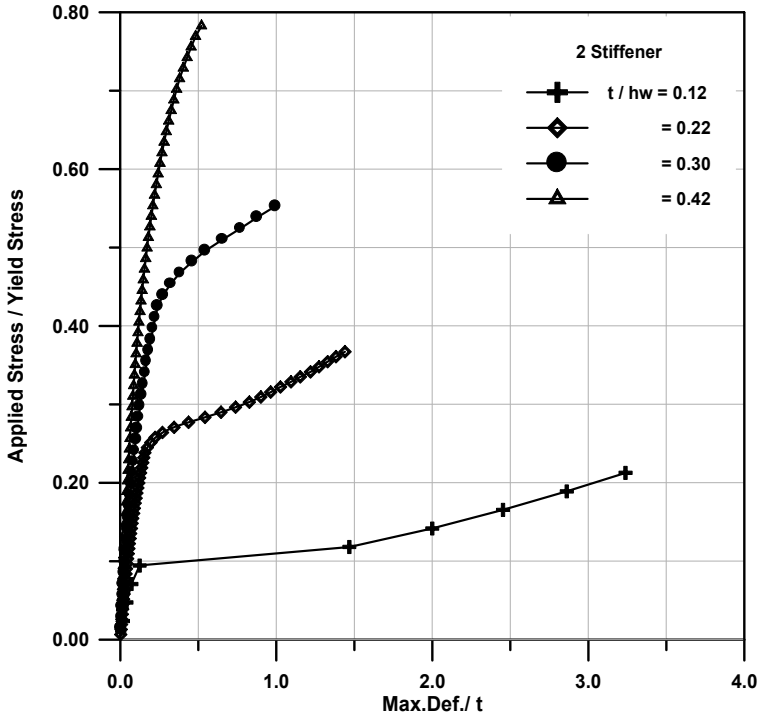

Fig.(5.38): Effect of Slenderness Ratio (B=3600, b_w=20, hw=50, tf=30, b_f=200, and aspect ratio = 0.667)

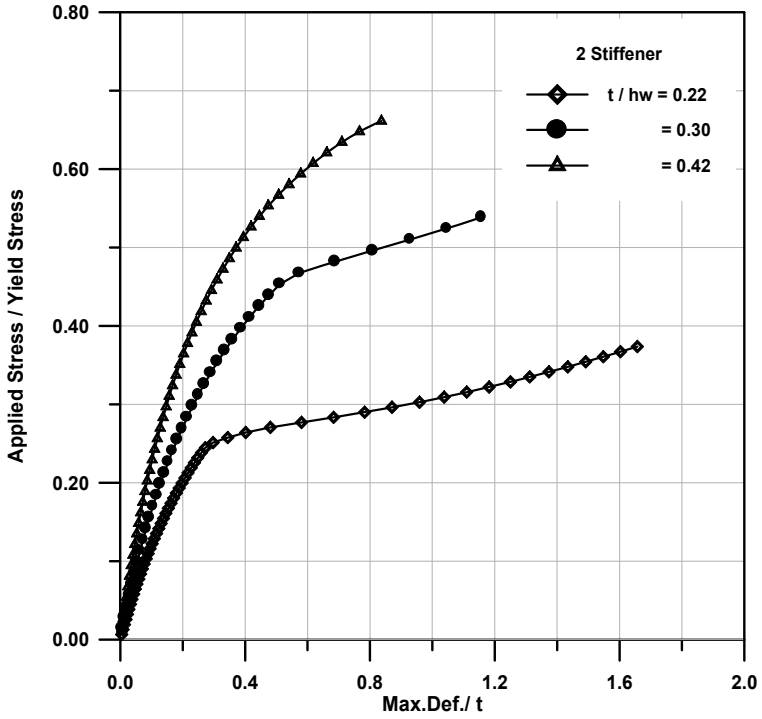

Fig.(5.39): Effect of Slenderness Ratio (B=3600, b_w=20, hw=50, tf=30, b_f=200, and aspect ratio = 0.5)

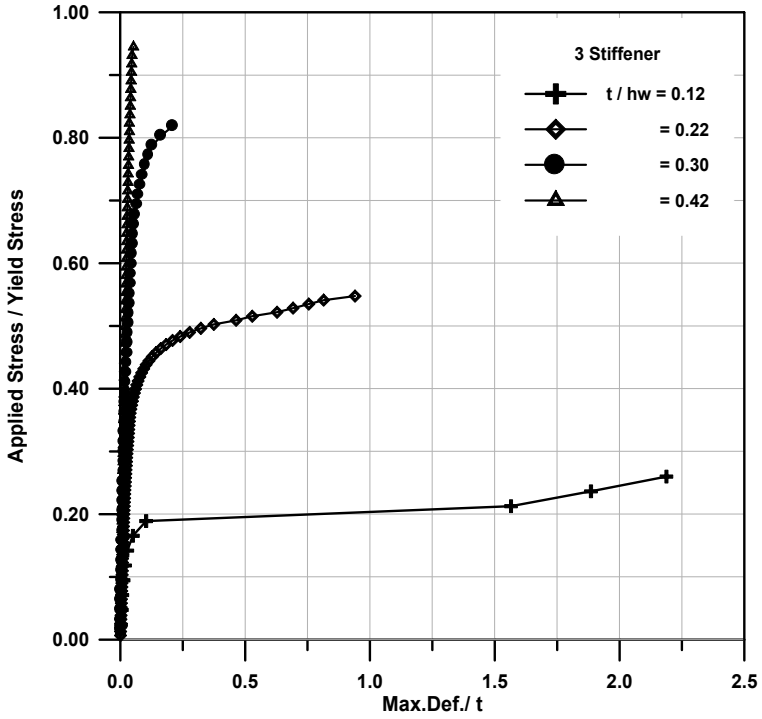

Fig.(5.40): Effect of Slenderness Ratio (B=3600, b_w=20, hw=50, tf=30, b_f=200, and aspect ratio = 1.5)

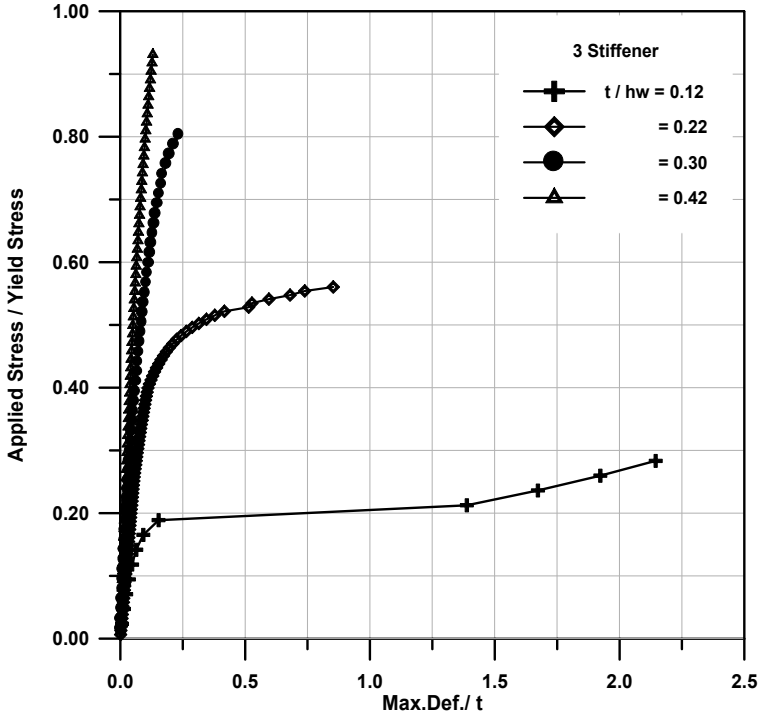

Fig.(5.41): Effect of Slenderness Ratio (B=3600, b_w=20, hw=50, tf=30, b_f=200, and aspect ratio = 1.0)

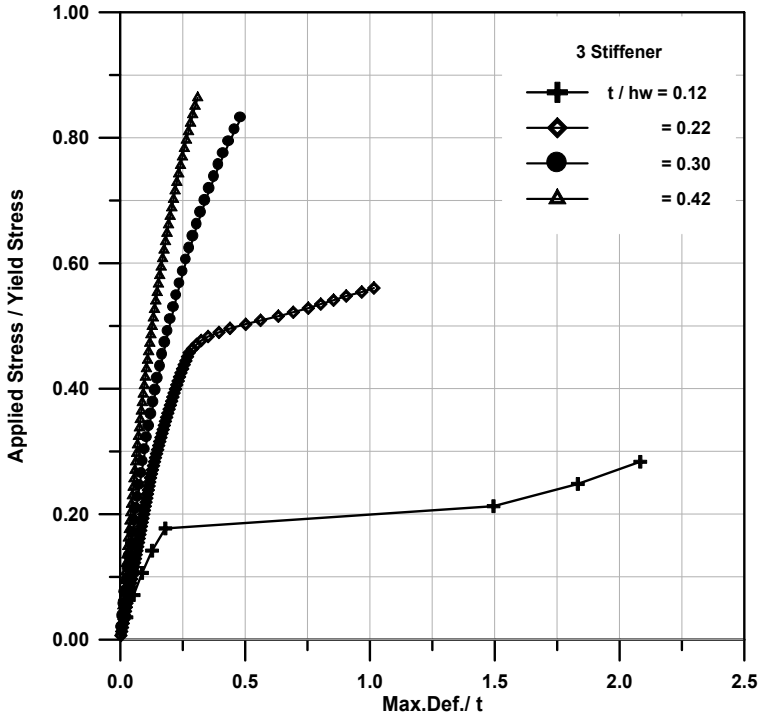

Fig.(5.42): Effect of Slenderness Ratio (B=3600, b_w=20, hw=50, tf=30, b_f=200, and aspect ratio = 0.667)

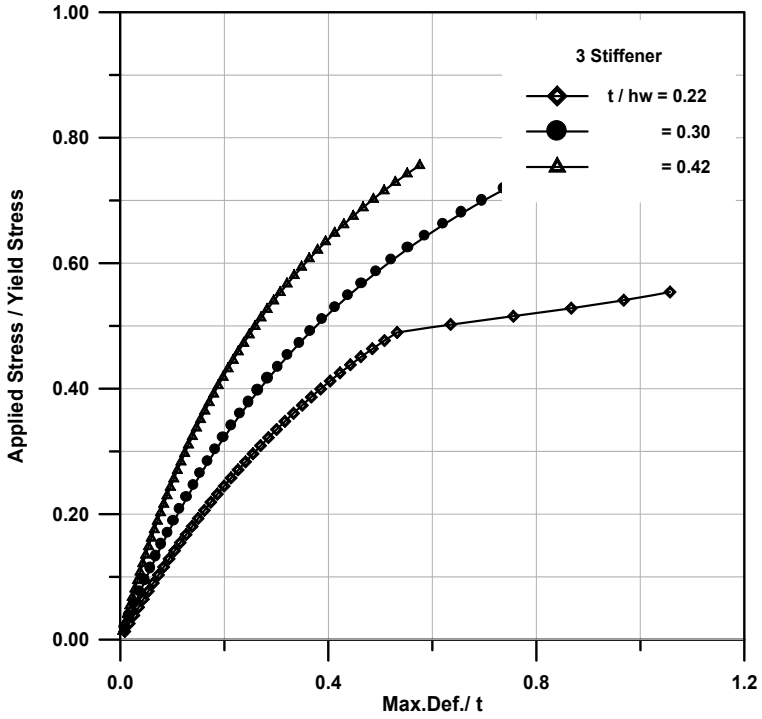

Fig.(5.43): Effect of Slenderness Ratio (B=3600, b_w=20, hw=50, tf=30, b_f=200, and aspect ratio = 0.5)

From these figures, it can be noticed that:

1. The decrease of the slenderness ratio (or increase of the thickness of plate to stiffener height ratio), the in-plane stiffeness of the plate increases and large amount of strength is obtained.
2. For 1-stiffener model, the increase in the in-plane stiffeness and post-buckling strength due to increase of the ($t / h_{w)}$ ratio from 0.12 for a slender plate to 0.42 for a stocky plate is (53 , 37, 30, 27%)of yield stress for plates having (aspect ratio =1.5, 1.0, 0.667, and 0.5) respectively.
3. The absolute maximum increase in strength due to decreasing the slenderness ratio from slender to a stocky plate is shown for the plate having three stiffeners and with aspect ratio equal to 1.5.
4. Increasing in thickness of the plate to stiffener's height ratio causes a gradual increase in strength with the increase in aspect ratios.

5.4.8 Strength-to-Weight Ratio

Table (5.4) gives the strength-to-weight ratio for different plates presented in this study. The strength of the plates can be noticed from the previous sections and the weight of these plates can be calculated as: weight= $[B*t + ns*(tw*hw + tf*hf)]$.

Table (5.4): Strength-to-Weight Ratio for Different Plates (MPa/mm^2) per Meter Length.

t/h_w	Aspect ratio=1.5	Aspect ratio=1.0	Aspect ratio=0.667	Aspect ratio=0.5

	ns=1	ns=2	ns=3	ns=1	ns=2	ns=3	ns=1	ns=2	ns=3	ns=1	ns=2	ns=3
0.42	2.77	3.40	3.45	2.07	3.19	3.40	1.85	3.08	3.15	1.73	2.60	2.76
0.30	2.08	2.80	3.85	1.75	2.87	3.78	1.64	2.87	3.91	1.69	2.80	3.88
0.22	1.86	2.38	3.19	1.70	2.50	3.26	1.66	2.42	3.26	1.62	2.46	3.22
0.12	1.46	1.25	2.15	1.46	1.25	2.34	1.61	2.11	2.34	1.63	1.40	2.41

CONCLUSIONS AND RECOMMENDATIONS

6.1 General

From the theoretical analysis and the comparison with available studies which are described in the previous chapter, the following conclusions can be drawn with regard to the results obtained for stiffened plates under specified load and boundary conditions.

The recommendations for future work are also presented in this chapter.

6.2 Conclusions

1. The main conclusion is that the stage of post-buckling of plates and stiffened plates is preferable to be taken into consideration for design purpose.
2. For crossover panels, the analytical procedures give a mean difference of about 0.074 and 0.087 for the local and overall buckling stresses respectively; therefore, these procedures are sufficiently accurate to predict the critical buckling stress.
3. The decrease of aspect ratio would produce an increase in out-of-plane deflection and in-plane stresses especially on the end bays.
4. The increase in slenderness ratio causes an increase in out-of-plane deflection, in-plane stresses, and the yield occurs in the skin of the plate. This problem is also shown when a high number of stiffeners is used.

5. The behavior of 3-stiffener model does not change when edge stiffeners are added (5-stiffener model) and only a small increase of in-plane stiffeness is noticed by (1.4, 4, 4%) of yield stress for plates having t/h_w ratio equal to 0.42 and aspect ratios equal to(1.0, 0.667, 0.5) respectively.
6. For design purpose it is ecconomic to use a 3-stiffener model because this model gives high strength-to-weight ratio (3.45, 3.85, 3.19, and 2.15) for plates having aspect ratio equal to 1.5 and t/h_w ratios equal to (0.42, 0.3, 0.22, and 0.12) respectively .
7. The best dimensions are noticed for plates having three intermediate stiffeners with 9.9 slenderness ratio (corresponding to $t/h_w = 0.3$) and with any aspect ratio since they have absolute maximum strength-to-weight ratios equal to (3.85, 3.78, 3.91, and 3.88) with aspect ratios equal to (1.5, 1.0, 0.667, and 0.5) respectively.

6.3 Recommendations

1. Behavior of a web plate in shear and compression with intermediate stiffeners.
2. Post-buckling analysis of stiffened plates under transverse compressive load.
3. Making a parametric study for an imperfect plate subjected to combined in-plane and lateral load.
4. Optimum design of the shape of stiffeners used in ship and marine structures.
5. Analyzing plates and shells stiffened by criss-crossing stiffeners.

Vitae

BAHAA H. MOHAMMAD **E-mail: Hussain_Bahaa@yahoo.com**

Personal Profile

Name:	**BAHAA HUSSAIN MOHAMMAD**
Date of Birth:	**August, 1, 1979.**
Marital Status:	**Single.**
Mobile:	**07801258370**
Tel.	**326510**
Address:	**Al-Aamel Quarter/ Karbala/ Iraq**

Educational Background

Bahaa Husain Mohamed El-Jeleahawy was born in Baghdad, Iraq the first of August 1979. Soon after he moved to Karbalaa with his family where he had his elementary, middle and high school education. In 1998 he was admitted in the College of Engineering at Babylon University. He graduated in 2002 with a B.S in civil Engineering. He obtained a Master Degree in structural Engineering in 2005.

ولد الباحث بهاء حسين محمد الجليحاوي في بغداد 1979 وفي نفس العام انتقل إلى كربلاء المقدسة مع عائلته وفيها أكمل الابتدائية والمتوسطة والإعدادية في عام 1998 دخل كلية الهندسة جامعة بابل وتخرج منها عام 2002 وفي عام 2005 حصل على ماجستير في علوم هندسة الإنشاءات عن أطروحته الموسومة " تحليل الانبعاج ِو ما بعدِ الانبعاج للصفائح المُجَسَأة بطريقةِ العناصر المحددةِ " بإشراف الأستاذ الدكتور حسين محمد حسين والأستاذ المساعد الدكتور هيثم حسن متعب الدعمي.

APPENDIX-A

This Appendix contains shade-coded Von Mises stress distribution gradients in the midthickness of the plates. All the plates were subjected to uniaxial compression load and the finite element program ANSYS (V.5.4) was used in the analysis. Only some plates are plotted to different yield locations in the entire model.

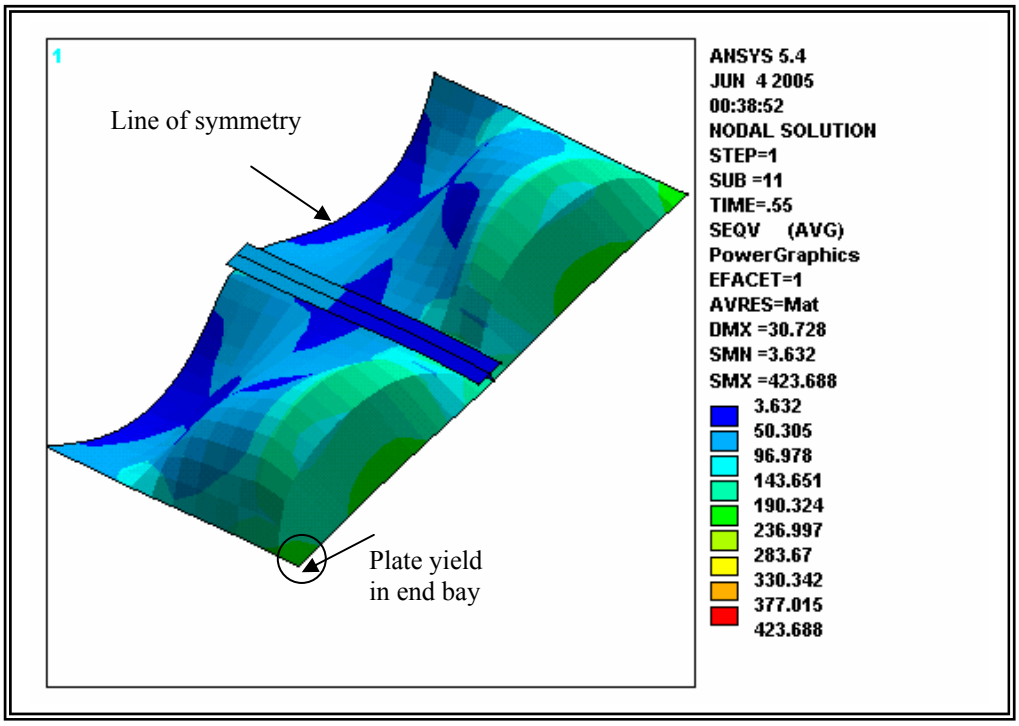

Fig.(A.1): Von-Mises Stress Distribution for Plate Having (B=3600, L=5400, t=6, t_w=20, h_w=50, t_f=30, b_f=200)

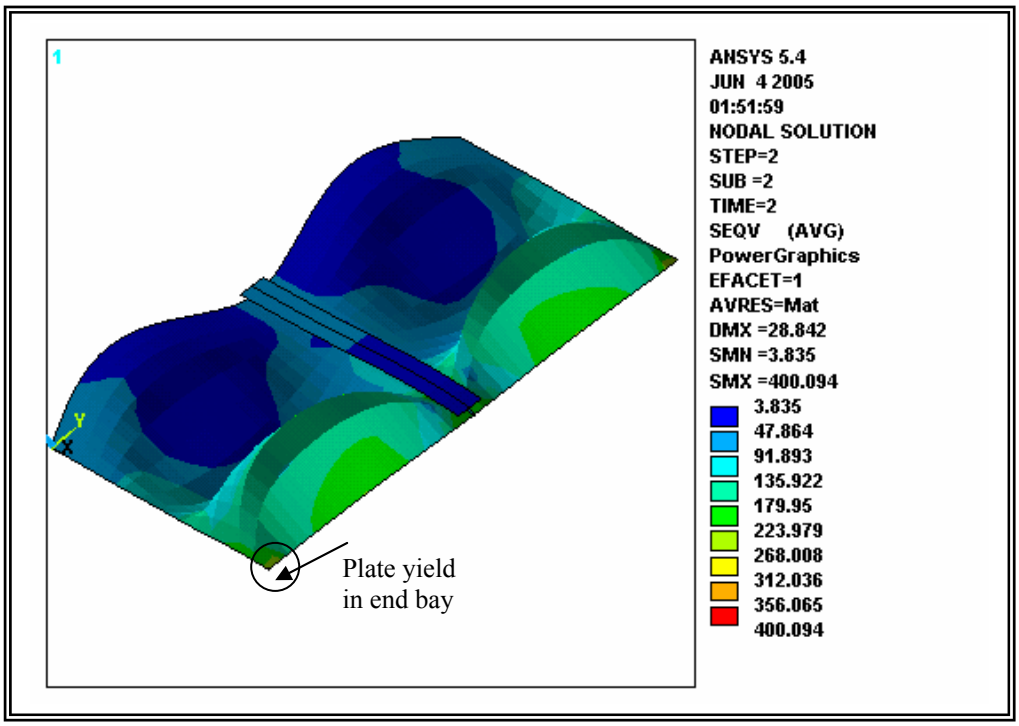

Fig.(A.2): Von-Mises Stress Distribution for Plate Having (B=3600, L=7200, t=6, t_w=20, h_w=50, t_f=30, b_f=200)

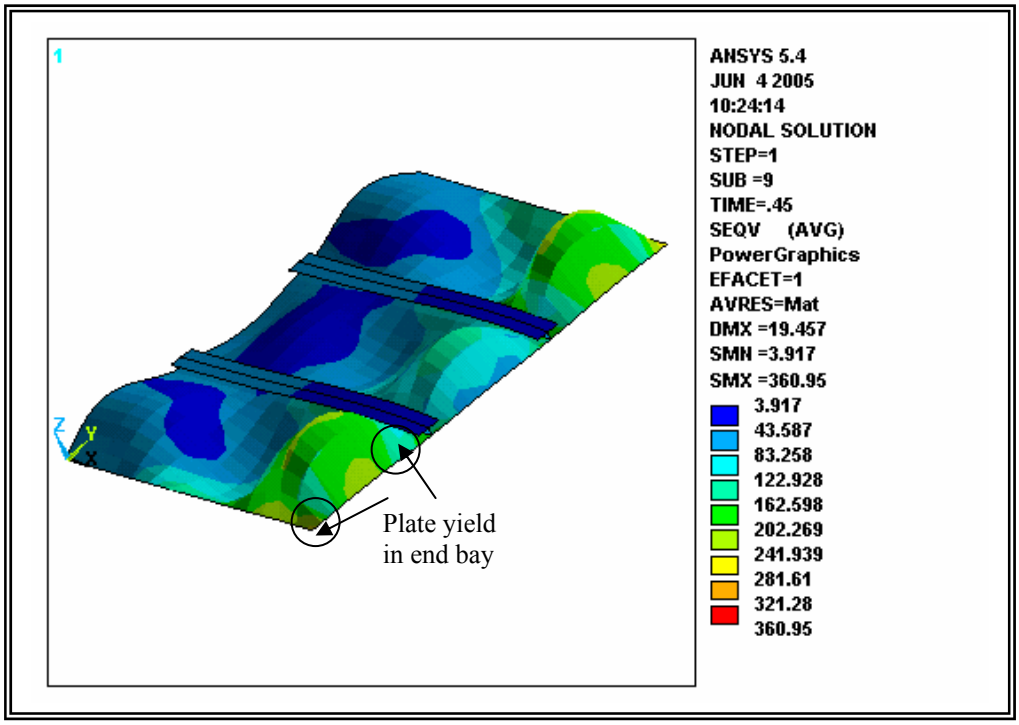

Fig.(A.3): Von-Mises Stress Distribution for Plate Having (B=3600, L=5400, t=6,t_w=20, h_w=50, t_f=30, b_f=200)

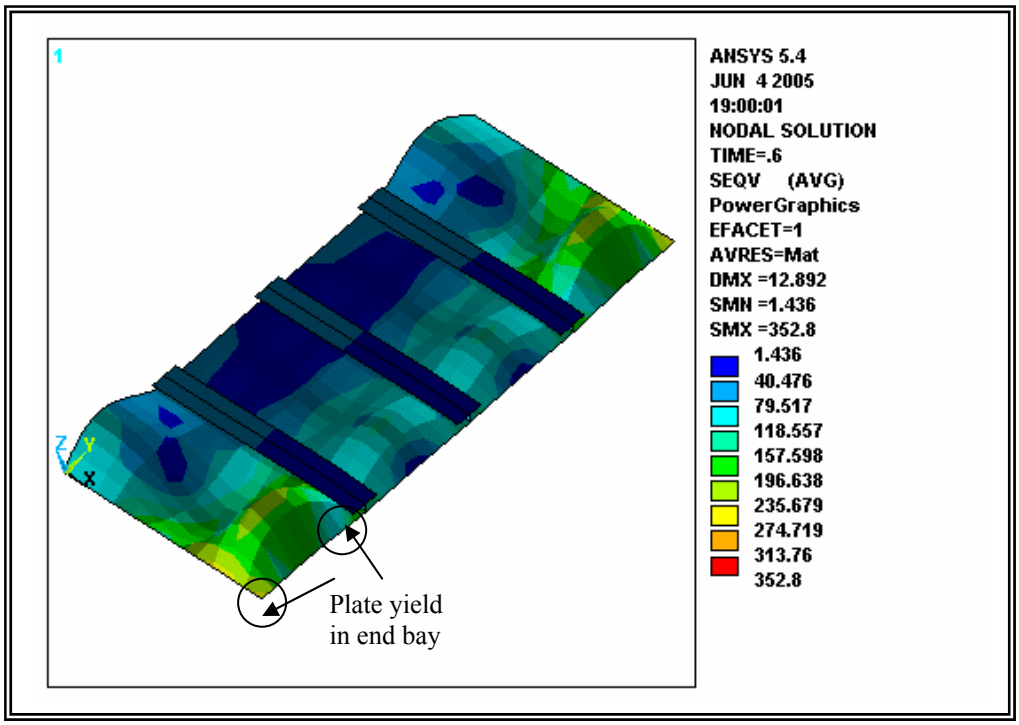

Fig.(A.4): Von-Mises Stress Distribution for Plate Having (B=3600, L=3600, t=6, t_w=20, h_w=50, t_f=30, b_f=200)

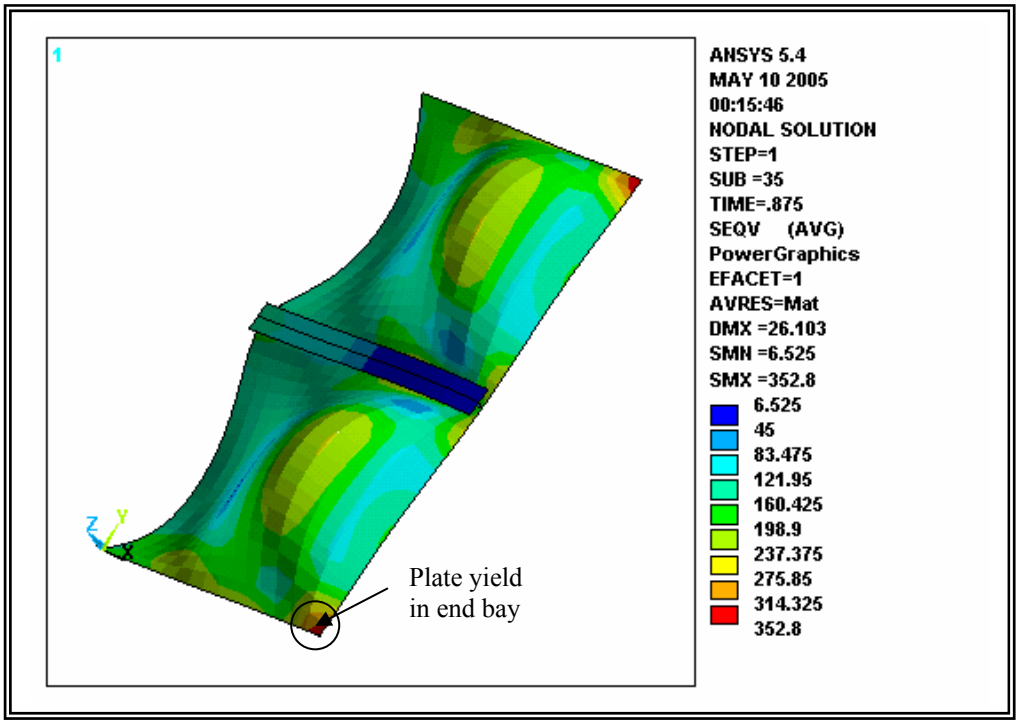

Fig.(A.5): Von-Mises Stress Distribution for Plate Having (B=3600, L=3600, t=11, t_w=20, h_w=50, t_f=30, b_f=200)

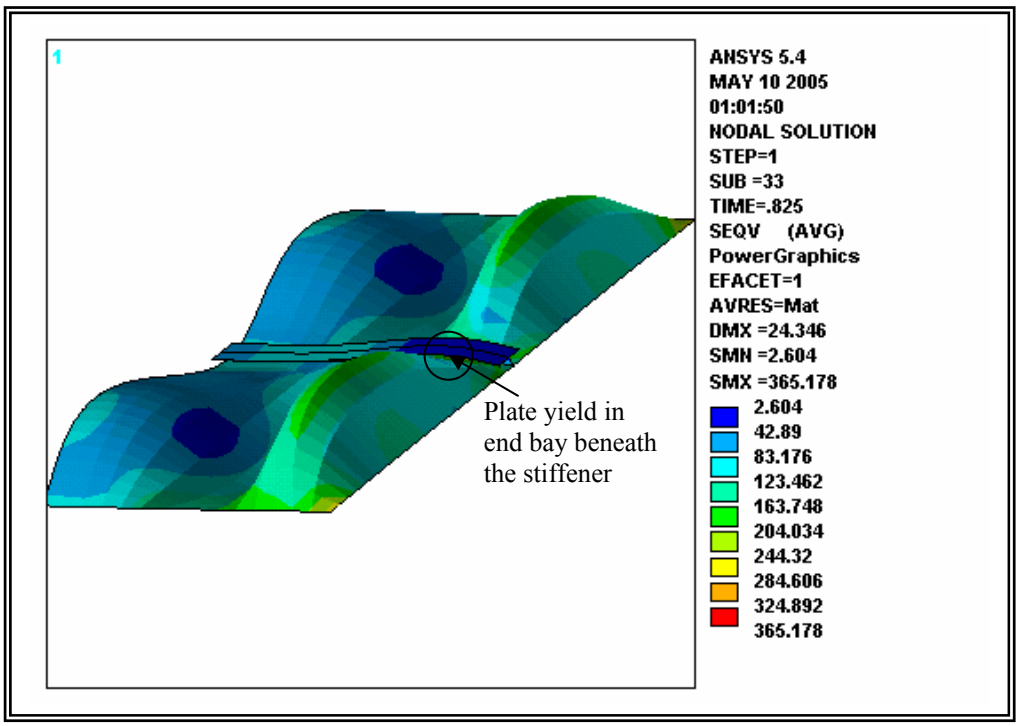

Fig.(A.6): Von-Mises Stress Distribution for Plate Having (B=3600, L=7200, t=11, t_w=20, h_w=50, t_f=30, b_f=200)

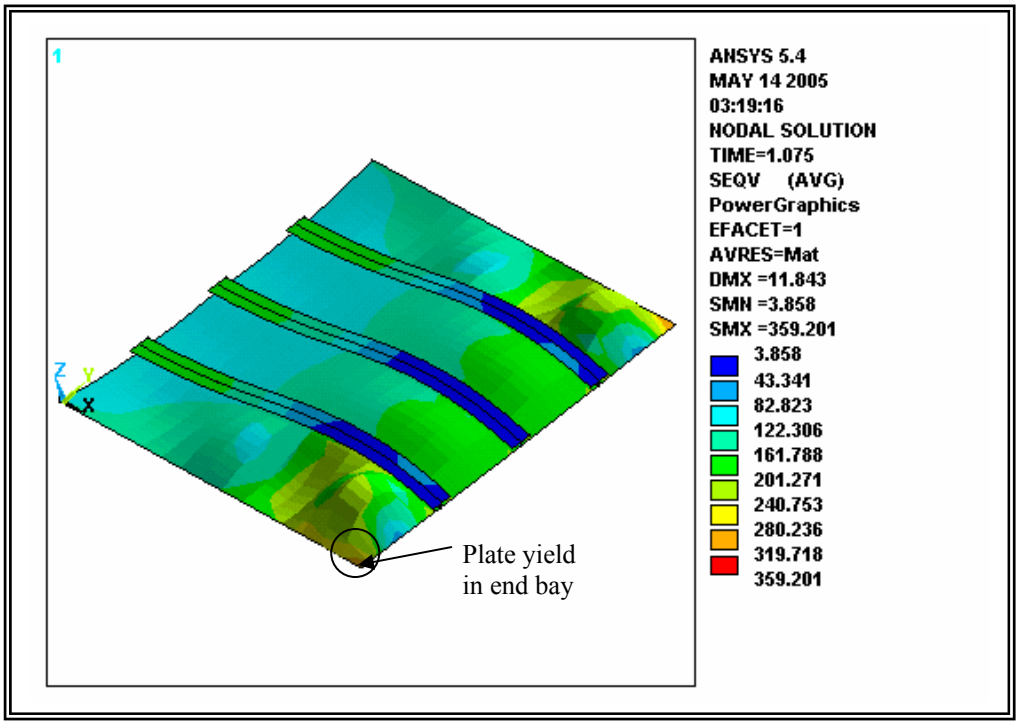

Fig.(A.7): Von-Mises Stress Distribution for Plate Having (B=3600, L=7200, t=11, t_w=20, h_w=50, t_f=30, b_f=200)

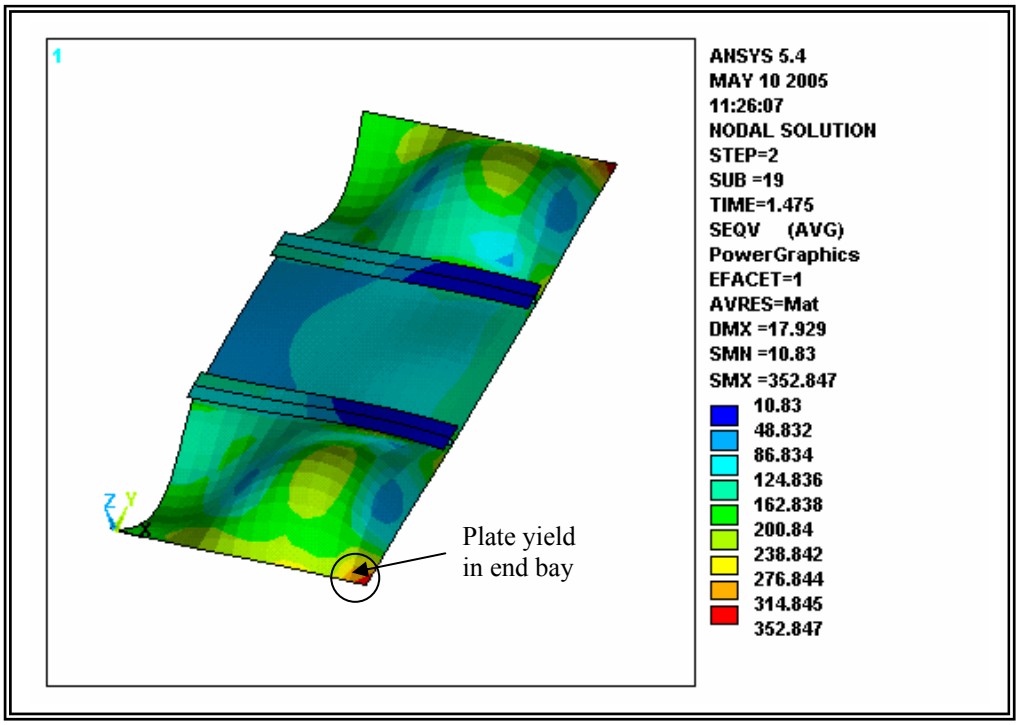

Fig.(A.8): Von-Mises Stress Distribution for Plate Having (B=3600, L=3600, t=11, t_w=20, h_w=50, t_f=30, b_f=200)

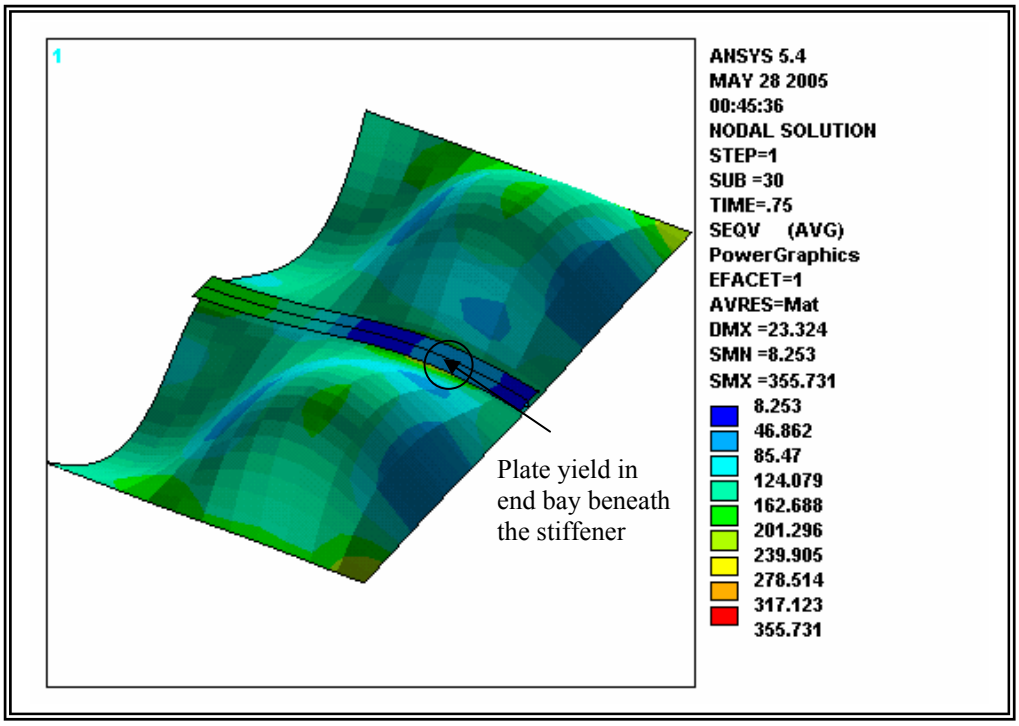

Fig.(A.9): Von-Mises Stress Distribution for Plate Having (B=3600, L=5400, t=15, t_w=20, h_w=50, t_f=30, b_f=200)

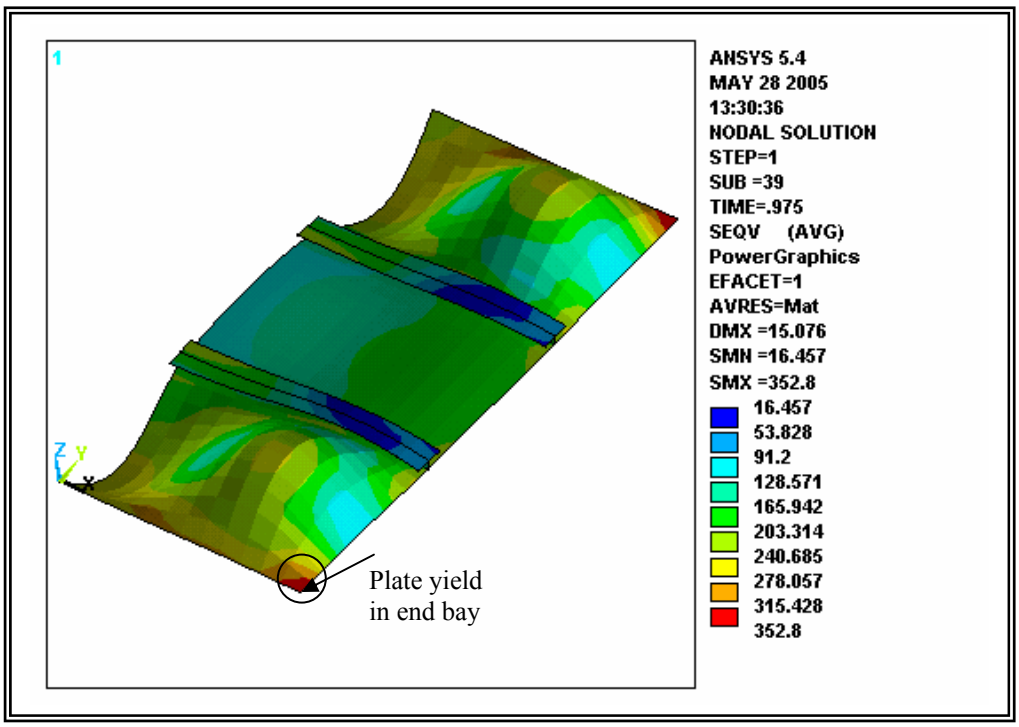

Fig.(A.10): Von-Mises Stress Distribution for Plate Having (B=3600, L=3600, t=15, t_w=20, h_w=50, t_f=30, b_f=200)

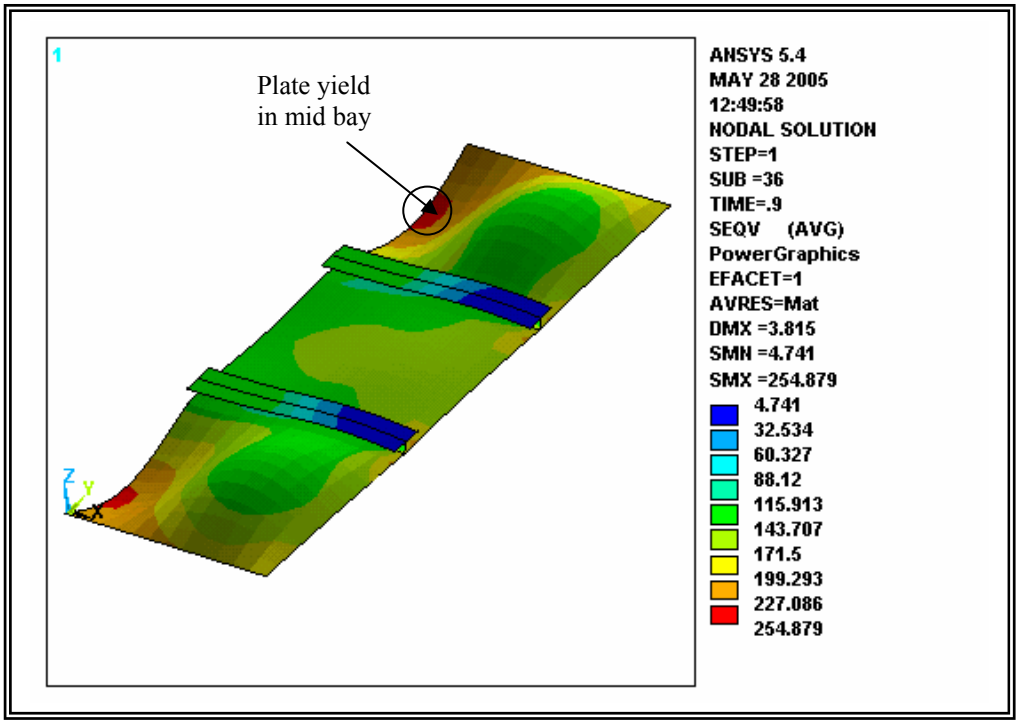

Fig.(A.11): Von-Mises Stress Distribution for Plate Having (B=3600, L=2400, t=15, t_w=20, h_w=50, t_f=30, b_f=200)

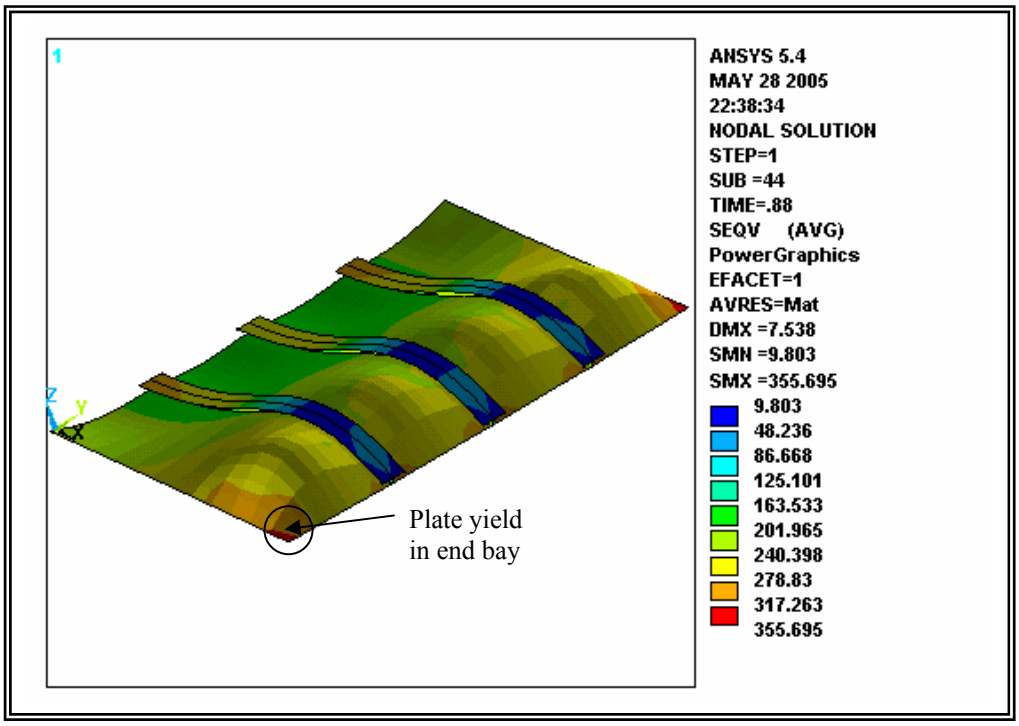

Fig.(A.12): Von-Mises Stress Distribution for Plate Having (B=3600, L=5400, t=21, t_w=20, h_w=50, t_f=30, b_f=200)

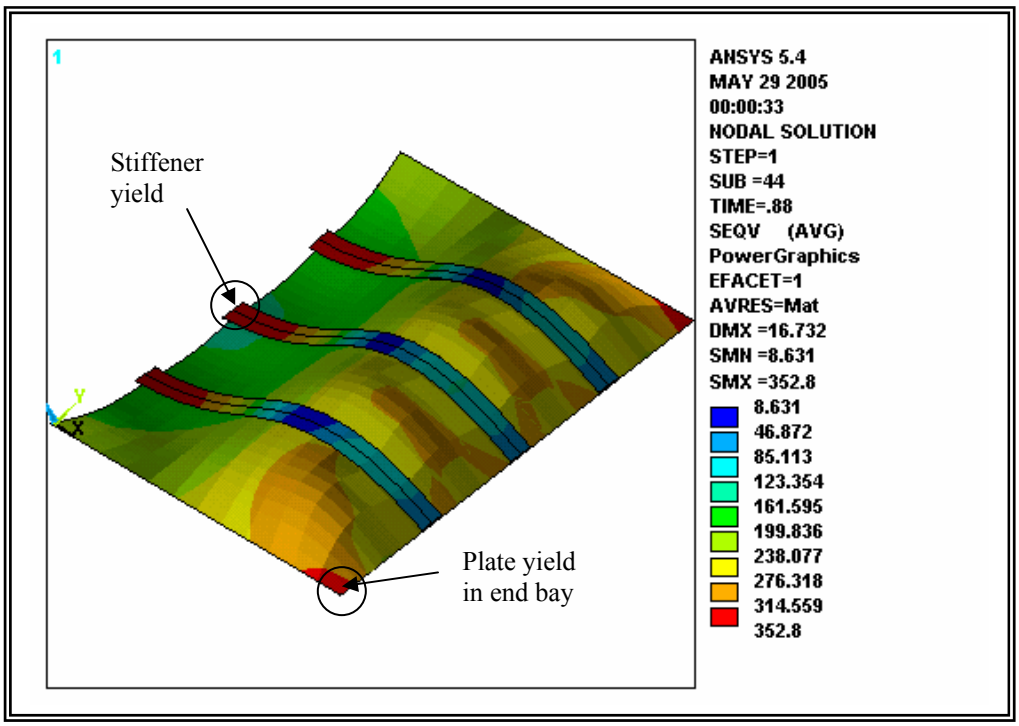

Fig.(A.13): Von-Mises Stress Distribution for Plate Having (B=3600, L=7200, t=15, t_w=20, h_w=50, t_f=30, b_f=200)

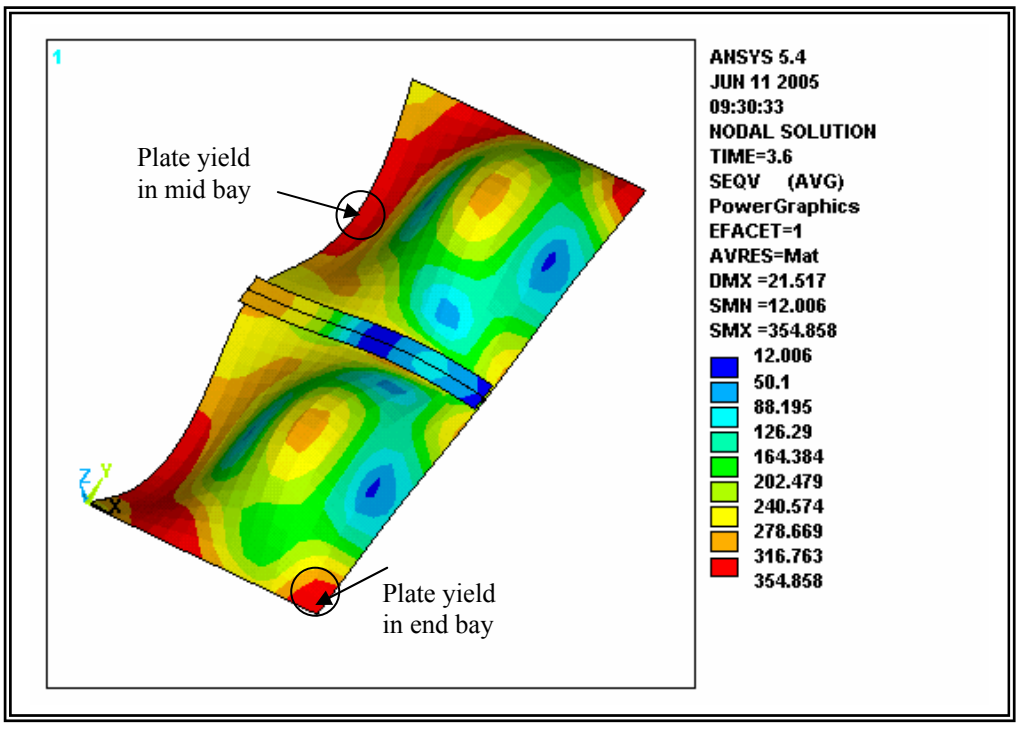

Fig.(A.14): Von-Mises Stress Distribution for Plate Having (B=3600, L=3600, t=21, t_w=20, h_w=50, t_f=30, b_f=200)

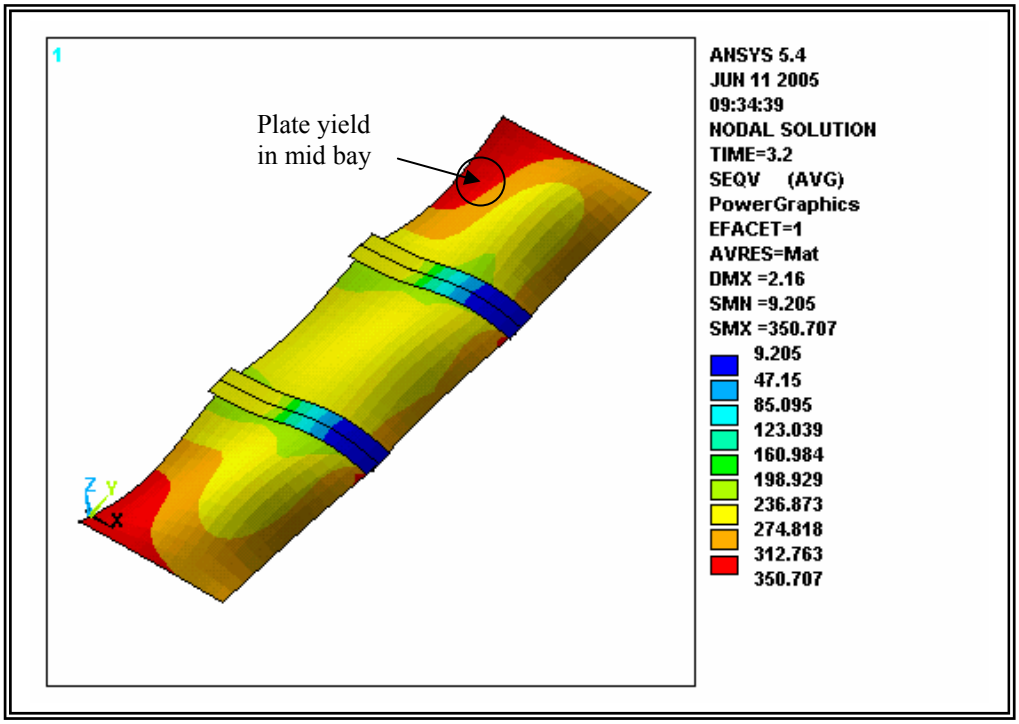

Fig.(A.15): Von-Mises Stress Distribution for Plate Having (B=3600, L=2400, t=21, t_w=20, h_w=50, t_f=30, b_f=200)

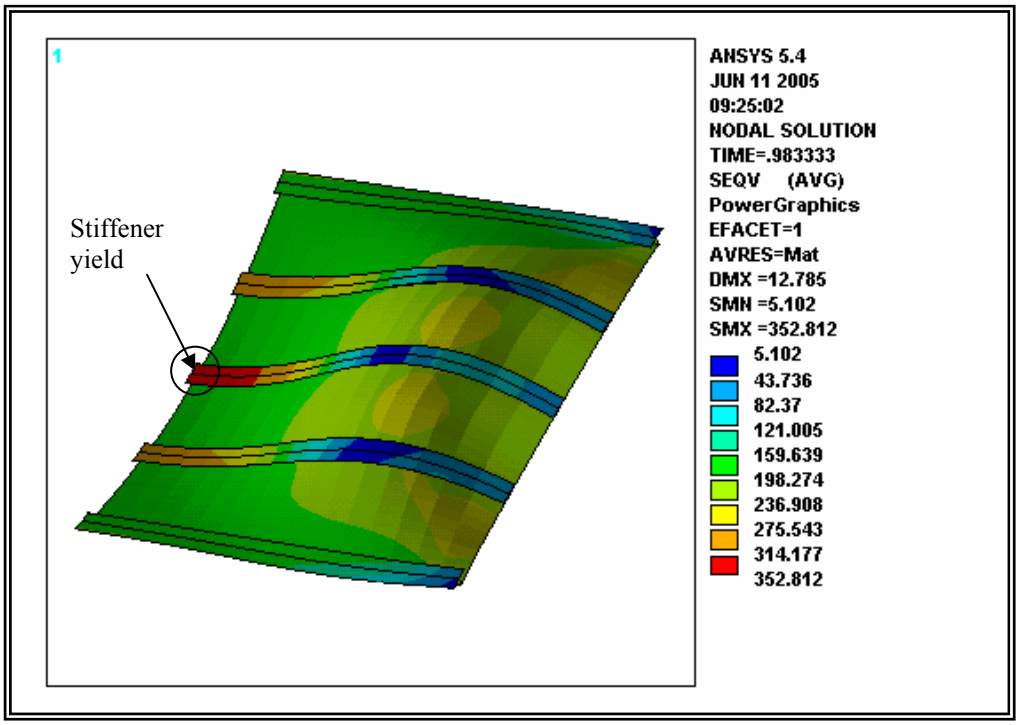

Fig.(A.16): Von-Mises Stress Distribution for Plate Having (B=3600, L=7200, t=21, t_w=20, h_w=50, t_f=30, b_f=200)

APPENDIX-B

This appendix show a review of *ANSYS* commands used to perform a square plate (3600x3600 mm) having one intermediate stiffener with t=6 mm , t_w=20 mm, h_w=50 mm, t_f=30 mm, b_f=200 mm.

```
/PREP7
ET,1,SHELL43
R,1,6, , , , ,
R,2,20,0,0,0,0,
R,3,30,0,0,0,0,
UIMP,1,EX, , ,205800,
UIMP,1,NUXY, , ,0.3,
TB,BKIN,0, , , ,
TB,BKIN,1, , , ,
TBMODIF,2,1,352.8
BLC4,0,0,1800,3600
FLST,5,2,4,ORDE,2
FITEM,5,2
FITEM,5,4
CM,_Y,LINE
LSEL, , , ,P51X
CM,_Y1,LINE
CMSEL,,_Y
LESIZE,_Y1, , ,40,1,
CMDEL,_Y
CMDEL,_Y1
FLST,5,2,4,ORDE,2
FITEM,5,1
FITEM,5,3
CM,_Y,LINE
LSEL, , , ,P51X
CM,_Y1,LINE
CMSEL,,_Y
LESIZE,_Y1, , ,15,1,
CMDEL,_Y
CMDEL,_Y1
CM,_Y,AREA
ASEL, , , ,       1
CM,_Y1,AREA
CHKMSH,'AREA'
CMSEL,S,_Y
AMESH,_Y1
CMDEL,_Y
CMDEL,_Y1
CMDEL,_Y2
```

```
TYPE,   1
MAT,      1
REAL,      3
ESYS,      0
K,5,1800,1800+100,63,
K,6,1800,1800-100,63,
K,7,0,1800+100,63,
K,8,0,1800-100,63,
FLST,2,4,3
FITEM,2,6
FITEM,2,5
FITEM,2,7
FITEM,2,8
A,P51X
FLST,5,2,4,ORDE,2
FITEM,5,6
FITEM,5,8
CM,_Y,LINE
LSEL, , , ,P51X
CM,_Y1,LINE
CMSEL,,_Y
LESIZE,_Y1, , ,15,1,
CMDEL,_Y
CMDEL,_Y1
FLST,5,2,4,ORDE,2
FITEM,5,5
FITEM,5,7
CM,_Y,LINE
LSEL, , , ,P51X
CM,_Y1,LINE
CMSEL,,_Y
LESIZE,_Y1, , ,2,1,
CMDEL,_Y
CMDEL,_Y1
CM,_Y,AREA
ASEL, , , ,      2
CM,_Y1,AREA
CHKMSH,'AREA'
CMSEL,S,_Y
AMESH,_Y1
CMDEL,_Y
CMDEL,_Y1
CMDEL,_Y2
FLST,5,32,1,ORDE,20
FITEM,5,37
FITEM,5,91
FITEM,5,130
FITEM,5,169
FITEM,5,208
FITEM,5,247
```

FITEM,5,286
FITEM,5,325
FITEM,5,364
FITEM,5,403
FITEM,5,442
FITEM,5,481
FITEM,5,520
FITEM,5,559
FITEM,5,598
FITEM,5,637
FITEM,5,659
FITEM,5,676
FITEM,5,691
FITEM,5,-704
NSEL,S, , ,P51X
NPLOT
/VIEW, 1 ,1,1,1
/ANG, 1
/REP,FAST
TYPE, 1
MAT, 1
REAL, 2
ESYS, 0
FLST,2,4,1
FITEM,2,659
FITEM,2,37
FITEM,2,637
FITEM,2,691
E,P51X
FLST,2,4,1
FITEM,2,691
FITEM,2,637
FITEM,2,598
FITEM,2,692
E,P51X
FLST,2,4,1
FITEM,2,692
FITEM,2,598
FITEM,2,559
FITEM,2,693
E,P51X
FLST,2,4,1
FITEM,2,693
FITEM,2,559
FITEM,2,520
FITEM,2,694
E,P51X
FLST,2,4,1
FITEM,2,694
FITEM,2,520

FITEM,2,481
FITEM,2,695
E,P51X
FLST,2,4,1
FITEM,2,695
FITEM,2,481
FITEM,2,442
FITEM,2,696
E,P51X
FLST,2,4,1
FITEM,2,696
FITEM,2,442
FITEM,2,403
FITEM,2,697
E,P51X
FLST,2,4,1
FITEM,2,697
FITEM,2,403
FITEM,2,364
FITEM,2,698
E,P51X
FLST,2,4,1
FITEM,2,698
FITEM,2,364
FITEM,2,325
FITEM,2,699
E,P51X
FLST,2,4,1
FITEM,2,699
FITEM,2,325
FITEM,2,286
FITEM,2,700
E,P51X
FLST,2,4,1
FITEM,2,700
FITEM,2,286
FITEM,2,247
FITEM,2,701
E,P51X
FLST,2,4,1
FITEM,2,701
FITEM,2,247
FITEM,2,208
FITEM,2,702
E,P51X
FLST,2,4,1
FITEM,2,702
FITEM,2,208
FITEM,2,169
FITEM,2,703

E,P51X
FLST,2,4,1
FITEM,2,703
FITEM,2,169
FITEM,2,130
FITEM,2,704
E,P51X
FLST,2,4,1
FITEM,2,704
FITEM,2,130
FITEM,2,91
FITEM,2,676
E,P51X
ALLSEL,ALL
VSEL,ALL
ASEL,ALL
LSEL,ALL
KSEL,ALL
ESEL,ALL
NSEL,ALL
EPLOT
/REPLO
/VIEW, 1 ,,,1
/ANG, 1
/REP,FAST
/AUTO, 1
/REP
FLST,2,2,1,ORDE,2
FITEM,2,37
FITEM,2,91
D,P51X, , , , , ,UY
FLST,2,32,1,ORDE,4
FITEM,2,1
FITEM,2,-17
FITEM,2,57
FITEM,2,-71
D,P51X, , , , , ,UZ,ROTY,ROTZ
FLST,2,44,1,ORDE,7
FITEM,2,7
FITEM,2,67
FITEM,2,267
FITEM,2,-305
FITEM,2,670
FITEM,2,681
FITEM,2,700
D,P51X, , , , , ,UZ
FLST,2,44,1,ORDE,5
FITEM,2,2
FITEM,2,17
FITEM,2,-56

```
FITEM,2,657
FITEM,2,-659
D,P51X, , , , , ,UZ,ROTX,ROTZ
FLST,2,44,1,ORDE,7
FITEM,2,1
FITEM,2,57
FITEM,2,72
FITEM,2,-110
FITEM,2,660
FITEM,2,675
FITEM,2,-676
D,P51X, , , , , ,UX,ROTY
/SOLU
FINISH
/SOLU
NLGEOM,1
NROPT,AUTO, ,
LUMPM,0
EQSLV,FRONT,1e-008,0,
SSTIF
PSTRES
TOFFST,0,
FLST,2,1,4,ORDE,1
FITEM,2,2
SFL,P51X,PRES,1000, ,
NSUBST,20
OUTRES,,1
SOLVE
/POST1
FINISH
/POST1
SET,FIRST
AVPRIN,0,0,
PLNSOL,S,EQV,0,1
SET,LIST,2
SET,1,6,1,
AVPRIN,0,0,
PLNSOL,S,EQV,0,1
/REPLOT,RESIZE
/REPLOT,RESIZE
AVPRIN,0,0,
PLNSOL,U,Z,0,1
SET,NEXT
AVPRIN,0,0,
PLNSOL,U,Z,0,1
FINISH
! /EXIT,ALL
```

REFERENCES

1. Aalami, B., and Chapman, I.C., "Large Deflection Behavior of Orthotropic Plates Under Transverse and In-Plane Loads", Proc.ICE, London, England Vol.42, Mar., 1969, pp.347-382.

2. Abbas, F.K, and Mathlum, M.K.," Large Deflection Elasto-Plastic Analysis of Plates by Finite Element Methods", Engineering and Technology, Baghdad, Vol.19, No.4, 2000, pp.88-108.

3. Abdel-Sayed, G., "Effective Width of Thin Plates in Compression", ASCE, J.Struct.Eng., Vol.95, No.St10, Oct., 1969, pp.2183-2203.

4. Amash, H.K.,"Post-Buckling and Post-Yielding Analysis of Imperfect Thin Plate by Finite Difference Method", M.Sc. Thesis, Department of Civil Eng., University of Babylon, Iraq, Feb., 2003.

5. ANSYS User's Manual (V-5.4), ANSYS Inc., 1997.

6. Basu, A.C., and Chapman, J.C.,"Large Deflection Behavior of Transversely Loaded Rectangular Orthotropic Plates", Proc. ICE, London, England, Vol.35, Sep., 1966, pp.79-110.

7. Biswarup, G., "Consequences of Simultaneous Local and Overall Buckling in Stiffened Panels", M.Sc. Thesis, Virginia Polytechnic Institute and State University, Blacksburg, April, 2003.

8. Bjelajac, N., "Evaluation of Post-Buckling Equilibrium Branches for Perfect and Imperfect Plates by Finite Difference Method", Numerical Methods in Continuum Mechanics, Liptovskk'y Ja'n, Slovac Republic, 2000, pp.1-18.

9. Bleich, F., "Buckling Strength of Metal Structures", McGraw-Hill, New York, 1952, cited in [7].

10. Bradfield, C.D., "An Evaluation of the Elastic-Plastic Analysis of Plates Loaded by Uniaxial In-Plane Compression", Int., J. Mech. Sci., Vol.24, No.3, 1982, pp.127-146.

11. Brebbia, C. and Connor, J., "Geometrically Nonlinear Finite Element Analysis", Journal of the Engineering Mechanics Division, Vol. 95, No. EM2, April 1969, pp.463-483, cited in [22].

12. Bryan, G. H., "On the Stability of a Plate Under Thrusts in Its Own Plane with Application to the Buckling of the Sides of Ships", Proc. London Math. Soc., Vol.22, 1891, pp.54-67, cited in [4].

13. Byklum, E., and Amdahl, J., "A Simplified Method for Elastic Large Deflection Analysis of Plates and Stiffened Panels Due to Local Buckling", Norwegian University of Science and Technology N-7491, 2002.

14. Byklum, E., and Amdahl, J., "Nonlinear Buckling Analysis and Ultimate Strength Prediction of Stiffened Steel and Aluminum Panels", Int. Conference on Advances in Struc. Eng. and Mech., Busan, Korea, Aug., 2002.

15. Chehil, D. S., and Dua, S. S., "Buckling of Rectangular Plates with General Variation in Thickness", ASME, J. Appl. Mech., Vol.40, 1973, pp.745-751.

16. Chen, Y., "Ultimate Strength Analysis of Stiffened Panels Using A Beam - Column Method", Ph.D. Dissertation, Virginia Polytechnic Institute And State University, Blacksburg, Janu., 2003.

17. Chin, C.K., Al-Bermani, F.G.A., and Kitipornchai, S., "Finite Element Method for Buckling Analysis of Plates Structure", ASCE, J.Struc.Eng. , Vol.119, No.4, Apr. 1993, pp.1050-1068.

18. Coan, J.M., "Large Deflection Theory for Plates with Small Initial Curvature Loaded in Edge Compression", ASME, J.Appl.Mech, Vol.18, June, 1951, pp.2979-2993.

19. Colville, J., Becker, E.B., and Furlong, R.W., "Large Deflection Analysis of Thin Plates", ASCE, J.Struc.Div. , Vol.99, No.ST3, Mar. 1973, pp.349-364.

20. Colville, J., and Kuen-Yaw Shye, "Post-Buckling Finite Element Analysis of Flat Plates", ASCE, J.Struc.Div., Vol.105, No.ST2, Feb. 1979, pp.297-311.

21. Crisfield, M.A., "Full-Range Analysis of Steel Plates Stiffened Plating Under Uniaxial Compression", Proc., ICE, Vol.59, Part 2, Dec. 1975, pp.593-624.

22. Elseifi, M. A., "A New Scheme for the Optimum Design of Stiffened Composite Panels with Geometric Imperfections", Ph.D. Dissertation, Virginia Polytechnic Institute And State University, Blacksburg, Nov., 1998.

23. Fok, C. D., "Effects of Initial Imperfections on the Elastic Post-Buckling Behavior of Flat Plates", Ph. D. Thesis, Monash University, 1980, cited in [4].

24. Fok, W.C., "Evaluation of Experimental Data of Plate Buckling", ASCE, J.Eng.Mech. , Vol.110, No.4, 1984, pp.577-588.

25. Frieze, P.A., Hobbs, R.E., and Dowling, P.J., "Application of Dynamic Relaxation to the Large Deflection Elasto-Plastic Analysis of Plates", Computers and Strucures, Vol.8, No.4, 1978, pp.301-310.

26. Harding, J.E., Hobbs, R.E., and Neal, B.G., "The Elasto-Plastic Analysis of Imperfect Square Plates Under In-Plane Loading", Proc.ICE, Part2, Vol.63, Mar., 1977, pp.137-158.

27. Husain, H.M., Al-Daami, H., and Amash, H.K., "Buckling Behavior of Rectangular Plate With Variable Thickness", Engineering and Technology,

Baghdad, Vol.21, No.10, 2002, pp.736-745.

28. Jayachandran, S.A, Gopalakrishnan, S., and Narayana, R., "Explicit Incremental Matrices for the Post-Buckling Analysis of Thin Plates with Small Initial Curvature", Struct.Eng.and Mech., Vol.12, No.30, 2001, pp.282-295.

29. Kassegne, S.K., and Reddy, J.N., "Local Behavior of Discretely Stiffened Composite Plates and Cylindrical Shells", Dep. of Mech. Eng., Texas A&M University, 1996.

30. Klitchieff, J.M., "On the Stability of Plates Reinforced by Longitudinal Ribs", J. Applied Mechanics, 18(4), 1951, pp. 364-366, cited in [7].

31. Kobayashi, H., and Sonoda, K., "Buckling of Rectangular Plates with Tapered Thickness", ASCE, J.Struct.Eng., Vol.116, No.5, May, 1990, pp.1278-1289.

32. Lam, S.S., "Post-Buckling Analysis of Strut with General Initial Imperfection", Int. J. Num. Mech. Eng., Vol.43, 1998, pp.1017-1028.

33. Lee, S.C., and Yoo, C.H., "Strength of Plate Girder Web Panels Under Pure Shear", ASCE, J.Struct.Eng., Vol.124, No.2, Feb., 1998, pp.184-194.

34. Lee, S.C., and Yoo, C.H., "Experimental Study on Ultimate Shear Strength of Web Panels", ASCE, J.Struct.Eng., Vol.128, No.8, Aug., 1999, pp.838-846.

35. Lee, S.C., Yoo, C.H., and Yoon, D.Y., "Behavior of Intermediate Transverse Stiffeners Attached on Web Panels", ASCE, J. Struct. Eng., Vol.128, No.3, March, 2002, pp.337-345.

36. Lin, T.H., and Ho, E.Y., "Elasto-Plastic Bending of Rectangular Plates with Large Deflection", Trans. ASME, Div., Vol.39, Dec., 1972, pp.978-982.

37. Little, G.H., "Rapid Analysis of Plate Collapse by Live-Energy Minimization", Int. J. Mech., Sci., Vol.19, 1977, pp.728-744.

38. Mathlum, M.K., "Large Deflection Elasto-Plastic Analysis of Plates by Finite Element Method", M.Sc. Thesis, Department of Building and Construction, University of Technology, Iraq, 1997.

39. Mirambell, E., Costa, J., and Arnedo, A., "Analytical and Experimental Study on the Behavior of Steel Panels Under Plane Compression", Proc. Int.Conf. On Steel Structures, CI-Premier Pte.Ltd, Jakarta, Indonesia, 1994, pp.205-212.

40. Mirambell, E., Zarate, A. V., "Web Buckling of Tapered Plate Girders", Proc. Inst. Civ.Eng.Struct.& Bldgs, Vol.140, Feb., 2000, pp.51-60.

41. Mohammed, A.M., "Effect of Initially Imperfect and Boundary Condition on the Buckling and Post-Buckling Behavior of Steel Plates", M.Sc. Thesis, Department of Building and Construction, University of Technology, Iraq, 2001.

42. Moxham, K.E., "Theoretical Prediction of the Strength of Welded Steel Plates in Compression", Cambridge University Report No.CUED/C-Struc. TR2, 1971, cited in [4].

43. Ohga, M., Shigematsu, T., and Kawagouchi, K., "Buckling Analysis of Thin-Walled Members with Variable Thickness", ASCE J. Struct. Eng., Vol.121, No.6, June, 1995, pp.919-924.

44. Paik, J.K., and Kim, Y., "A Simplified Finite Element Method for the Ultimate Strength Analysis of Plates with Initial Imperfection", Journal of the Society of Naval Architects of Korea, Vol.26, No.1, Mar., 1989, pp.24-38.

45. Paik, J.K., Ham, J.H., and Ko, J.H., "A New Plate Buckling Design Formula", Journal of the Society of Naval Architects of Japan, Vol.172, 2nd

Report, Dec., 1992, pp.417-428.

46. Paik, J.K., Thayamballi, A.K., "Buckling Strength of Steel Plating with Elastically Restraining Edges", Thin-Walled Structures, Vol.37, 2000, pp.27-55, cited in [7].

47. Park, O., Haftka, R.T., Sankar, B.V, Starnes, J.H., and Nagendra, S., "Analytical and Experimental Study of a Blade Stiffened Panel in Axial Compression", Corporate Research and Development, Jan., 2000.

48. Rerkshanandana, N., Usami, T., and Karasudhi, P., "Ultimate Strength of Eccentrically Loaded Steel Plates and Box Sections", Computers and Structures, Vol.13, 1981, pp.467-481.

49. Rushton, K.R., "Post-Buckling of Tapered Plates", Int.J.Mech.Sci., Vol.11, 1969, pp.461-480.

50. Salvadori, M.G., "Numerical Computation of Buckling Loads by Finite Differences", ASCE, Trans., Dec., 1949, pp.590-636, cited in [4].

51. Sherbourne, A.N., and Korol, R.M., "Post-Buckling of Axially Compressed Plates", ASCE, J. Struc. Div., Vol.98, No.ST10, Oct., 1972, pp.2223-2234.

52. Shnan, W.F., "A Proposed Plastic Collapse Mechanism for the Prediction of Ultimate Load Capacity of Plated Structures", M.Sc. Thesis, Dep. of Building and Construction Eng., Univ. of Tech., Baghdad, 2001.

53. Sridhran, S., and Graves-Smith, T.R., "Post-Buckling Analysis with Finite Strips", ASCE, J. Eng. Mech. Div., Vol.107, No.EM5, Oct., 1981, pp.869-888.

54. Stein, M., "Behavior of Buckling Rectangular Plates", ASCE, J. Eng. Mech. Div., Vol.86, No.EM2, Apr., 1960, pp.59-76.

55. Sun, G., and Williams, F.W., "An Initial Post-Buckling Analysis for Prismatic Plate Assemblies Under Axial Compression", Int.J. Solids Structures, Vol.34, No.28, 1997, pp.3705-3725.

56. Sun, G., Kennedy, D., and Williams, F.W., "A Post-Buckling Analysis for Isotropic Prismatic Plate Assemblies Under Axial Compression", Int.J. Mech. Sci., Vol.42, 2000, pp.1783-1803.

57. Turvey, G.J., and Salehi, M., "Elasto-Plastic Response of Uniformly Loaded Sector Plates: Full-Section Yield Model Predictions and Spread of Plasticity", Computers and Structures, Vol.79, 2001, pp.2335-2348.

58. Tvergaard, V., "Influence of Post-Buckling Behavior on Optimum Design of Stiffened Panels", Int. J.Solids Structures, Vol.9, 1973, pp.1519, cited in [7].

59. Ueda, Y., and Yao, T., "The Plastic Node Method: A New Method of Plastic Analysis", Computer Methods in Applied Mechanics and Engineering, Vol.34, 1982, pp.1089-1104.

60. Ueda, Y., Rashed, S.M.H., and Paik, J.K., "An Incremental Galerkin Method for Plates and Stiffened Plates", Computers and Structures, vol.27, no.1, 1987, pp.147-156.

61. Usami, T., "Post-Buckling of Plates in Compression and Bending", ASCE, J. Struc. Eng., Vol.108, No. ST3, Mar., 1982, pp.591-609.

62. Usami, T., "Effective Width of Locally Buckled Plates in Compression and Bending", ASCE, J. Struc. Eng., Vol.119, No. 5, May, 1993, pp.1358-1337.

63. Wah, T., "Large Deflection Theory of Elasto-Plastic Plates", ASCE, J. Eng. Mech. Div., Vol.84, No.EM4, Oct., 1958, pp.1-24.

64. Whitney, J., "Structural Analysis of Laminated Anisotropic Plates",

Technomic Publishing Co., Inc., 1987, cited in [22].

65. Williams, D.G. and Walker, A.C. "Explicit Solution for the Design of Initially Deformed Plates Subjected to Compression" Proc., ICE, London, England, Vol.59, Part 2, 1975, pp.763-787.

66. Yamaki, N., "Post-Buckling Behavior of Rectangular Plates with Small Initial Curvature Loaded in Edge Compression", ASME Trans., J.Appl. Mech., Vol.26, 1959, pp.407-414.

67. Zou, G., and Qiao, P., "Higher Order Finite Strip Method for Post-Buckling Analysis of Imperfect Composite Plates", J. Eng. Mech., Vol.128, No.9, Sep., 2002, pp.1008-1015.